

An Optimal Control Framework for Flight Management Systems

Jesus Villarroel

A Thesis
in
The Department
of
Electrical and Computer Engineering

Presented in Partial Fulfillment of the Requirements
for the Degree of Master of Applied Science (Electrical and Computer Engineering) at
Concordia University
Montréal, Québec, Canada

February 2015

© Jesus Villarroel, 2015

**CONCORDIA UNIVERSITY
SCHOOL OF GRADUATE STUDIES**

This is to certify that the thesis prepared

By: Jesus Villarroel

Entitled: An Optimal Control Framework for Flight Management Systems

and submitted in partial fulfillment of the requirements for the degree of

Master of Applied Science (Electrical & Computer Engineering)

complies with the regulations of the University and meets the accepted standards with respect to originality and quality.

Signed by the final examining committee:

_____	Chair
Dr. S. Hashtrudi Zad	
_____	Examiner
Dr. C. Skonieczny	
_____	External Examiner
Dr. A. Akgunduz	
_____	Supervisor
Dr. L. Rodrigues	

Approved by _____
Dr. A.R. Sebak, Graduate Program Director

Dr. A. Asif, Dean

Faculty of Engineering & Computer Science

February 16, 2015

ABSTRACT

An Optimal Control Framework for Flight Management Systems

Jesus Villarroel

In the present day, the aviation sector is one of the largest contributor of carbon dioxide emissions in the world. As air traffic growth is expected to outweigh the industry's efforts to reduce air pollution, the problem of minimizing fuel consumption in commercial flight becomes of utmost importance. This thesis proposes an optimal control framework for the optimization of aircraft trajectories in Flight Management Systems (FMS), focusing on the problem known as the Economy Mode. This problem consists of minimizing the direct operating cost of the flight in compliance with a crew-supplied cost index.

The objective of the FMS is to obtain optimal true airspeed references that will then be followed by the pilot or the autopilot. The optimal top-of-climb and top-of-descent must be computed as well. A novel approach is proposed based on solving the problem analytically using a combination of Pontryagin's maximum principle and the Hamilton-Jacobi-Bellman equation. For the cruise phase, a sub-optimal algebraic solution for the true airspeed is obtained in a state-feedback form, which reduces to the well-known maximum range case when the cost index vanishes. For the climb and the descent, the sub-optimal speed is the positive root inside the aircraft's flight envelope of a 5th degree polynomial whose coefficients involve only the state variables and the aircraft-specific coefficients, which can be found easily with fast-converging algorithms such as Newton's method. The exact optimal trajectories are computed numerically using the shooting method, and simulations show that the sub-optimal trajectories are close enough for all practical purposes. Moreover, the trajectories exhibit the expected behavior regarding the locations of the top-of-climb and top-of-descent. Having attained an analytic solution for the cruise and a computationally inexpensive formulation for the climb and the descent, the need to have a performance database in the system is eliminated thus making its implementation faster in real-time.

Overall, the developments presented in this work not only provide a very efficient means of implementing the optimal speed schedules in an on-board FMS, but also extend the theory of aircraft performance to the more general minimum-cost case based on the cost index.

ACKNOWLEDGEMENTS

I would like to give very special thanks to my academic supervisor, Dr. Luis Rodrigues, for his invaluable teachings, guidance and support during the course of my research, without which this work would have not been possible. I would like also to extend my gratitude to Mitacs and TRU Simulation + Training (formerly Mechtronix) for providing financial support, and for giving me the opportunity to obtain much-valued work experience as an intern by applying the results of my work in a practical environment.

Thanks to all of my friends and peers at the Hybrid Control Systems (HYCONS) Laboratory: Azita, Javier, Julia, Manuel, Miad, Michael Di Perna, Michael El-Jiz, Qasim and Sina. Thank you all for your continued support, encouragement and for the good times that we spent together in the laboratory.

Last but not least, I would like to thank all of my family for their unconditional love and support. Special thanks to my uncle Jorge for his help and guidance both in my academic and personal life. Finally, I want to give very, very special thanks to my mother Carmen Elena for being the cornerstone of all that I have achieved so far. This work is for you.

Contents

List of Symbols	xii
List of Acronyms	xv
1 Introduction	1
1.1 Motivation	1
1.2 Flight Management System Description	2
1.3 Economy Mode and Cost Index	4
1.4 Objective	6
1.5 Literature Survey	7
1.5.1 Optimal Control	7
1.5.2 Flight Management Systems	8
1.5.3 Optimal Control Applied to Aircraft Trajectory Optimization	9
1.6 Methodology	11
1.7 Contributions	12
1.8 Structure of the Thesis	13
2 Theoretical Preliminaries	14
2.1 Aircraft Performance	14
2.1.1 The International Standard Atmosphere (ISA) Model	14
2.1.2 Aerodynamic Forces Acting on an Airplane	17

2.1.3	Equations of Motion in the Longitudinal Plane	19
2.1.4	Flight Envelope	22
2.1.5	Specific Fuel Consumption	24
2.1.6	Cruise Performance	25
2.1.7	Maximum Rate of Climb and Rate of Descent Speeds	27
2.2	Optimization and Optimal Control	29
2.2.1	Necessary and Sufficient Conditions for Optimality	29
2.2.2	Optimal Control Problem	31
2.2.3	Pontryagin's Maximum Principle	34
2.2.4	The Shooting Method	36
2.2.5	The Hamilton-Jacobi-Bellman Equation	39
2.2.6	Combining the Hamilton-Jacobi-Bellman Equation with the Maximum Principle	41
3	Optimal Solutions for Cruise	43
3.1	Assumptions	43
3.2	Maximum Endurance OCP	45
3.3	Economy Mode OCP for Cruise	50
3.3.1	Longitudinal Flight	50
3.3.2	Extension to Lateral Flight	56
3.4	Validation Results	62
3.4.1	Aircraft Model Used for the Simulations	62
3.4.2	Shooting Method for Cruise	63
3.4.3	Comparison between the optimal and sub-optimal trajectories	65
4	Optimal Solutions for Climb and Descent	68
4.1	Assumptions	68
4.2	Maximum Rate of Climb and Minimum Rate of Descent OCPs	70

4.2.1	Maximum Rate of Climb	70
4.2.2	Minimum Rate of Descent	75
4.3	Economy Mode OCP for Climb	79
4.4	Validation of Climb Results	88
4.4.1	Shooting Method for Climb	89
4.4.2	Comparison between the optimal and sub-optimal trajectories	90
4.5	Economy Mode OCP for Descent	94
4.6	Validation of Descent Results	103
4.6.1	Shooting Method for Descent	103
4.6.2	Comparison between the optimal and sub-optimal trajectories	105
4.7	Practical consideration: Estimation of the Top-of-Descent	109
5	Conclusions and Future Work	111
5.1	Conclusions	111
5.2	Extensions	113
A	Validation Code for the Cruise Phase	122
B	Validation Code for the Climb Phase	130
C	Validation Code for the Descent Phase	136

List of Figures

1.1	Block diagram of a Flight Management System.	2
1.2	Effect of CI on the longitudinal profile.	5
2.1	ISA variation of the temperature with respect to altitude.	15
2.2	Aerodynamic forces acting on a wing.	17
2.3	Coordinate systems for an aircraft flying in the longitudinal plane.	20
2.4	Forces acting on an aircraft flying in the longitudinal plane.	21
2.5	Sketch of a typical flight envelope.	24
2.6	Spring-damper system used for the shooting method example.	38
3.1	Aircraft flying in a horizontal plane.	57
3.2	Centripetal force in a coordinated turn.	59
3.3	Comparison between the optimal and sub-optimal cruise speeds for different cost indexes.	66
3.4	Costate J_W^* in cruise as a function of the range for different cost indexes.	66
4.1	Comparison between the optimal and sub-optimal climb speeds for different cost indexes.	91
4.2	Costate J_W^* in climb as a function of time for different cost indexes.	93
4.3	Climb vertical profile for different values of CI.	94
4.4	Comparison between the optimal and sub-optimal descent speeds for different cost indexes.	106

4.5	Costate J_W^* in descent as a function of time for different cost indexes.	107
4.6	Descent vertical profile for different values of CI.	108
4.7	Estimating the top-of-descent.	110
A.1	Simulink block diagram of the cruise 2PBVP.	128
A.2	Simulink block diagram of the sub-optimal cruise validation system.	128
B.1	Simulink block diagram of the climb 2PBVP.	133
B.2	Simulink block diagram of the sub-optimal climb validation system.	135
C.1	Simulink block diagram of the descent 2PBVP.	139
C.2	Simulink block diagram of the sub-optimal descent validation system.	141

List of Tables

- 2.1 Shooting method progression for the spring-damper system example. 39
- 3.1 Cruise fuel, time and cost comparison for different values of CI. 67
- 4.1 Climb fuel, time, range and cost comparison for different values of CI. 92
- 4.2 Descent fuel, time, range and cost comparison for different values of CI. 108

List of Symbols

a	Temperature lapse rate
α	Angle of attack
c	Wing chord length
C_D	Drag coefficient
$C_{D,0}$	Zero-lift (or parasitic) drag coefficient
$C_{D,2}$	Induced drag coefficient
C_I	Cost index
C_L	Lift coefficient
C_{L_0}	Zero-angle-of-attack lift coefficient
C_{L_α}	Stability derivative of the lift coefficient with respect to angle of attack
$C_{L_{max}}$	Maximum lift coefficient
C_{M_o}	Pitching moment coefficient
d_0	Parasitic component of the steady-flight drag function
d_1	Induced component of the steady-flight drag function
D	Drag force
f_f	Fuel flow rate
$f_{f_{cl}}$	Climb fuel flow rate
$f_{f_{cr}}$	Cruise fuel flow rate
f_{f_d}	Descent fuel flow rate
g	Gravitational constant

γ	Flight path angle
H	Hamiltonian
h	Density altitude
h_0	Density altitude of the initial waypoint
h_c	Cruise density altitude
h_f	Density altitude of the final waypoint
J	Cost functional/ cost-to-go
L	Lift force
M	Mach number
M_{MO}	Maximum operating Mach number
M_o	Pitching moment
p	Atmospheric pressure
p_1	Atmospheric pressure at the start of the troposphere layer
p_s	Standard sea-level pressure
ρ	Atmospheric density
ρ_1	Atmospheric density at the start of the troposphere layer
ρ_s	Standard sea-level density
R	Gas constant for air
R_e	Reynolds number
S	Wing planform area
\mathcal{S}	Target set
S_{FC}	Specific fuel consumption
θ	Heading angle
T	Thrust force
T_c	Maximum climb thrust force
T_i	Idle thrust force
T_{max}	Maximum thrust force

T_s	Maximum sea-level climb thrust force
\mathcal{T}	Atmospheric temperature
\mathcal{T}	Atmospheric temperature at the tropopause layer
\mathcal{T}_s	Standard sea-level temperature
u	Control vector
μ	Air viscosity, bank angle
v	True airspeed (TAS)
v_{cr}	Estimated cruise true airspeed
v_s	Stall speed
v_{vert}	Vertical speed (rate of climb, rate of descent)
v_w	Headwind speed
W	Aircraft gross weight
\widetilde{W}	Fuel consumed
x	Aircraft range or horizontal distance
x_0	Horizontal coordinate of the initial waypoint
x_c	Horizontal coordinate of the top-of-climb
x_d	Horizontal coordinate of the top-of-descent
x_f	Horizontal coordinate of the final waypoint
ζ	State vector

List of Acronyms

2PBVP	Two-point boundary value problem
ATC	Air Traffic Control
CDU	Control Display Unit
CI	Cost Index
ECON	Economy (mode)
FMS	Flight Management System
FPM	Flight Plan Management
TFP	Final Turn Point
HJB	Hamilton-Jacobi-Bellman
ISA	International Standard Atmosphere
ITP	Initial Turn Point
LRC	Long Range Cruise (mode)
OCP	Optimal Control Problem
ODE	Ordinary Differential Equation
PDE	Partial Differential Equation
ROC	Rate of Climb
RTA	Required Time of Arrival
SFC	Specific Fuel Consumption
SID	Standard Instrument Departure
STAR	Standard Terminal Arrival Route

TAS	True Airspeed
TC	Turn Center
TOC	Top-of-climb (waypoint)
TOD	Top-of-descent (waypoint)

Chapter 1

Introduction

1.1 Motivation

Carbon dioxide (CO₂) emissions in the world have increased steadily during the last two decades. According to the Netherlands Environmental Assessment Agency, China emitted 10300 million metric tons of CO₂ in 2013 making it the largest emitter in the world, followed by the United States at 5300 million metric tons [1]. The same report identifies international transport as the most significant factor in global carbon emissions, a fact that is supported by the U.S. Energy Information Administration [2], which states that the transportation sector is the largest contributor of CO₂ emissions in the country, emitting around 2400 million metric tons in 2013. In addition, recent research suggests that air traffic growth will outweigh the industry's efforts to reduce CO₂ emissions unless ticket prices begin to increase by at least 1.4% annually [3]. Furthermore, the decrease in oil prices by more than half in the end of 2014 is expected to have a negative impact on the environment in oil-importing countries, as investment in alternate technologies is discouraged and consumers use more gasoline and larger, less fuel efficient vehicles [4]. Taking all this information into account, the problem of minimizing fuel consumption in commercial flights becomes of utmost importance and could potentially reduce CO₂ emissions by a significant amount. In an aircraft, the task of optimizing its trajectory is carried out by the on-board flight management system.

1.2 Flight Management System Description

Flight Management Systems (FMS) are the master computers of an aircraft. Since their introduction in 1982, they have become a staple in every modern aircraft thanks to their capability of significantly reducing the workload of the crew. This is done by interfacing with all the navigation systems in order to produce the best possible measurements, providing the tools for an easy flight plan assembly, synthesizing optimal trajectories and even guiding the aircraft in order to follow those trajectories, amongst other things. All these functions are readily accessible to the pilot through a single control panel called the Control Display Unit (CDU) [5].

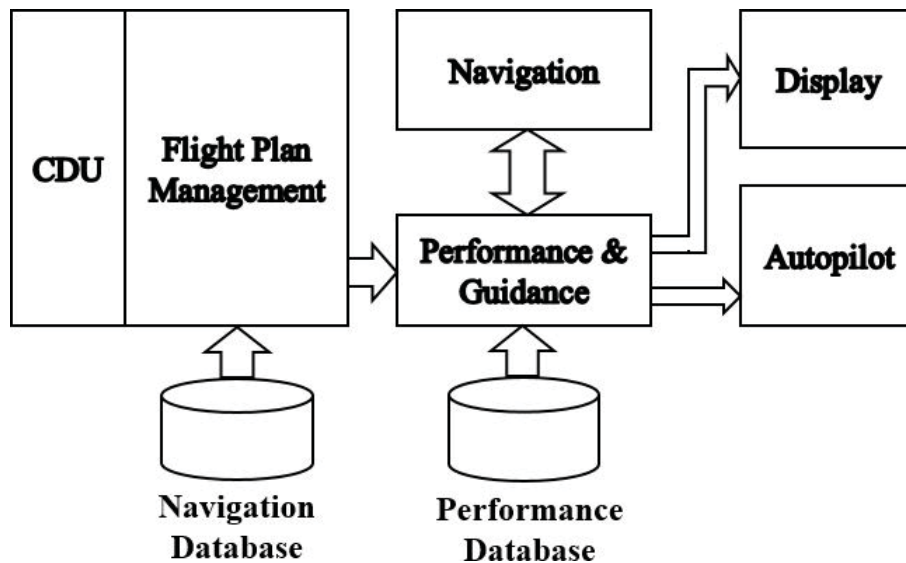


Figure 1.1: Block diagram of a Flight Management System.

A typical FMS consists of several subsystems as shown in Fig. 1.1 [6, 7]. A flight plan, comprised of a series of waypoints describing latitude/longitude pairs and possibly speed, time or altitude constraints (at or above, at or below, etc.), is put together by the Flight Plan Management (FPM) module. It communicates with an up-to-date Navigation Database containing a list of airports, their Standard Instrument Departure (SIDs) and Standard Terminal Arrival Route (STARs) procedures, waypoints, airways and navigation aids. The pilot inputs the desired flight plan and controls the FMS via the Control Display Unit (CDU).

The Navigation block determines the best estimate of the position and velocity of the aircraft as well as the wind velocity by merging the information from the Inertial Reference System (IRS), Global Positioning System (GPS) and other navigation systems using Kalman filtering techniques.

The Performance and Guidance module is the most relevant to this work. It is concerned with generating a trajectory that minimizes a given performance measure, such as the rate of climb (ROC), aircraft range and overall trip cost. The FMS assumes that the *longitudinal* (vertical) and lateral dynamics of the aircraft can be decoupled. The different *performance modes* available, named after the performance measure that they minimize, provide different optimal trajectories., such as [7]:

- **Economy (ECON) Mode:** Minimize total operating cost of the flight (all flight phases).
- **Required Time of Arrival (RTA):** Reach a waypoint at a specified time (all flight phases).
- **Long Range Cruise (LRC):** Yield the trajectory that gives 99% of fuel efficiency (cruise only).
- **Maximum Endurance:** Maximize the time that the aircraft can stay in the air with the current fuel reserves (cruise only).
- **Maximum Rate of Climb:** Minimize the time to reach cruise altitude (climb only).
- **Maximum Angle of Climb:** Maximize the climb angle (climb only).

The longitudinal trajectory is in the form of an optimal true airspeed command, thrust target, the top-of-climb (TOC) and top-of-descent (TOD) waypoints, with the cruising altitude being a fixed, crew-entered value determined by Air Traffic Control (ATC). After the optimization is carried out, the system predicts the estimated time of arrival, fuel remaining, speed and altitude at each waypoint. Since commercial aircraft fly in quasi-steady flight

conditions where accelerations are very small, the thrust is usually constrained to offset the effect of the aerodynamic forces or is set to pre-determined climb or descent rating. As a result, it can be computed in a straightforward manner once the speed is known, the latter becoming the most important parameter involved in the optimization.

In a typical FMS, the optimized speed schedules for the different modes are computed off-line and stored in the Performance Database, which also contains the data regarding the aerodynamic, propulsion and fuel consumption of the aircraft necessary to carry out performance predictions [6, 8]. The lateral path is generated based on the flight plan by the Guidance block according to a fixed set of rules, which is then shown in the Multi-function/Navigation Display. This module also sends pitch, thrust and steering commands to the autopilot to ensure that the aircraft follows the computed lateral and longitudinal trajectories. Other useful information, such as the desired track and cross-track error, is calculated and displayed as well.

It is important to note that the FMS is a reference generator: It computes set-points that are then furnished to a separate autopilot system whose task is to follow those targets using the aircraft's flight controls such as the elevator, ailerons and throttle. As a result, the FMS can be thought of as an outer control loop in the control system, and the dynamics of the aircraft associated with the speed and flight path angle can be neglected. Such dynamics then become the concern of the inner loop consisting of the autopilot and auto throttle.

1.3 Economy Mode and Cost Index

The main focus of this thesis is the Economy (ECON) Mode, which is also the default mode in a FMS and the most important. It is concerned with minimizing the *total operating cost* of the flight, expressed by the performance measure

$$\text{Total Operating Cost} = C_f \Delta f + C_t \Delta t,$$

where Δf is the total weight of fuel consumed, Δt is the trip time, C_f is the cost of fuel per unit of weight and C_t is the cost of the flight per unit time, comprising hourly maintenance costs, flight crew salaries, leasing costs, amongst others [9, 10]. If C_f is factored from the equation we get

$$\text{Total Operating Cost} = C_f \left(\Delta f + \frac{C_t}{C_f} \Delta t \right) = C_f (\Delta f + C_I \Delta t)$$

Since C_f is constant, the problem of minimizing the total operating cost is equivalent to minimizing the total cost in a *fuel-equivalent* form, expressed as follows:

$$\text{Total Fuel-Equivalent Operating Cost} = \Delta f + C_I \Delta t \quad (1.1)$$

Equation (1.1) computes the total operating cost in terms of a single parameter called the *Cost Index* (CI) C_I , which can be interpreted as the fuel-equivalent cost of time. A CI of zero corresponds to a small C_t or a large C_f , which is equivalent to minimizing fuel consumption disregarding time, while a maximum CI correspond to a large C_t which can be interpreted as minimizing the trip time regardless of the amount fuel consumed. Thus, being a convenient way of biasing the FMS between saving fuel or minimizing flight time, the ECON Mode finds the optimal trajectory that minimizes (1.1) for a given, crew-entered CI [11].

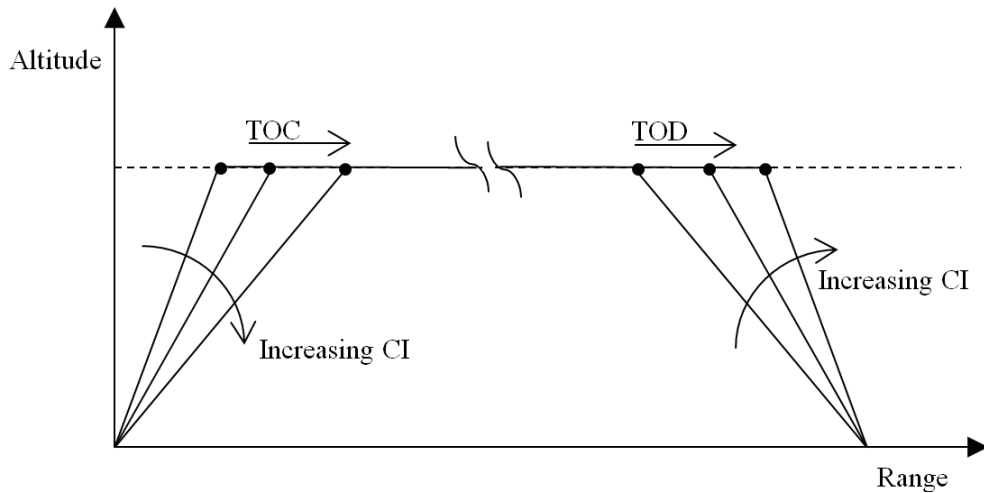


Figure 1.2: Effect of CI on the longitudinal profile.

The effects of CI on the longitudinal profile are well known. As depicted in Fig. 1.2, increasing CI during climb makes the climb angle shallower and pushes farther the TOC, while in descent the TOD starts later and the descent slope becomes steeper; during cruise at a constant altitude, a higher CI simply increases the true airspeed and the aircraft burns more fuel [9, 11, 12]. The opposite behaviors of the TOC and TOD might seem counter-intuitive at first, since the descent can be thought as a climb backwards in time, but the main difference between the two phases is the engine’s thrust setting: A high value known as the *maximum climb thrust* is used while climbing, whereas a low value known as the *idle thrust* is used while descending [13].

The CI’s units and range of allowable values vary depending on the FMS manufacturer and aircraft type. For example, Boeing defines the cost index in dollars per hour divided by cents per pound, as explained in [12]. In this work, it is assumed that CI is given in pounds per seconds (lb/s).

1.4 Objective

As explained in Section 1.2, current FMS contain a Performance Database that stores the optimal speed schedules for the aircraft in question, which are computed prior to the installation. The procedure used to generate this data is classified information. While storage space might not be an issue in today’s systems, employing performance tables to obtain the speed targets would often require interpolation between the sampling points, as opposed to implementing a real-time scheme in which the optimal references would be computed directly. In particular, analytic solutions require the least amount of storage space and computational time. To the best of the author’s knowledge, most of the open literature regarding trajectory optimization of aircraft either do not consider the performance modes present in a FMS, or propose algorithms that require off-line computations or are too taxing for an on-board, real-time implementation. As a result, finding an explicit, analytic feedback law for the speed schedules would not only supply a very efficient means of implementation in a FMS,

but would also provide an elegant theoretical contribution to the performance analysis of aircraft.

The objective of this thesis is to obtain *state-feedback* laws for the optimal true airspeeds that generate cost-optimal trajectories in terms of CI for the different phases of flight, preferably as explicit analytic solutions, suitable for implementation in a real FMS. Sub-optimal solutions are acceptable, provided that they are sufficiently close to the optimal and easily implementable. The Range, Endurance, Maximum Rate of Climb and Minimum Rate of Descent problems are also considered.

1.5 Literature Survey

1.5.1 Optimal Control

Optimal control theory is the branch of control systems that is concerned with finding the control inputs for a system that optimize a given performance measure [14]. After determining the state-space representation of the system and defining the performance measure, an Optimal Control Problem (OCP) is formulated and solved using different techniques. There exists two main approaches to solving OCPs: The maximum principle which is based on calculus of variations, and dynamic programming leading to the Hamilton-Jacobi-Bellman (HJB) equation, based on Bellman's principle of optimality. Nowadays, optimal control theory is well known and documented, and several books have been released on the matter, including [14–17].

The maximum principle was invented by Russian mathematician Lev Pontryagin et al. in 1956, and first published in English in reference [18]. This approach yields a Two-Point Boundary Value Problem (2PBVP) which can be solved analytically in some cases, but generally require using a computer. An important drawback of the maximum principle is that, since 2PBVPs specify some conditions at the initial time and others at the final time, the optimal trajectories and controls attained are usually described in an open-loop fashion,

that is, as a function of the time (or the independent variable used). Ideally, it would be preferable if the control inputs were given in a state-feedback form, as it would be valid for different initial conditions and it would account for deviations from the optimal trajectory due to potential disturbances.

In 1957, at around the same time when the maximum principle was proposed, dynamic programming was formulated by Richard Bellman and published in [19]. Based on the principle of optimality, this approach provides state-feedback targets but is more computationally intensive. It demands more storage capacity, as the state-space must be partitioned into a grid and processed every iteration to obtain the minimal cost-to-go [14]. Its continuous-time equivalent is the HJB equation which involves a nonlinear Partial Differential Equation (PDE) and a boundary condition that must be satisfied by the optimal cost. It has the same advantage as dynamic programming of providing a state-feedback control law, but obtaining an analytical solution to the HJB is usually very difficult, if not impossible, for most problems. Nevertheless, an important contribution regarding the solution of PDEs that has been applied to the HJB equation is the development of viscosity solutions, proposed by P. Lions et al. in [20] (viscosity solutions are not utilized in this work).

1.5.2 Flight Management Systems

The actual algorithms used in a real FMS to generate the performance database are classified information. However, there exists some publications by Boeing and Airbus that provide the intuition behind the speed schedules that are provided by the performance module of the FMS. For example, [10] is a thorough discussion on aircraft performance by Boeing including the different performance modes available for each phase of flight in detail, for which examples in the form of plots and charts are provided without specifying the methodology to obtain the speed targets. A series of articles published in Boeing Aero Magazine, cited in [11, 12, 21, 22], summarize the impact of different speed schedules on fuel and cost savings during takeoff, climb, cruise and descent, including the effect of the CI on the TOC and TOD. Similar

documents by Airbus include [9, 13].

In the open literature, Sam Lidén from Honeywell (a manufacturer of FMS) has been an important contributor on the topic. In [6] he presents the history of FMS and their evolution in time, while in [23] he discusses issues regarding the implementation of the RTA mode in FMS, which involves computing the CI that meets a time arrival constraint at a given waypoint. He has also published several patents, including [24] for a FMS that minimizes operating costs including the arrival error, and [25] for a method for computing optimum altitude steps considering the effect of winds.

Within Concordia University, a laboratory-based test bed for FMS is developed in [26] based on a commercial flight simulation software to obtain the aircraft aerodynamic data. A communication interface between this software and the FMS is developed, as well as a graphical user interface to operate the test bed.

1.5.3 Optimal Control Applied to Aircraft Trajectory Optimization

There has been several contributions in the open literature regarding the optimization of aircraft trajectories in FMS since the 1980's, most of which have been based on the theory of optimal control, involving the definition of an OCP and solving it using the techniques mentioned in section 1.5.1.

The maximum principle has been the most applied approach to the optimization of aircraft trajectories. Books such as [17, 27] apply this approach to the minimum fuel, minimum time, maximum-range and maximum rate-of-climb for aircraft problems. Some of the first algorithms for the generation of on-board minimum cost trajectories in FMS using an energy-state aircraft model, where it is assumed that energy increases monotonically during climb, stays constant during cruise and decreases monotonically during the descent, can be found in [28–31]. ATC constraints in these works are either neglected or incorporated in the form of step-climbs. Computing a CI that meets a time of arrival constraint at a certain waypoint,

which is the strategy used by FMS in the RTA mode, is discussed using the Maximum Principle in [32,33]. A more recent work discusses “next generation” FMS [34], assuming that the aircraft stays very close to the optimal trajectory allowing to linearize the model about the trajectory and to design a feedback autopilot. However, the cost functional discussed in section 1.3 for the Economy mode is not considered, with a quadratic cost functional being used instead.

Dynamic programming has also been considered in aerospace applications, in works such as [35], in which issues such as the size of the solution space and enforcing constraints are discussed. In [36] the Economy Mode is addressed and expanded by adding “at or before” and “at or after” time constraints, along with several improvements to reduce computation times. The generation of maximum-range trajectories during descent for commercial aircraft in engine-out situations using dynamic programming has been considered in [37]. Very recent publications include [38], in which minimum fuel trajectories are obtained for all flight phases while taking the wind profile into account and ATC constraints. Finally, the HJB equation has been applied to trajectory optimization of aerial vehicles, in works such as [39], where an explicit solution is attained for the minimum time trajectory of a glider in a competition, and [40], where a numerical method is developed to solve the HJB equation based on viscosity solutions.

Finally, as a result of the increased computational power for on-board flight management computers, other methods have emerged that do not rely on the classic optimal control theory. Instead, these methods rely on converting the OCP into a nonlinear program, such as [41], or a finite-dimensional optimization, as in [42], and solving the resulting problem using numerical algorithms or specialized solvers. In [43], a method is developed to obtain the performance bound of minimum time and minimum fuel descent trajectories, also considering the case of RTA, and the optimal trajectory is generated using a numerical method known as the Gauss pseudo-spectral method. Reference [44] considers the so-called inverse dynamics method to generate minimum-time trajectories, in which the OCP is transformed into a nonlinear

program and the optimal trajectory is parametrized using polynomials.

Even though the ECON problem has been treated extensively in the open literature, most of the contributions are centered around the previously mentioned approaches which resort to complicated numerical methods, and generally obtain time-dependent descriptions of the optimal trajectories which require a-priori offline computations. To the best of the authors' knowledge, there has been no attempt, at least in the open literature, to obtain explicit, analytic solutions to the ECON problem in a state-feedback form. As a result, the following methodology will be proposed to attain the objective of this work.

1.6 Methodology

The ECON mode will be formulated and solved as an OCP for each of the flight phases: climb, cruise and descent. The model of an aircraft flying in the longitudinal plane will be considered in state-space form, and assumptions will be made to simplify and make it more tractable for algebraic manipulations. To solve the OCP, both the Pontryagin's Maximum Principle and the Hamilton-Jacobi-Bellman equation will be used.

To validate the attained solutions, the Two-Point Boundary Value Problems (2PBVPs) derived from the Maximum Principle will be solved directly by the means of a shooting method in Matlab and Simulink. The shooting method is an iterative algorithm that solves 2PBVPs by reducing them to initial value problems. This method is not suitable for a real-time implementation, as it relies on integrating the governing equations of the 2PBVP problem each iteration which is generally time consuming, and it requires an initial estimate of the unknown initial conditions from practical experience or trial and error. However, the trajectories resulting from the shooting method can be considered as optimal, which are then compared to the ones generated by the proposed solutions. An aircraft model based on the Gulfstream Aerospace's G-IV aircraft is used for the simulations.

1.7 Contributions

The following results are obtained in this thesis:

- The well-known true airspeed targets for maximum rate of climb, minimum rate of descent, maximum range and maximum endurance are obtained by formulating each scenario as an OCP and solving it by applying classical optimal control techniques. From a theoretical point of view, this is the first time that these problems have been approached from this perspective.
- For the cruise phase of the flight, a sub-optimal analytic expression in state-feedback form is derived for the true airspeed in ECON mode. Moreover, when CI vanishes, the solution reduces to the maximum-range speed which is known to be equivalent to the minimum fuel per unit distance case. Simulation results show that the relative error between the optimal cost (obtained by solving the OCP directly using the shooting method) and the cost resulting from applying the analytic law is less than or equal to $1 \cdot 10^{-2}\%$ for the cases presented in this thesis, making the sub-optimal approach good enough for practical purposes. To the best of the author's knowledge, this is the first time that an algebraic expression has been proposed for the solution of this problem.
- For the climb and descent phases, a 5th degree polynomial in terms of the sub-optimal speed is obtained, its coefficients involving only the states of the aircraft. The roots of such polynomial can be found on-line by fast-converging algorithms such as Newton's method. The latter is arguably one of the simplest numerical methods available, making this approach suitable for implementation in a real-time FMS. As in the cruise phase, simulations show that, for the cases studied in this thesis, the relative error between the optimal and sub-optimal cost is less than $1 \cdot 10^{-3}\%$, and therefore the sub-optimal trajectory is close enough to the optimal one for practical purposes.

1.8 Structure of the Thesis

Chapter 2 starts by the Theoretical Preliminaries, covering the basic background material required for understanding the rest of the thesis. It is followed by Chapter 3, which formulates and solves the OCPs for Maximum Endurance and ECON during the cruise phase. For the latter, a sub-optimal analytic expression for the optimal speed is found, which is compared to the solution obtained by the shooting method at the end of the chapter. Next, Chapter 4 applies the same treatment to the climb and descent phases, addressing the Maximum Rate of Climb, Minimum Rate of Descent and ECON problems. A polynomial is found, one of its roots being the sub-optimal speed target, which is also compared to the shooting method solution following the same approach as in the cruise. Lastly, Chapter 5 draws the main conclusions of this thesis and provides extensions for future work.

Chapter 2

Theoretical Preliminaries

2.1 Aircraft Performance

The material covered in this section is based on [5, 45–48].

2.1.1 The International Standard Atmosphere (ISA) Model

Aircraft fly in the Earth’s atmosphere and, as a result, the latter has great influence on the aerodynamic and propulsion properties of the airplane. The main variables that must be considered in the atmosphere are the density ρ , viscosity μ and pressure p , all of which can be considered as depending on the air temperature \mathcal{T} . The real atmosphere is constantly changing, so there does not exist a “normal” atmosphere, but the International Standard Atmosphere (ISA) has been defined as a baseline to obtain standardized conditions from which analyses can be made. A day whose conditions match the ones in the ISA model is called a *standard day*.

The ISA assumes that the gravitational constant g is equal to its value at sea level and defines the variation of \mathcal{T} with altitude h based on empirical data. As shown in Fig. 2.1, the ISA divides the atmosphere in three layers: The *troposphere* from sea level to 36150 ft. where \mathcal{T} decreases linearly, one section of the *stratosphere* called the *tropopause* from 36150

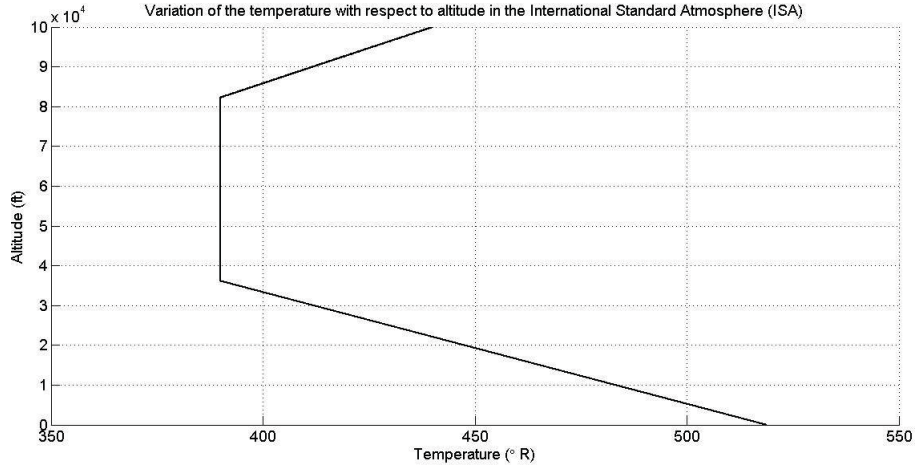


Figure 2.1: ISA variation of the temperature with respect to altitude.

ft. to 82300 ft. where \mathcal{T} remains constant, and the last region from 82300 ft. until 154000 ft. where \mathcal{T} increases linearly.

Let

$$\mathcal{T}_s = 518.69 \text{ }^\circ\text{R}$$

$$p_s = 2116.2 \text{ lb/ft}^2$$

$$\rho_s = 0.002377 \text{ slug/ft}^3,$$

be the standard sea-level temperature, pressure and density, respectively. From the ISA definition of temperature, the equation of state of a perfect gas and the hydrostatic equation, it can be shown that in the troposphere the following expressions are valid:

$$\mathcal{T} = \mathcal{T}_s + ah \tag{2.1a}$$

$$p = p_s \left(\frac{\mathcal{T}}{\mathcal{T}_s} \right)^{-\frac{g}{aR}} \tag{2.1b}$$

$$\rho = \rho_s \left(\frac{\mathcal{T}}{\mathcal{T}_s} \right)^{-\left(\frac{g}{aR}+1\right)}, \tag{2.1c}$$

where

$$a = -0.00356 \text{ }^\circ\text{R/ft}$$

$$g = 32.17 \text{ ft/s}^2$$

$$R = 1718 \text{ lb ft slug}^{-1} \text{ }^\circ\text{R}^{-1}$$

are the temperature lapse rate, gravitational constant and gas constant for air, respectively.

Similarly, for the tropopause layer, let

$$h_1 = 36150 \text{ ft}$$

$$\mathcal{T}_1 = 389.99 \text{ }^\circ\text{R}$$

$$p_1 = 472.2 \text{ lb/ft}^2$$

$$\rho_1 = 7.0539 \cdot 10^{-4} \text{ slug/ft}^3,$$

be the altitude, temperature, pressure and density at the point where the tropopause starts, then the temperature remains constant, and the pressure and density are given by:

$$p = p_1 e^{-\frac{g(h-1)}{RT}} \quad (2.2a)$$

$$\rho = \rho_1 e^{-\frac{g(h-1)}{RT}} \quad (2.2b)$$

Commercial aircraft never fly in the highest region of the stratosphere, therefore the equations for that layer will not be covered here. The main factor that influences aerodynamic forces is the density, making (2.1c) and (2.2b) the most important expressions for performance analysis.

The ISA model is general enough to allow predicting the atmospheric conditions even in a non-standard day. This is achieved by the means of the *density altitude*, which is the altitude above sea level in a standard day at which the standard density would be equal to the actual density experienced by the aircraft. In colloquial terms, it is the altitude that

the aircraft “feels” in the ISA. Strictly speaking, the variable h used throughout this work must correspond to the density altitude to account for *ISA deviations*. Then, if the density altitude is known, parameters such as the density and pressure can be computed using the formulas presented in this section. The density altitude can be computed in real aircraft from the *pressure altitude* read by the altimeter and the outside air temperature, and performance charts for determining its value are usually available to pilots [5]. The exact procedure to obtain density altitude is beyond the scope of this work and will not be discussed further.

2.1.2 Aerodynamic Forces Acting on an Airplane

The aerodynamic forces are a consequence of the movement of a body immersed in a fluid; they are caused by the pressure and shear stress exerted by the fluid on the body’s exposed surfaces. For an aircraft flying in the longitudinal plane, the fluid is the air present in the atmosphere and the main bodies that generate aerodynamic forces are the wings, the fuselage and the nacelles. Such forces are the *lift* which is perpendicular to the free-stream velocity, and the *drag* which is parallel to it. These components, along with the *pitching moment* about a point where the forces are considered to act on the airfoil of the wing (normally the quarter-chord point), will completely describe the physical effects on the body due to aerodynamics, as shown in Fig. 2.2.

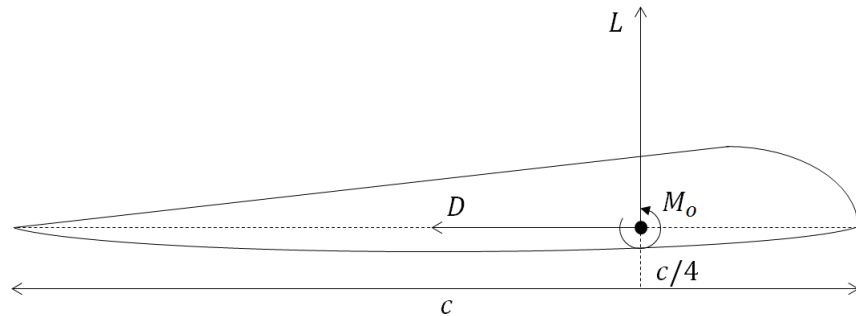


Figure 2.2: Aerodynamic forces acting on a wing.

It is standard practice in this area of expertise to describe the aerodynamic forces in terms of *coefficients*, in such a way that two aircraft of identical geometric shape but different sizes

exposed to the same flow conditions yield the exact same coefficient values, a fact that propelled the creation of wind tunnels. The lift, drag and pitching moment are therefore given by

$$L = \frac{1}{2}C_L(\alpha, R_e, M)\rho S v^2 \quad (2.3a)$$

$$D = \frac{1}{2}C_D(\alpha, R_e, M)\rho S v^2 \quad (2.3b)$$

$$M_o = \frac{1}{2}C_{M_o}(\alpha, R_e, M)\rho S c v^2, \quad (2.3c)$$

where it can be seen that the coefficients are assumed to depend on the angle of attack α , Reynolds number R_e and the Mach number M . The nature of these dependencies vary according to the shape of the airfoil. There exists an underlying assumption: commercial aircraft fly in a *quasi-steady* regime, meaning that accelerations and moments are very small, and that the control surfaces deflect slowly and in small increases. As a result, it can be assumed that control surface deflections do not effect aerodynamic forces. There are more general models that account for these dependencies, but for performance analysis of commercial aircraft, the equations presented here provide sufficient precision.

A functional relationship often used for the lift in aircraft performance is given by

$$C_L = C_{L_0}(M) + C_{L_\alpha}(M)\alpha,$$

where C_{L_0} and C_{L_α} are known aircraft-dependent functions. This expression is considered valid until the lift coefficient reaches a known maximum value $C_{L_{max}}$, after which the approximately-linear relationship between C_L and α is broken and C_L drops rapidly. If this situation is reached, it is said that the aircraft has *stalled*, and we can compute the corresponding *stall speed* by using $C_{L_{max}}$ and (2.3a) to obtain:

$$v_s = \sqrt{\frac{2W}{\rho S C_{L_{max}}}} \quad (2.4)$$

In (2.4) we have assumed that the lift equals the aircraft gross weight, an approximation that is commonly used for commercial aircraft flying in quasi-steady conditions. It will allow us to compute C_L using the weight, resulting in a required angle of attack such that the lift coefficient equation is satisfied.

The drag is expressed as a function of the lift coefficient as follows:

$$C_D = C_{D,0} + C_{D,2}C_L^2 \quad (2.5)$$

This well-known equation is called the *drag polar*. Generally speaking, the coefficients $C_{D,0}$ and $C_{D,2}$ should depend on the Mach number, specially in transonic and supersonic flight where shockwaves form around the wings, greatly increasing the drag. For most commercial aircraft (which fly at a Mach number of less than 0.8), they can be assumed constant.

There exists well-known expressions to model the pitching moment coefficient C_{M_0} . However, this work involves commercial aircraft flying in quasi-steady conditions where the rotational dynamics of the aircraft can be neglected. As a result, the pitching moment coefficient is not relevant to our discussion and will not be covered here.

2.1.3 Equations of Motion in the Longitudinal Plane

It is assumed that the Earth is flat and an inertial reference frame. As shown in Fig. 2.3, the following coordinate systems are defined:

- The Earth coordinate system $x_e y_e z_e$, attached to the surface of the Earth at sea level with \hat{y}_e pointing into the plane, such that the $x_e z_e$ plane becomes the longitudinal plane in which the aircraft flies.
- The horizon coordinate system $x_h y_h z_h$, whose origin is located at the center of gravity of the aircraft and its axes stand parallel to the Earth axes.
- The body axes system $x_b y_b z_b$, which is attached to the airplane at its center of gravity,

such that \hat{x}_b points along the nose of the aircraft and the $y_w z_w$ plane is its plane of symmetry (see Fig. 2.3).

- The wind axes system $x_w y_w z_w$, which moves with the airplane with the origin at its center of gravity, and \hat{x}_w is in the same direction as the velocity vector v . It is tilted relative to the horizon system by the *flight path angle* γ , and the body axes are tilted with respect to the wind axes by the *angle of attack* α .

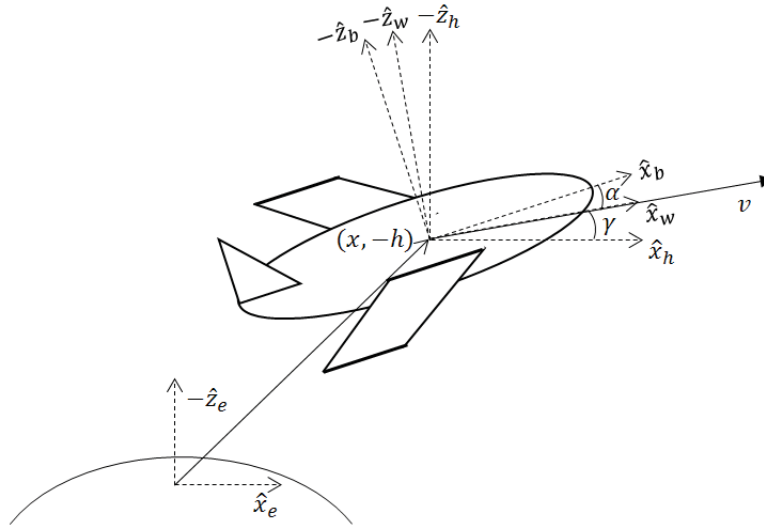


Figure 2.3: Coordinate systems for an aircraft flying in the longitudinal plane.

In the equations of motion derived below, the kinematic equations describe the position $(x, -h)$ of the aircraft with respect to the Earth coordinate system (note that \hat{z}_e points towards the center of the Earth). Newton's equations state that the sum of the forces shown in Fig. 2.4 equal the time rate of change of linear momentum, and are written on the wind axes system. Based on these considerations, it can be shown that the so-called wind axes

state-space model of an aircraft flying in the longitudinal plane is given by

$$\begin{aligned}
 \dot{x} &= v \cos \gamma \\
 \dot{h} &= v \sin \gamma \\
 \dot{v} &= \left(\frac{g}{W} \right) (T \cos \alpha - D - W \sin \gamma) \\
 \dot{\gamma} &= \left(\frac{g}{Wv} \right) (T \sin \alpha + L - W \cos \gamma) \\
 \dot{W} &= -S_{FC}(h, v, T)T,
 \end{aligned} \tag{2.6}$$

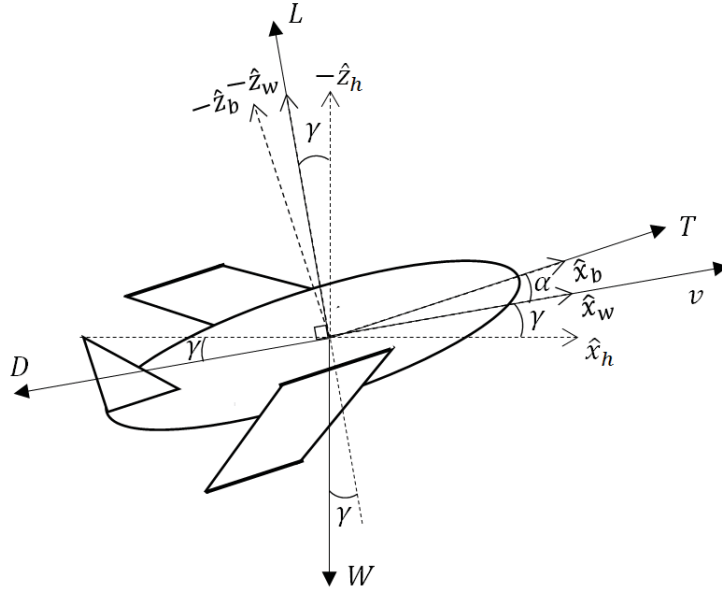


Figure 2.4: Forces acting on an aircraft flying in the longitudinal plane.

where the control inputs are the angle of attack α and the engine thrust T , and L and D are given by (2.3a) and (2.3b), respectively. The Specific Fuel Consumption (SFC), S_{FC} , is explained briefly in Section 2.1.5. This model neglects rotational dynamics. However, as explained in Section 2.1.2, commercial aircraft fly in quasi-steady conditions, and therefore we can assume that moments are negligible.

2.1.4 Flight Envelope

In Section 2.1.2 the stall speed, given by (2.4), was introduced. The stall speed becomes a lower bound on the valid range of True Airspeeds (TAS) that the aircraft may fly at, for a given value of altitude and weight. It makes sense to ask then if there exists an upper bound on the TAS as well, and in which region of space can the aircraft sustain steady, level flight. Such region is called the *flight envelope*, and is usually given by a curve plotted in the speed-altitude plane consisting of the locus of maximum and minimum velocities, for a particular weight.

An upper and lower bound on the TAS can be estimated as a consequence of the engine limitations and drag characteristics of the airplane: Assume that the aircraft flies in steady, level-flight. In (2.6), the derivatives of v and γ become zero, as well as $\dot{\gamma}$. If we let $T \sin(\alpha) \ll W$ and assume $T \cos(\alpha) \approx T$, then the neglected dynamics yield the following balance of forces:

$$L = W \tag{2.7}$$

$$T = D \tag{2.8}$$

Equations (2.7) and (2.8) are frequently used in the performance analysis of aircraft during cruise. When in level flight, the amount of thrust needed to equal the drag as in (2.8) is called the *thrust required*. Let the engine thrust T be constrained to a given range

$$T_i \leq T \leq T_{max}(h), \tag{2.9}$$

where the idle thrust T_i and maximum thrust T_{max} are known for a particular engine. In fact, the latter is normally a decreasing function of h in turbojet and turbofan engines, and is specified in tabular or graphical form. Then, combining the expression for the drag (2.3b)

and (2.8), we get:

$$T = \frac{1}{2}C_D\rho S v^2$$

Substituting the drag coefficient (2.5) gives

$$T = \frac{1}{2} (C_{D,0} + C_{D,2}C_L^2) \rho S v^2,$$

which, after solving for C_L in (2.3a) and accounting for (2.7), becomes:

$$T = \frac{C_{D,0}\rho S v^2}{2} + \frac{2C_{D,2}W^2}{\rho S v^2} \quad (2.10)$$

When $T = T_{max}(h)$, solving for v in (2.10) will yield the maximum and minimum velocities for which the thrust can equal drag and level flight can be sustained, for each value of altitude and weight. Normally, it is expected that solving (2.10) will yield two positive values for v , the maximum and the minimum, until an altitude where the maximum thrust has decreased to the point where both bounds coincide into a single, positive value. When that case happens, we have reached the maximum altitude or *absolute ceiling* at which level flight can be attained, with a rate of climb (ROC) equal to zero.

Generally speaking, it is expected that the stall speed v_s is of larger magnitude than the minimum v obtained using (2.10) for most altitudes. Moreover, in order to protect the structural integrity of the airplane, real aircraft are also constrained to operate below a maximum Mach number M_{MO} and *service ceiling* h_{max} (defined as the height at which $ROC < 100$ feet-per-minute). An accurate depiction of the flight envelope should therefore account for these structural constraints as well as the stall speed and maximum speed due to the thrust required limitation. A not to-scale drawing illustrating the shape of a typical flight envelope is shown in Fig. 2.5.

To summarize, the flight envelope of the aircraft will yield constraints in its states and

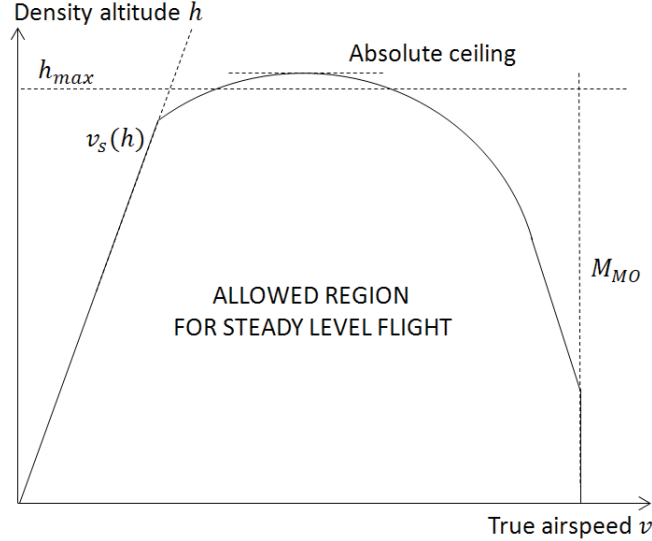


Figure 2.5: Sketch of a typical flight envelope.

control variables of the form:

$$\begin{aligned}
 h &\leq h_{max} \\
 v_{min}(h, W) &\leq v \leq v_{max}(h, W) \\
 T_i &\leq T \leq T_{max}(h)
 \end{aligned}
 \tag{2.11}$$

One should also consider that the weight must be less or equal than a specified maximum take-off weight.

2.1.5 Specific Fuel Consumption

The *thrust specific fuel consumption*, or simply Specific Fuel Consumption (SFC), is defined for turbojet and turbofan engines as the weight of fuel burned per unit of thrust per unit of time, so it can be thought of as a measure of how efficient the engine is at generating thrust with respect to the amount of fuel consumed. From the weight dynamics in (2.6), we see that

$$f_f = -\dot{W} = S_{FC}(h, v, T)T, \tag{2.12}$$

where f is called the fuel flow rate, and is the weight of fuel burned per unit of time. Solving

for S_{FC} yields

$$S_{FC} = \frac{f_f}{T}, \quad (2.13)$$

therefore the units of the SFC is [1/time]. It is accustomed to use hours as the unit of time when specifying the SFC. For propeller and reciprocating engines, the SFC is defined in terms of the engine shaft power instead of thrust. However, it is possible to convert the SFC for a propeller-driven/reciprocating engine to an *equivalent* thrust specific fuel consumption and vice versa. The reader should consult [46] for more details. As a result, we will consider (2.13) as a general expression for SFC that encompasses all engine types.

Generally speaking, SFC is considered as a function of thrust, speed and altitude (to be specific, it depends on the density, but the latter depends on height in the ISA model), and may vary drastically from one engine to another. In the performance analysis literature, simpler models are used where SFC may be constant, altitude-dependent or a function of both altitude and Mach number. This work will consider SFC to be a given function of h

$$S_{FC} = S_{FC}(h), \quad (2.14)$$

where its dependency can be linear, quadratic or any other model that fits the data. Its nature does not affect the results obtained in this thesis.

2.1.6 Cruise Performance

Maximum Range Speed

The range of an aircraft is defined as the total ground distance it can travel for a given amount of fuel. To obtain the maximum range of an aircraft, one seeks to maximize its *fuel mileage* or *specific range*, a measure of the distance traversed per unit weight of fuel. The specific range is given by the ground speed (which we assume is equal to TAS due to the

absence of wind) divided by the fuel flow rate, that is

$$r_s \equiv \frac{v}{f_f},$$

which, after substituting f_f using (2.12), becomes:

$$r_s = \frac{v}{S_{FC}T} \quad (2.15)$$

Note that (2.15) is in units of distance divided by fuel weight, as desired. Integrating r_s with respect to the weight from the initial gross weight W_0 to the zero fuel weight W_1 would then yield the range:

$$\text{Range} = \int_{W_1}^{W_0} r_s dW$$

There exists several approaches in the literature to estimate the range; we are interested, however, in obtaining the maximum range speed, which as explained previously is the one that maximizes (2.15). It can be shown that for jet-driven aircraft, under steady flight conditions where (2.7) and (2.8) hold, the maximum range speed can be computed as follows [46]:

$$v_{range} = \left(\frac{2W}{\rho S} \sqrt{\frac{3C_{D,2}}{C_{D,0}}} \right)^{1/2} \quad (2.16)$$

It must be emphasized once more that (2.16) is the groundspeed for maximum range, which equals TAS under zero-wind conditions only. In addition, it is well-known that this solution yields the best fuel economy: given a certain distance to cover, flying at (2.16) ensures that the amount of fuel consumed per unit distance is minimized. This fact will be remarked in Chapter 3 as a way to verify the ECON speed, which must match the minimum fuel case when CI is zero.

Maximum Endurance Speed

Endurance is defined as the amount of time an aircraft can fly with a given amount of fuel. It is different from the concept of range in the sense that time is now the variable of interest, not distance, and as a result endurance is more important in surveillance missions or when executing holding patterns, where the aircraft's autonomy is more important. The fuel flow rate f_f as defined in (2.12) plays the same role as the specific range in the case of endurance, since minimizing it with respect to v yields the speed at which endurance is maximized. Similar to the range, integrating the fuel flow rate with respect to the weight yields the endurance.

As in the previous section it can be shown that, for jet-powered aircraft under steady flight conditions, the speed for maximum endurance is given by the expression (see [46])

$$v_{endurance} = \left(\frac{2W}{\rho S} \sqrt{\frac{C_{D,2}}{C_{D,0}}} \right)^{1/2}, \quad (2.17)$$

which is the same value that minimizes the drag. It is tempting but incorrect to think that maximizing endurance implies maximum fuel economy, since maximizing the time that the aircraft can fly does not imply that it will reach its destination in a fuel-efficient manner. Therefore, flying at the maximum range speed (2.16) will result in minimal fuel consumption for the flight.

2.1.7 Maximum Rate of Climb and Rate of Descent Speeds

For an aircraft climbing (resp. descending) in quasi-steady flight conditions, the rate of climb (resp. rate of descent) is defined as the vertical speed of the aircraft, given by

$$v_{vert} = \frac{v(T - D)}{W}, \quad (2.18)$$

where

$$T = \begin{cases} T_c & : \gamma > 0 \quad (\text{during climb}) \\ T_i & : \gamma < 0 \quad (\text{during descent}) \end{cases}.$$

In the previous expression T_c is the maximum climb thrust or thrust available, while T_i is the idle thrust value. We assume that both are independent of v . To maximize v_{vert} during climb (resp. minimize during the descent), (2.18) is differentiated with respect to v and equated to zero, known as the necessary condition of optimality (explained in section 2.2.1). For steady flight conditions, the drag is given by [45]

$$D(h, v, W) = d_0(h)v^2 + \frac{d_1(h, W)}{v^2},$$

where

$$\begin{aligned} d_0 &= \frac{1}{2}C_{D,0}\rho S \\ d_1 &= \frac{2C_{D,2}W^2}{\rho S}. \end{aligned}$$

As a result, from differentiating (2.18) and setting it to zero, we get

$$T - D - vD_v = 0,$$

in which we substitute the expression for the drag yielding

$$3d_0v^4 - Tv^2 - d_1 = 0.$$

This expression can be solved for v^2 , which is given by

$$v^2 = \frac{T \pm \sqrt{T^2 + 12d_0d_1}}{6d_0},$$

or, after replacing d_0 and d_1 and taking the positive sign:

$$v^2 = \frac{T + \sqrt{T^2 + 12C_{D,0}C_{D,2}W^2}}{3C_{D,0}\rho S} \quad (2.19)$$

Expression (2.19) computes the speed for the maximum rate of climb when $T = T_c$, and similarly for the minimum rate of descent when $T = T_i$.

2.2 Optimization and Optimal Control

The material in this section is based on [14, 17, 27, 49–51].

2.2.1 Necessary and Sufficient Conditions for Optimality

The necessary and sufficient conditions for solving a point-wise, finite-dimensional optimization problem will be reviewed. Suppose that we want to minimize a given function $H : \mathbb{R}^n \times \mathbb{R}^m \rightarrow \mathbb{R}$, that is

$$\min_u H(x, u),$$

with respect to the decision variables or *control vector* u , which is of the form:

$$u = [u_1 \cdots u_m]^T$$

Assuming that there are no constraints on u and that the first and second partial derivatives of H exist everywhere, then the necessary conditions for a minimum are [49]:

$$\frac{\partial H}{\partial u} \Big|_{u^*} = 0 \quad (2.20a)$$

$$\frac{\partial^2 H}{\partial u^2} \Big|_{u^*} \geq 0 \quad (2.20b)$$

Points u^* that satisfy these conditions are called *stationary points*. Note that, since u is a vector, condition (2.20a) implies that each component of the gradient $\partial H / \partial u_i, i = 1, \dots, m$

must vanish, and condition (2.20b) reads that the Hessian matrix $\partial^2 H / \partial u^2$ must be positive semidefinite.

The *sufficient condition for optimality* is given by [49]

$$\frac{\partial^2 H}{\partial u^2} \Big|_{u^*} > 0 \tag{2.21}$$

For maximization problems, it can be shown that the sign in (2.21) must be negative. If (2.21) is satisfied, then u^* minimizes H . Note that (2.20b) and (2.21) differ only in the greater or equal sign and, as a result, it is common practice to prove only (2.20a) and (2.21) when solving optimization problems.

Note that H is a function of two variables: x and u . Often one wants to optimize a multi-variable function with respect to only one of the variables, such as u . Such is the case here, where the other variables are treated as constants and partial derivatives are used in the necessary and sufficient conditions.

Condition (2.21) implies that the Hessian with respect to u of H must be positive definite. A useful method for determining the positive definiteness of a matrix is by the means of *Sylvester's criterion*, which states that a symmetric matrix A is positive definite if and only if its *leading principal minors* are all positive. The k th leading principal minor of a matrix is defined as the determinant of its upper-left k -by- k matrix. As a result, to test the positive definiteness of A , we compute the determinant of each k -by- k submatrix, including A itself. All of these determinants must be positive for A to be positive definite.

For example, if we have a symmetric 2-by-2 matrix

$$A = \begin{bmatrix} a & b \\ b & d \end{bmatrix},$$

then the following expressions must be satisfied:

$$\begin{aligned} a &> 0 \\ ad - b^2 &> 0 \\ d &> 0 \end{aligned}$$

This work will use the necessary and sufficient conditions presented in this section to minimize a function called the Hamiltonian with respect to u , where the latter is subject to *strict* inequality constraints. It is important to note that the existence of these constraints does not invalidate the conditions presented here. For instance, suppose that u is constrained to lie inside a set Ω , described by the vector g composed of p strict inequality constraints

$$\Omega = \{u : g(u) < 0\},$$

then u^* must satisfy (2.20a), (2.21) and $g_i(u^*) < 0, i = 1, \dots, p$. That is, u^* must lie in the interior of Ω , where the constraints g are not effective and can the problem can be treated as an unconstrained one. Optimization of functions subject to less-or-equal or equality constraints is not carried out in this thesis and therefore will not be covered in the theoretical preliminaries.

2.2.2 Optimal Control Problem

An Optimal Control Problem (OCP) differs from a point-wise, finite-dimensional optimization problem in two fundamental components: the existence of a dynamic system and the performance measure.

A dynamic system could be a physical body (such as an aircraft) or any process whose outputs vary *dynamically* as the inputs are applied. Such process needs a mathematical description that accurately describes its response with respect to the control inputs. A well-

known mathematical representation of dynamic systems is the *state space representation*, in which the system is characterized by a set of *state variables*

$$\zeta_1(t), \dots, \zeta_n(t),$$

and the *control inputs*

$$u_1(t), \dots, u_m(t),$$

which are a function of time just like the states. Then, the relationship between the state variables and control inputs is given by the set of Ordinary Differential Equations (ODEs)

$$\begin{aligned} \dot{\zeta}_1(t) &= f_1(\zeta_1(t), \dots, \zeta_n(t), u_1(t), \dots, u_m(t), t) \\ \dot{\zeta}_2(t) &= f_2(\zeta_1(t), \dots, \zeta_n(t), u_1(t), \dots, u_m(t), t) \\ &\vdots \\ \dot{\zeta}_n(t) &= f_n(\zeta_1(t), \dots, \zeta_n(t), u_1(t), \dots, u_m(t), t), \end{aligned}$$

or, in more compact form:

$$\dot{\zeta}(t) = f(\zeta(t), u(t), t) \tag{2.22}$$

In (2.22), we denote $\zeta = [\zeta_1 \cdots \zeta_n]^T$ as the state vector, $u = [u_1 \cdots u_m]^T$ as the control vector and $f = [f_1 \cdots f_n]^T$ as the dynamic function, which is generally nonlinear and time-varying. The state space representation is widely used in control systems and provides a universal framework for the analysis of dynamic systems. Section 2.1.3 will present a model of an aircraft in state space form, which will be used in this work.

The performance measure, or *cost functional*, mathematically defines the criterion that will be used to quantitatively assess the performance of the system. A *functional* is a real-valued function that takes arguments from a space of functions, effectively making it a “func-

tion of a function”. In optimal control, cost functionals of the form

$$J(\zeta(t_0), u(t_0), t_0) = \int_{t_0}^{t_f} L(\zeta(t), u(t), t) dt + \phi(\zeta(t_f), t_f) \quad (2.23)$$

are used, in which t_0 and t_f are the initial and final time, respectively, and ϕ and L are scalar functions. For any initial state $\zeta(t_0)$ and control function $u(t)$ the state is driven by (2.22) for $t \in [t_0, t_f]$, and the cost functional (2.23) assigns a real number to the resulting state and control history. Then, J gives us a quantitative measure of the performance of the system for that particular control input. Simple examples of cost functionals include those used in minimum time problems

$$J = \int_{t_0}^{t_f} dt = t_f - t_0,$$

and quadratic cost functionals that minimize the energy spent by the control signal

$$J = \int_{t_0}^{t_f} u^T(t) R u(t) dt$$

Having defined its main components, an OCP is formulated as follows: find the optimal control function $u^*(t)$ that minimizes the cost functional (2.23), where the optimal state trajectory $\zeta^*(t)$ is generated by the system dynamics (2.22) evaluated for $u^*(t)$. The optimization is also subject to initial and final conditions on the state, and constraints on ζ and u are described as a set of *admissible* states \mathcal{Z} and control inputs \mathcal{U} , respectively. Mathematically, we write:

$$J^*(t_0) := \inf_{u(t)} \left\{ \int_{t_0}^{t_f} L(\zeta(t), u(t), t) dt + \phi(\zeta(t_f), t_f) \right\}$$

s.t.

$$\dot{\zeta}(t) = f(\zeta(t), u(t), t) \quad (2.24)$$

$$\zeta(t) \in \mathcal{Z}, \quad u(t) \in \mathcal{U}$$

$$\zeta(t_0) = \zeta_0$$

$$\psi(\zeta(t_f), t_f) = 0$$

Note that, while the initial condition ζ_0 and the initial time t_0 are considered as given, the final condition $\zeta(t_f)$ and the final time t_f *do not* have to be specified. In (2.24) we have written that the final state and time must satisfy equality constraints $\psi(t_f, \zeta(t_f)) = 0$. This encompasses the case where final conditions are given as well. In other words, we want $(t_f, \zeta(t_f))$ to belong to a *target set*:

$$\mathcal{S} = \{(\zeta(t_f), t_f) : \psi(\zeta(t_f), t_f) = 0\} \quad (2.25)$$

The final time t_f is then defined as the smallest time such that $(t_f, \zeta(t_f))$ enters \mathcal{S} . The different types of OCPs are then represented by the choice of \mathcal{S} . For instance, a fixed-time, free-endpoint problem has a target set of the form $\mathcal{S} = t_1 \times \mathbb{R}^n$, with t_1 known. It is important to consider that \mathcal{S} must be a closed set for t_f to be well defined.

The two main approaches used for solving OCPs, the Maximum Principle and Dynamic Programming, will be the subject of the following subsections.

2.2.3 Pontryagin's Maximum Principle

The Maximum Principle is a technique that provides necessary conditions that must be met by a minimizing control $u(t)$. Assume an OCP of the form (2.24) with unspecified terminal time t_f . Then, the system dynamics (2.22) and the final state constraints are adjoined to the cost functional (2.23) yielding

$$\begin{aligned} \bar{J} = & \int_{t_0}^{t_f} \left[L(\zeta(t), u(t), t) + \lambda^T(t) \left(f(\zeta(t), u(t), t) - \dot{\zeta}(t) \right) \right] dt \\ & + \phi(\zeta(t_f), t_f) + \nu^T \psi(\zeta(t_f), t_f), \end{aligned}$$

with $\lambda(t)$ being n time-varying *Lagrange multipliers* or *costates*, and ν being also lagrange multipliers of the same dimension as ψ . Define the *Hamiltonian* as:

$$H(\zeta(t), u(t), \lambda(t), t) = L(\zeta(t), u(t), t) + \lambda^T(t) f(\zeta(t), u(t), t) \quad (2.26)$$

It follows from calculus of variations that the necessary conditions for obtaining an optimal J^* are [17]:

$$\dot{\zeta} = f(\zeta, u, t) \quad (2.27)$$

$$\dot{\lambda} = - \left(\frac{\partial H}{\partial \zeta} \right)^T \quad (2.28)$$

$$\frac{\partial H}{\partial u} = 0 \quad (2.29)$$

$$\lambda(t_f) = \left(\frac{\partial \phi}{\partial \zeta} + \nu^T \frac{\partial \psi}{\partial \zeta} \right) |_{t_f} \quad (2.30)$$

$$\left(\frac{\partial \phi}{\partial t} + \nu^T \frac{\partial \psi}{\partial t} + H \right) |_{t_f} = 0 \quad (2.31)$$

$$\psi(\zeta(t_f), t_f) = 0 \quad (2.32)$$

Equations (2.27) and (2.32) are re-statements of the system dynamics and the final state constraints, respectively. On the other hand, (2.28) and (2.30) have effectively augmented the system by providing additional dynamics and boundary conditions for the costates, while u must be a stationary point of H as stated in (2.29). Equation (2.31) results from the fact that the final time is not prescribed. In summary, the resulting problem is called a *two-point boundary value problem* (2PBVP) because the boundary conditions for the state are given at the initial time ζ_0 , while the ones for the costates λ_f are given at the final time via (2.30).

The approach presented in this section is the most frequently used in the literature when dealing with OCPs. However, its main disadvantage is that the optimal control policy is specified as a function of the costates, which must be obtained by integrating (2.28) backwards in time subject to their boundary conditions. As a result, the control input is obtained as a function of time. The 2PBVP can be solved numerically using the celebrated shooting method, which will be explained briefly in the next section.

2.2.4 The Shooting Method

The shooting method is a numerical technique to solve 2PBVPs, such as the ones formulated using the maximum principle, by reducing it to an initial value problem. Suppose we have a system described by n first order ODEs with some boundary conditions given at the initial time and others given at the final time, that is:

$$\begin{aligned}\dot{\zeta}(t) &= f(\zeta(t), t), \quad t \in [t_0, t_f] \\ \zeta_i(t_0), \quad &i = 1, \dots, q \quad \text{specified} \\ \zeta_j(t_f), \quad &j = q, \dots, n \quad \text{specified}\end{aligned}$$

Normally, if $\zeta_i(t_0)$ were specified $\forall i = 1, \dots, n$, the trajectory $\zeta(t)$ would easily be generated by integrating the state equation with the help of a computer. The main idea behind the shooting method is to guess an initial condition for the states ζ_j , integrate the ODEs to obtain the corresponding trajectory, then guess a new (and hopefully more accurate) initial condition based on the error between the values of ζ_j at t_f and their prescribed ones. The algorithm would stop when the error in the final conditions are small enough, or when the difference between consecutive values of the initial conditions (also known as seeds) becomes negligible.

Letting $\zeta^{(k)}(t)$ denote the state trajectory at the k^{th} iteration, the following pseudo-code is an example of a generic shooting algorithm:

1. Choose initial seeds $\zeta_j^{(0)}(t_0)$
2. Let $k = 0$
3. Do:
 - (a) Simulate the system by integrating the equations forward
 - (b) $\epsilon_j = \zeta_j^{(k)}(t_f) - \zeta_j(t_f)$

- (c) Compute next seed $\zeta_j^{(k+1)}(t_0)$ as a function of $\zeta_l^{(k)}(t_0)$, ϵ_l and $l = q, \dots, n$, using a given update law
 - (d) $k = k + 1$
4. Until $\sum_{j=q}^n |\epsilon_j| < \text{tolerance}$ OR $k \geq \text{Max. Iterations}$

The 2PBVPs resulting from the Maximum Principle fit into the framework of the shooting method: in this case, the dynamics of the costates J_ζ^* are appended to the ones of the original state variables ζ to form an “augmented” system in which some boundary conditions will be prescribed at the initial time, and others at the final time. The optimal control input u is obtained at every time-step by solving for it using the necessary condition of optimality (2.29) (which could have an algebraic solution or be a transcendental equation; the way it is solved would depend on the problem). As a result, the methodology discussed in this section applies to the Maximum Principle, making the shooting method an attractive approach to numerically solving OCPs.

It is important to note that the system’s governing equations must be integrated until the final time each iteration, which could be a time consuming process especially for complex systems. In addition, it requires selecting $\zeta_j^{(0)}(t_0)$ from practical experience or trial and error. Thus, even though it can yield precise numerical solutions to 2PBVPs, it is not suitable for a real-time system implementation. However, it can be used to validate sub-optimal solutions to OCPs off-line, as is the case in this thesis.

The main challenges when implementing the shooting algorithm include selecting the initial seed for the states $\zeta_j(t_0)$, specifically if they do not have an obvious physical meaning, and choosing an appropriate update law for the subsequent guesses. A generally accepted expression for an update law is [27]

$$\zeta_j^{(k+1)}(t_0) = \zeta_j^{(k)}(t_0) - \sum_{l=q}^n \beta_l \left(\zeta_l^{(k)}(t_f) - \zeta_l(t_f) \right) \quad (2.33)$$

where β_l are tuning parameters. This work will use update laws of such type. To illustrate

the shooting method, consider the spring-damper system in Fig. 2.6 where $m = 4$ lb is the body's mass, $k = 16$ lb/s² is the spring constant and $c = 4.8$ lb/s. This system is described by the state-space model

$$\begin{bmatrix} \dot{\zeta}_1(t) \\ \dot{\zeta}_2(t) \end{bmatrix} = \begin{bmatrix} 0 & 1 \\ -\omega_n^2 & -2\xi\omega_n \end{bmatrix} \begin{bmatrix} \zeta_1(t) \\ \zeta_2(t) \end{bmatrix}, \quad (2.34)$$

where the damping coefficient ξ and the natural frequency ω_n are given by

$$\xi = \frac{c}{2\sqrt{km}} = 0.3$$

$$\omega_n = \sqrt{\frac{k}{m}} = 2 \text{ rad/s.}$$

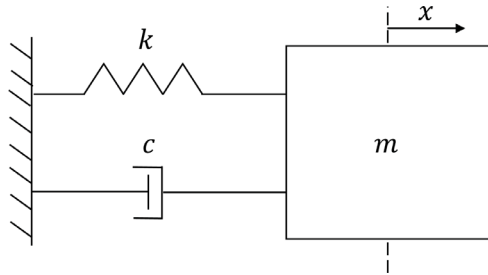


Figure 2.6: Spring-damper system used for the shooting method example.

In (2.34), ζ_1 is horizontal position of the body while ζ_2 is its speed. Suppose that we want to find an initial position $\zeta_1(0)$ such that the body reaches $\zeta_1(t_f) = 0$ with speed $\zeta_2(t_f) = -0.35$ ft/s (equivalent to 10.6 cm/s) within $t_f = 4$ s. The left sign implies that the direction of the velocity is towards the left. We assume that the body is released with no initial speed, that is $\zeta_2(0) = 0$. Putting everything together we have the following initial and final conditions

$$\zeta_1(0) \quad \text{unspecified,} \quad \zeta_1(t_f) = 0$$

$$\zeta_2(0) = 0, \quad \zeta_2(t_f) = -0.35.$$

The shooting method will be used to obtain $\zeta_1(0)$. It follows the algorithm specified above, where the update law for $\zeta_1^{(k+1)}(0)$ is based on (2.33) and is given by

$$\zeta_1^{(k+1)}(0) = \zeta_1^{(k)}(0) - \beta_1 \left(\zeta_1^{(k)}(t_f) - \zeta_1(t_f) \right) - \beta_2 \left(\zeta_2^{(k)}(t_f) - \zeta_2(t_f) \right),$$

where $\beta_1 = 1$ and $\beta_2 = -0.8$ s, which were tuned using trial and error. The stopping tolerance was set to 0.1. Table 2.1 shows the progression of $\zeta_1^{(k)}(0)$ and the sum of the errors ϵ throughout the algorithm, which was executed in Matlab. The initial seed was set to $\zeta_1^{(0)}(0) = 2.5$ ft. It can be concluded that the algorithm converged in 5 iterations, and the desired initial condition was found to be $\zeta_1(0) = 1.87$ ft. For this initial condition, the corresponding final conditions were $\zeta_1(t_f) = 0.08$ ft and $\zeta_2(t_f) = -0.35$ ft/s, which are close enough to the desired values.

Table 2.1: Shooting method progression for the spring-damper system example.

Iteration (k)	$\zeta_1^{(k)}(0)$ in ft	Error (ϵ)
1	2.5	0.23
2	2.29	0.18
3	2.12	0.15
4	1.98	0.11
5	1.87	0.09

2.2.5 The Hamilton-Jacobi-Bellman Equation

The Hamilton-Jacobi-Bellman (HJB) equation results from the application of Bellman’s Principle of Optimality using a dynamic programming approach. Such principle states that:

“An optimal policy has the property that whatever the initial state and initial decision are, the remaining decisions must constitute an optimal policy with regard to the state resulting from the first decision” [52].

The principle of optimality allows us to derive optimal control inputs in a *state-feedback law*: given an initial state ζ_1 , the optimal control is determined solely by the cost from that

state until the final state ζ_f . Based on the cost functional (2.23), define the *cost-to-go* as:

$$J(\zeta(t), u(t), t) = \int_t^{t_f} L(\zeta(t), u(t), t) dt + \phi(\zeta(t_f), t_f) \quad (2.35)$$

For a given initial state and time $(\zeta(t), t)$, and control input $u(t), t \in [t, t_f]$, equation (2.35) returns the cost to be incurred from that given point until the final time, using the prescribed control history. The additive property of the *optimal* cost-to-go allows splitting it as follows, for some time increment Δt :

$$J^*(\zeta(t), t) = \inf_{u(\tau), t \leq \tau \leq t + \Delta t} \left\{ \int_t^{t + \Delta t} L(\zeta(\tau), u(\tau), \tau) d\tau + J^*(\zeta(t + \Delta t), t + \Delta t) \right\} \quad (2.36)$$

In (2.36) the superscript * denotes that the cost-to-go is optimal. It can be shown that, by letting Δt converge to zero and using Taylor series, (2.36) yields a partial differential equation that must be satisfied by the optimal cost-to-go, given by

$$0 = J_t^*(\zeta(t), t) + \min_{u(t)} H(\zeta(t), u(t), J_\zeta^*(\zeta(t), t), t), \quad (2.37)$$

with

$$H(\zeta(t), u(t), J_\zeta^*(\zeta(t), t), t) = L(\zeta(t), u(t), t) + J_\zeta^* \dot{\zeta}, \quad (2.38)$$

and boundary condition:

$$J^*(\zeta(t_f), t_f) = \phi(\zeta(t_f), t_f) \quad \text{s.t.} \quad (\zeta(t_f), t_f) \in \mathcal{S} \quad (2.39)$$

Equation (2.37) is the celebrated HJB equation, , with H being the Hamiltonian. A subscript as in J_t^* denotes the partial derivative of J^* with respect to t , and similarly for the rest of the variables. Note that the boundary condition (2.39) is satisfied only in the target set, which is given by (2.25). If an optimal u^* that minimizes H is found using the

necessary and sufficient conditions stated in section 2.2.2, then it is guaranteed that such function minimizes J .

2.2.6 Combining the Hamilton-Jacobi-Bellman Equation with the Maximum Principle

The Maximum Principle can be used in conjunction with the HJB equation to solve a given OCP. Both approaches are connected by the means of the Hamiltonian. Comparing H in (2.37) with (2.26), it can be shown that, as expected, the partial derivatives of the optimal cost-to-go J_ζ^* correspond to the costates that appear in the Maximum Principle, that is

$$J_\zeta^*(t) = \lambda^T(t). \quad (2.40)$$

As a result of (2.40), equations (2.28), (2.30) and (2.31) can be used to obtain information regarding the time evolution and the final values of the partial derivatives of the optimal cost. Thus, when solving OCPs analytically a combination of the Maximum Principle and the HJB equation provides the best insight regarding the optimal solution. In subsequent developments, (2.26), (2.28) and (2.30) will be written as follows:

$$H(\zeta(t), u(t), J_\zeta^*(t), t) = L(\zeta(t), u(t), t) + J_\zeta^*(t)f(\zeta(t), u(t), t) \quad (2.41)$$

$$j_\zeta^* = - \left(\frac{\partial H}{\partial \zeta} \right)^T \quad (2.42)$$

$$J_\zeta^*(t_f) = \left(\frac{\partial \phi}{\partial \zeta} + \nu^T \frac{\partial \psi}{\partial \zeta} \right) \Big|_{t_f} \quad (2.43)$$

An important result that greatly simplifies the analysis of OCPs using the HJB equation is that, if the Hamiltonian (2.38) is *not* an explicit function of time (i.e. $\partial H / \partial t = 0$) and the final time t_f is free, then H must vanish along the optimal trajectory, implying that $J_t^* = 0$

and the HJB equation reduces to [14]

$$0 = \min_{u(t)} H(\zeta(t), u(t), J_{\zeta}^*(\zeta(t), t)) \quad (2.44)$$

As explained previously, the main advantage of the HJB equation is that it yields an optimal control function in state-feedback form. However, solving this equation analytically is extremely difficult. Nevertheless, there exist OCPs of practical interest, such as some of the problems presented in this thesis, for which the HJB can be solved. The result is an algebraic solution for the state-feedback controller, which is arguably the most desirable type of solution for implementation purposes.

Chapter 3

Optimal Solutions for Cruise

3.1 Assumptions

Section 2.1.3 presented the equations of motion of an aircraft flying in the longitudinal plane. In order to make (2.6) more tractable for performance computations, some assumptions must be made based on the quasi-steady flight conditions in which modern commercial aircraft fly. Such tractability is important if one wants to find an analytical solution to the resulting OCP; otherwise, the mathematical expressions involved would be too complicated to manipulate algebraically.

The assumptions made for the cruise segment of the flight are the following:

- The aircraft flies at a given, constant altitude constrained by Air Traffic Control (ATC) as is the case with real FMS. This assumption makes γ , $\dot{\gamma}$ and \dot{h} equal to zero.
- The altitude, speed and thrust values lie in the interior of the flight envelope given by the constraints (2.11). As a result, we do not need to enforce them in the mathematical formulation of the OCP.
- The angle of attack α is small, allowing to write $\cos \alpha \approx 1$ and $\sin \alpha \approx \alpha$. This assumption is standard practice in performance analysis for commercial aircraft.

- The component of the thrust perpendicular to the velocity vector, $T\alpha$, is much smaller than L and W . The thrust force is usually around one order of magnitude smaller than the weight, therefore multiplying it by a small angle will effectively make it negligible.
- Accelerations are negligible due to the steady-flight condition, and as a result we can assume that \dot{v} is approximately zero. Moreover, as explained previously in Section 1.2, the FMS is not charged with reaching the optimal setpoints using the aircraft's flight controls, so we can take v as a control signal, leaving its dynamics to the autopilot.

In light of these assumptions, the simplified aircraft model for steady level flight in the longitudinal plane is obtained as

$$\begin{aligned}\dot{x} &= v \\ \dot{W} &= -S_{FC}D\end{aligned}\tag{3.1}$$

$$L = W\tag{3.2}$$

$$T = D\tag{3.3}$$

The last two equations come from \dot{v} and $\dot{\gamma}$ being equal to zero, using the assumptions mentioned above (including $T\alpha \ll W$). Note that they allow computing the required control inputs to follow a given aircraft configuration in steady level flight. On one hand, (3.2) effectively constrains the angle of attack to a value such that the lift balances the weight at any given altitude and airspeed. On the other hand, (3.3) states that the *thrust required* to sustain steady level flight will always be equal to the drag, implying that the thrust setpoint provided by the FMS is easily computed during cruise provided that the optimal TAS is found.

From (2.3a) and (3.2) we can solve for the lift coefficient as follows:

$$\begin{aligned} L = W &= \frac{1}{2}C_L\rho S v^2 \\ C_L &= \frac{2W}{\rho S v^2} \end{aligned} \quad (3.4)$$

Substituting (3.4) into the drag coefficient (2.5) yields

$$C_D = C_{D,0} + C_{D,2} \left(\frac{2W}{\rho S v^2} \right)^2,$$

which is then used in conjunction with (2.3b) to obtain the equation for the drag in quasi-steady flight regime

$$D = \frac{1}{2}C_{D,0}\rho S v^2 + \frac{2C_{D,2}W^2}{\rho S v^2} \quad (3.5)$$

Note that under the assumptions made, the drag becomes a function of h (indirectly through the density ρ), v and W . In subsequent developments (3.5) will be written as a function of TAS as follows:

$$D(h, v, W) = d_0(h)v^2 + \frac{d_1(h, W)}{v^2} \quad (3.6)$$

Obviously, the coefficients d_0 and d_1 are given by:

$$\begin{aligned} d_0 &= \frac{1}{2}C_{D,0}\rho S \\ d_1 &= \frac{2C_{D,2}W^2}{\rho S} \end{aligned} \quad (3.7)$$

3.2 Maximum Endurance OCP

To illustrate the usefulness of formulating optimization problems involving dynamic systems in the framework of the optimal control theory, this section will present a simple problem: obtaining the TAS that maximizes the endurance of the aircraft during cruise.

Suppose that the aircraft weight W_c at TOC is given, and that W_d is the final weight at which descent can be safely carried out in a given mission. The maximum endurance problem seeks to maximize the amount of time that the aircraft can stay in the air, that is, it maximizes the functional

$$J = \int_{t_c}^{t_d} dt,$$

where the final time t_d has to be free for the problem to make sense. Since no final value for the range $x(t_d)$ is prescribed, the \dot{x} equation in (3.1) becomes irrelevant, reducing the dynamics to a 1st order system. As a result, the OCP formulation is given by:

$$\begin{aligned} J^* &= \max_{v(t), t_d} \int_{t_c}^{t_d} dt \\ \text{s.t.} & \\ \dot{W} &= -S_{FC}D \\ W(t_c) &= W_c, W(t_d) = W_d \end{aligned} \tag{3.8}$$

The following theorem states the solution to OCP (3.8).

Theorem 3.2.1. *The optimal solution to OCP (3.8) is given by*

$$v^2 = \frac{2W}{\rho S} \sqrt{\frac{C_{D,2}}{C_{D,0}}}, \tag{3.9}$$

and the optimal cost-to-go J^* is

$$J^* = \frac{1}{2S_{FC}\sqrt{C_{D,0}C_{D,2}}} \log\left(\frac{W}{W_d}\right). \tag{3.10}$$

Proof. We begin by writing the Hamiltonian as shown in (2.41)

$$H = 1 - J_W^* S_{FC}D, \tag{3.11}$$

which, in accordance with both the Maximum Principle and the HJB equation approach, must be maximized with respect to $v(t)$ (because this is a maximization problem). The necessary condition explained in Section 2.2.1 is used

$$\frac{\partial H}{\partial v} = -J_W^* S_{FC} D_v = 0$$

In the above equation, D_v denotes the partial derivative of the drag with respect to the speed. It follows that either J_W^* , D_v or both must vanish for every t . However, from the sufficient condition for optimality, we get

$$\frac{\partial^2 H}{\partial v^2} = -J_W^* S_{FC} D_{vv} < 0,$$

implying

$$J_W^* > 0, \tag{3.12}$$

since S_{FC} is positive and D is convex with respect to the speed. As a result, the necessary condition becomes

$$D_v = 0 \tag{3.13}$$

Using (3.6) as the expression for the drag, condition (3.13) can be used to solve for the optimal v :

$$2d_0v - \frac{2d_1}{v^3} = 0 \rightarrow v^4 = \frac{d1}{d0}$$

Considering (3.7), the speed for maximum endurance is obtained as

$$v^2 = \frac{2W}{\rho S} \sqrt{\frac{C_{D,2}}{C_{D,0}}},$$

which is equal to (3.9) and coincides with (2.17) as presented in Section 2.1.6. In this case, the value of this approach is that it allows obtaining an expression for the optimal cost-to-go, which must satisfy the HJB equation (2.37). Since H does not depend explicitly on time and

t_d is free, then from (2.44) we get that the HJB equation

$$0 = J_t^*(\zeta(t), t) + \min_{v(t)} H(\zeta(t), v(t), J_\zeta^*(\zeta(t), t), t),$$

reduces to

$$\min_{v(t)} H(\zeta(t), v(t), J_\zeta^*(\zeta(t), t), t) = \min_{v(t)} \{1 - J_W^* S_{FC} D\} = 0 \quad (3.14)$$

that is, the Hamiltonian must vanish along the optimal trajectory. The boundary condition for the cost-to-go is obtained by applying (2.39) to this problem, that is:

$$J^*(t_d) = 0 \quad \text{s.t.} \quad W(t_d) = W_d \quad (3.15)$$

Moreover, using (2.42) from the Maximum Principle, we obtain an equation for the time derivative of J_W^* , given by

$$\begin{aligned} \dot{J}_W^* &= -\frac{\partial H}{\partial W} = J_W^* S_{FC} D_W \\ &= J_W^* S_{FC} \frac{4C_{D,2}W}{\rho S v^2}, \end{aligned} \quad (3.16)$$

where (3.5) was used for the drag. From (3.14) evaluated at the optimal v , we can solve for J_W^*

$$J_W^* = \frac{1}{S_{FC} D},$$

where the drag must be evaluated at the optimal v . Substituting (3.9) into (3.5) yields

$$D = 2W \sqrt{C_{D,0} C_{D,2}} \quad (3.17)$$

When (3.17) is replaced into J_W^* we get

$$J_W^* = \frac{1}{2W S_{FC} \sqrt{C_{D,0} C_{D,2}}} \quad (3.18)$$

To prove that J_W^* satisfies (3.16), the time derivative of (3.18) is taken using the state equation for \dot{W} and (3.17) for D to obtain

$$\frac{d}{dt} \left(\frac{1}{2WS_{FC}\sqrt{C_{D,0}C_{D,2}}} \right) = -\frac{2S_{FC}\sqrt{C_{D,0}C_{D,2}}\dot{W}}{(2WS_{FC}\sqrt{C_{D,0}C_{D,2}})^2} = \frac{S_{FC}D}{2W^2S_{FC}\sqrt{C_{D,0}C_{D,2}}},$$

which, after considering (3.18) and (3.17) becomes

$$\frac{S_{FC}D}{2W^2S_{FC}\sqrt{C_{D,0}C_{D,2}}} = \frac{S_{FC}D}{W} J_W^* = 2S_{FC}\sqrt{C_{D,0}C_{D,2}} J_W^*.$$

This is the same expression as (3.16) with v^2 substituted by (3.9). The obtained J_W^* also satisfies (3.12), the sufficient condition to maximize the Hamiltonian. The optimal cost-to-go is therefore obtained by integrating (3.18) with respect to W :

$$J^* = \frac{1}{2S_{FC}\sqrt{C_{D,0}C_{D,2}}} \int \frac{1}{W} dW = \frac{\log(W)}{2S_{FC}\sqrt{C_{D,0}C_{D,2}}} + C$$

The constant C is determined by the boundary condition (3.15), which must be satisfied by J^* :

$$J^*(W_d, t_d) = \frac{\log(W_d)}{2S_{FC}\sqrt{C_{D,0}C_{D,2}}} + C = 0 \rightarrow C = -\frac{\log(W_d)}{2S_{FC}\sqrt{C_{D,0}C_{D,2}}}$$

As a result, the optimal cost function is

$$J^* = \frac{1}{2S_{FC}\sqrt{C_{D,0}C_{D,2}}} \log \left(\frac{W}{W_d} \right).$$

□

By adopting an analytic approach to solving OCPs, it was possible to solve the maximum endurance problem for an aircraft in cruising flight, recovering the well-known result for the maximum endurance speed presented in Section 2.1.6, and also obtaining the expression for the optimal cost-to-go (3.10). It seems reasonable then to apply the same set of tools to the ECON problem in order to solve for the most economical speed target in terms of CI. Such

is the purpose of the next section.

3.3 Economy Mode OCP for Cruise

Section 3.3.1 will derive and solve the ECON mode OCP for cruise in longitudinal flight, followed by section 3.3.2 which shows that the approach can be extended to handle turns in the lateral plane.

3.3.1 Longitudinal Flight

Problem Formulation

The ECON mode for cruise will now be formulated as an OCP with a structure as in (2.24). As explained in Section 1.3, its purpose is to minimize the total operating cost of the flight, given by (1.1). This performance measure can be rewritten as a cost functional in integral form as

$$J = \int_{t_c}^{t_d} (f_f + C_I) dt$$

Here, t_d is the unspecified time at which the TOD is reached, and t_c is the time at which the cruise phase begins. The fuel flow rate f_f , defined in (2.12), becomes

$$f_f = S_{FC}D,$$

after (3.3) is taken into account. When f_f is substituted into the cost functional, we get

$$J = \int_{t_c}^{t_d} (S_{FC}D + C_I) dt \tag{3.19}$$

The ECON OCP during cruise can now be stated as follows:

$$J^* = \min_{v(t), t_d} \int_{t_c}^{t_d} (S_{FC}D + C_I) dt$$

s.t.

$$\dot{x} = v(t) \tag{3.20}$$

$$\dot{W} = -S_{FC}D$$

$$x(t_c) = x_c, \quad x(t_d) = x_d$$

$$W(t_c) = W_c$$

Optimal solution

The following result gives the solution to this problem.

Theorem 3.3.1. *The optimal solution to the economy mode OCP stated in (3.20) is given*

by

$$v = \sqrt{\frac{C_I + \sqrt{C_I^2 + 12(1 - J_W^*)^2 S_{FC}^2 C_{D,0} C_{D,2} W^2}}{(1 - J_W^*) S_{FC} C_{D,0} \rho S}}, \tag{3.21}$$

where the time derivative of J_W^ is given by*

$$\dot{J}_W^* = (J_W^* - 1) \frac{4S_{FC} C_{D,2} W}{\rho S v^2}, \tag{3.22}$$

with final condition

$$J_W^*(t_d) = 0. \tag{3.23}$$

Proof. To solve (3.20), the Hamiltonian

$$\begin{aligned}
H(\zeta(t), v(t), J_\zeta^*(\zeta(t), t), t) &= L + J_\zeta^* \dot{\zeta} \\
&= S_{FC}D + C_I + J_x^* v - J_W^* S_{FC}D \\
&= (1 - J_W^*) S_{FC}D + J_x^* v + C_I
\end{aligned} \tag{3.24}$$

must be minimized with respect to $v(t)$ (because this is a minimization problem), implying that the necessary condition for optimality must be satisfied:

$$\frac{\partial H}{\partial v} = (1 - J_W^*) S_{FC}D_v + J_x^* = 0,$$

which allows solving for J_x^* yielding

$$J_x^* = -(1 - J_W^*) S_{FC}D_v. \tag{3.25}$$

From the sufficient condition for a minimum, we get

$$\frac{\partial^2 H}{\partial v^2} = (1 - J_W^*) S_{FC}D_{vv} < 0,$$

which is equivalent to

$$(1 - J_W^*) > 0,$$

resulting in

$$J_W^* < 1,$$

because S_{FC} is a positive quantity independent of v , and the curvature of the drag as a function of the speed is positive. Next, note that the Hamiltonian (3.24) is not an explicit function of time, and that t_d is unspecified. As a result, the HJB equation

$$0 = J_t^*(\zeta(t), t) + \min_{v(t)} H(\zeta(t), v(t), J_\zeta^*(\zeta(t), t), t),$$

reduces to

$$\min_{v(t)} H(\zeta(t), v(t), J_\zeta^*(\zeta(t), t), t) = 0, \quad (3.26)$$

that is, $J_t^* = 0$. We substitute (3.24) into (3.26) to obtain

$$\min_v \{(1 - J_W^*)S_{FC}D + J_x^*v + C_I\} = 0,$$

or, at the optimal speed

$$(1 - J_W^*)S_{FC}D + J_x^*v + C_I = 0.$$

After replacing J_x^* from the necessary condition (3.25) and the drag from (3.6), we obtain the following polynomial in terms of v :

$$(1 - J_W^*)S_{FC}D - (1 - J_W^*)S_{FC}vD_v + C_I = 0 \quad (3.27)$$

$$\equiv (1 - J_W^*)S_{FC}d_0v^4 - C_Iv^2 - 3(1 - J_W^*)S_{FC}d_1 = 0 \quad (3.28)$$

This biquadratic equation can be solved easily by letting $z = v^2$, leading to

$$(1 - J_W^*)S_{FC}d_0z^2 - C_Iz - 3(1 - J_W^*)S_{FC}d_1 = 0,$$

whose solution can be found by the formula

$$z = \frac{C_I + \sqrt{C_I^2 + 12(1 - J_W^*)^2S_{FC}^2d_0d_1}}{2(1 - J_W^*)S_{FC}d_0}.$$

Since $C_I^2 + 12(1 - J_W^*)^2S_{FC}^2d_0d_1 > C_I^2$, and C_I can only take positive values, it is true that $\sqrt{C_I^2 + 12(1 - J_W^*)^2S_{FC}^2d_0d_1} > C_I$. Therefore the solution with the negative sign is eliminated as it would yield a complex solution for z . To express it in terms of more physically

meaningful quantities, the expressions for d_0 and d_1 are substituted using (3.7) to obtain

$$v^2 = \frac{C_I + \sqrt{C_I^2 + 12(1 - J_W^*)^2 S_{FC}^2 C_{D,0} C_{D,2} W^2}}{(1 - J_W^*) S_{FC} C_{D,0} \rho S}.$$

This equation computes the TAS that minimizes the operating costs of the cruise phase analytically as a function of W , C_I , ρ and J_W^* . Note that J_x^* does not appear in this equation (a predictable result since the initial and final conditions of x are fixed), making J_W^* the only unknown in (3.21). Using the costate equation (2.42) and the Hamiltonian (3.24) allows studying the time derivative of J_W^* . We get

$$\dot{J}_W^* = -\frac{\partial H}{\partial W} = (J_W^* - 1) \frac{4S_{FC} C_{D,2} W}{\rho S v^2}$$

Considering the general form of an OCP in (2.24), there is no terminal cost making the terminal cost function $\phi = 0$ and, since $x(t_d)$ is the only prescribed final condition, the terminal constraint function $\psi = x - x_d$. Then the final value of J_W^* is given by (2.43) as follows:

$$J_W^*(t_d) = \left(\frac{\partial \phi}{\partial W} + \nu \frac{\partial \psi}{\partial W} \right) \Big|_{t_d} = 0$$

□

Remark: When $C_I = 0$, the solution sought is the airspeed for minimum fuel per unit distance, which is known to coincide with the maximum range solution [17]. This is indeed the case if C_I vanishes in (3.21), yielding

$$v = \sqrt{\frac{2W}{\rho S} \sqrt{3 \frac{C_{D,2}}{C_{D,0}}}}, \quad (3.29)$$

which is identical to the maximum range speed presented in equation (2.16) of the theoretical preliminaries.

Deriving a sub-optimal control law

Considering that J_W^* must be less than one as specified in (3.3.1), we will now proceed to make the assumption that \dot{J}_W^* is negligible, allowing to approximate J_W^* by its final value, zero, as per (3.23). This assumption implies that either the product $S_{FC}C_{D,2}W$ is small or that $\rho S v^2$ is large in (3.22). S_{FC} and $C_{D,2}$ are generally very small quantities, whereas W , S , and v tend to be large. As an example, let $C_{D,2} = 0.08$, $S = 950 \text{ ft}^2$ and $S_{FC} = 1.92 \times 10^{-4} \text{ 1/s}$. These values were taken from the G-IV aircraft model used in the simulations, which is presented formally in section 3.4.1. Moreover, let $W = 74600$ (the maximum takeoff weight for this aircraft) and $\rho = 1.07 \times 10^{-3} \text{ slug/ft}^3$, the density at 25000 ft obtained using (2.1c). For the following values of v , we obtain these results for $S_{FC}C_{D,2}W$, $\rho S v^2$ and their quotient

$$\begin{aligned}
 v = 650 \text{ ft/s} : \quad & S_{FC}C_{D,2}W = 1.15 \text{ lbf/s}, \quad \rho S v^2 = 4.29 \times 10^5 \text{ lbf}, \quad \text{Quotient} = 2.68 \times 10^{-6} \text{ 1/s} \\
 v = 700 \text{ ft/s} : \quad & S_{FC}C_{D,2}W = 1.15 \text{ lbf/s}, \quad \rho S v^2 = 4.98 \times 10^5 \text{ lbf}, \quad \text{Quotient} = 2.31 \times 10^{-6} \text{ 1/s} \\
 v = 750 \text{ ft/s} : \quad & S_{FC}C_{D,2}W = 1.15 \text{ lbf/s}, \quad \rho S v^2 = 5.72 \times 10^5 \text{ lbf}, \quad \text{Quotient} = 2.01 \times 10^{-6} \text{ 1/s}.
 \end{aligned}$$

It can be seen that, for this example, $S_{FC}C_{D,2}W$ is considerably smaller than $\rho S v^2$, therefore the assumption that \dot{J}_W^* is negligible, leading to $J_W^* \approx 0$, is reasonable from a physical point of view. Under these considerations, it is possible to derive a *sub-optimal* feedback law for v after substituting $J_W^* = 0$ in (3.21), yielding

$$v = \sqrt{\frac{C_I + \sqrt{C_I^2 + 12S_{FC}^2 C_{D,0} C_{D,2} W^2}}{S_{FC} C_{D,0} \rho S}}. \quad (3.30)$$

A validation of the assumption $J_W^* \approx 0$ is made in section 3.4 by solving the OCP using the shooting method numerically, and comparing its optimal trajectory with the sub-optimal one obtained using (3.30). However, prior to presenting the validation results, it will be shown that the results obtained in this section are also valid when the aircraft is turning, provided that its bank angle is small.

Remark 2: Having neglected J_W^* , it is possible to determine the minimum and maximum values of CI such that the aircraft remains inside the flight envelope. From (3.27) with $J_W^* \approx 0$, we can solve for C_I to obtain

$$C_I = S_{FC}d_0v^2 - \frac{3S_{FC}d_1}{v^2}.$$

If the above equation is evaluated at the minimum speed v_{min} and the maximum speed v_{max} , which are part of the flight envelope as shown in (2.11), the corresponding CIs will be the minimum and maximum, respectively.

3.3.2 Extension to Lateral Flight

The previous section discussed the case of an aircraft flying in cruise at constant altitude while minimizing the flight's operating cost. In this section, the effect of turning on the aircraft's Economy Mode performance will be studied. Turns usually happen during the cruise when transitioning from one waypoint to another, and are produced by banking the aircraft by deflecting the ailerons that are located on the wings. An FMS decouples longitudinal and lateral dynamics. Nevertheless, this section will account for the lateral dynamics in the OCP and verify that under the right assumptions it is in fact possible to carry decouple both dynamics.

We want the aircraft to perform a coordinated turn starting at a point in the horizontal plane, called the Initial Turn Point (ITP), by tracing a curve in space with a given turn radius and Turn Center (TC) until the given Final Turn Point (FTP) is reached, at which longitudinal flight is resumed. The situation is depicted in Fig. 3.1, where θ is the heading angle and μ is the bank angle. Both μ and the true airspeed v are to be determined by the FMS. We assume that the aircraft is at the ITP at the initial time. Under these conditions,

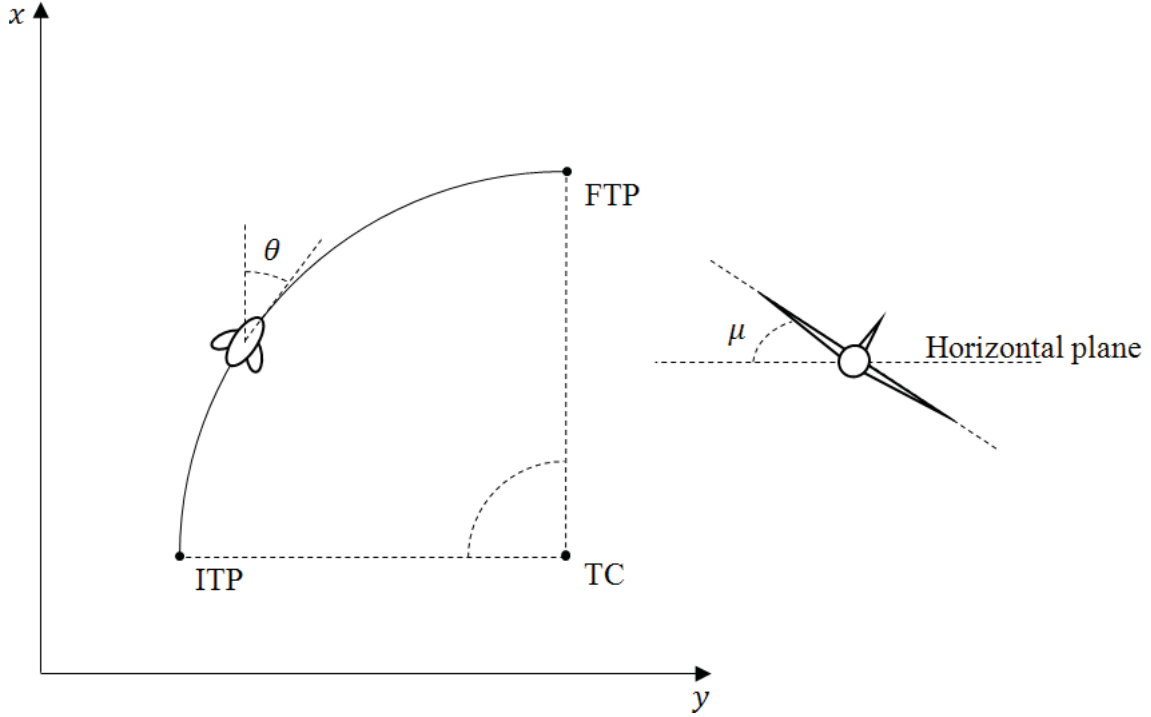


Figure 3.1: Aircraft flying in a horizontal plane.

it can be shown that the dynamics in (2.6) can be extended to [47]:

$$\begin{aligned}
 \dot{x} &= v \cos(\theta) \cos(\gamma) \\
 \dot{y} &= v \sin(\theta) \cos(\gamma) \\
 \dot{h} &= v \sin(\gamma) \\
 \dot{V} &= \frac{g}{W} (T \cos(\alpha) - D - W \sin(\gamma)) \\
 \dot{\gamma} &= \frac{g}{Wv} [(T \sin(\alpha) + L) \cos(\mu) - W \cos(\gamma)] \\
 \dot{\theta} &= \frac{g}{Wv \cos(\gamma)} (T \sin(\alpha) + L) \sin(\mu) \\
 \dot{W} &= -S_{FC}T
 \end{aligned} \tag{3.31}$$

We proceed to make the following assumptions, most of which coincide with the longitudinal case:

- The aircraft flies at a given, constant altitude constrained by Air Traffic Control (ATC) as is the case with real FMS. This assumption makes γ , $\dot{\gamma}$ and \dot{h} equal to zero.

- The altitude, speed and thrust values lie in the interior of the flight envelope given by the constraints (2.11). As a result, we do not need to enforce them in the mathematical formulation of the OCP.
- The angle of attack α is small, allowing to write $\cos \alpha \approx 1$ and $\sin \alpha \approx \alpha$. This assumption is standard practice in performance analysis for commercial aircraft.
- The component of the thrust perpendicular to the velocity vector, $T\alpha$, is much smaller than L and W .
- Accelerations are negligible due to the steady-flight condition, and as a result we can assume that \dot{v} is approximately zero.
- The bank angle μ is sufficiently small such that $\cos(\mu) \approx 1$.

Under these assumptions, (3.31) simplifies to

$$\begin{aligned}
 \dot{x} &= v \cos(\theta) \\
 \dot{y} &= v \sin(\theta) \\
 \dot{\theta} &= \frac{g}{Wv} L \sin(\mu) \\
 \dot{W} &= -S_{FC}T \\
 L &= W \\
 T &= D
 \end{aligned} \tag{3.32}$$

In addition to the last two constraints, we must enforce that

$$L \sin(\mu) = \frac{Wv^2}{gr}, \tag{3.33}$$

which implies that the horizontal component of the lift must provide the centripetal force used for performing the turn of radius r as shown in Fig. 3.2, where \hat{y}_w and \hat{z}_w are part of the wind axes system. Note that, after the turn radius is given and the above constraint is

enforced, the the equations for x and y in (3.32) become irrelevant to the problem, as μ is constrained such that the FTP is reached at some point in time.

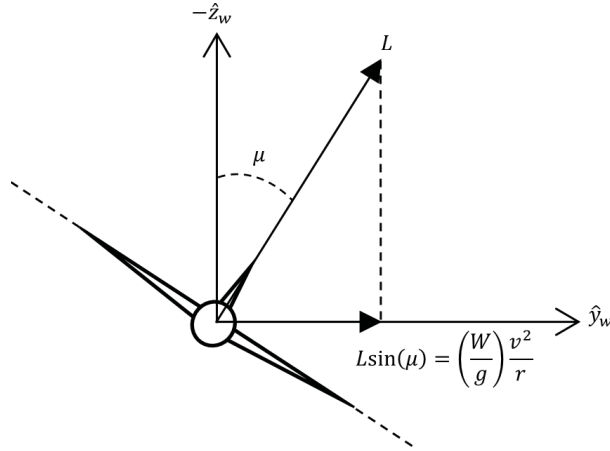


Figure 3.2: Centripetal force in a coordinated turn.

Note that the last assumption allows using (3.6) as an expression for the drag. Strictly speaking, it should be modified such that

$$D(h, v, W) = d_0(h)v^2 + \frac{d_1(h, W)}{v^2 \cos^2(\mu)},$$

where d_0 and d_1 are given by (3.7). However, since $\cos(\mu) \approx 1$, the above expression simplifies to (3.6).

Putting everything together, we can formulate the OCP

$$J^* = \min_{u(t), t_d} \int_{t_c}^{t_d} (S_{FC}D + CI) dt$$

s.t.

$$\dot{\theta} = \frac{g}{Wv} L \sin(\mu)$$

$$\dot{W} = -S_{FC}D$$

$$\theta(0) = \theta_0, \theta(t_f) = \theta_f$$

$$W(0) = W_0,$$

where $u = [v \ \mu]^T$, and θ_0 and θ_f are known as the *inbound* and *outbound* course respectively. Briefly considering $L \cos(\mu) = W$ instead of $L = W$ in (3.32), and from (3.33), we can solve for μ as a function of v , yielding

$$\tan(\mu) = \frac{v^2}{rg}. \quad (3.34)$$

In addition, using (3.33) allows writing $\dot{\theta}$ as

$$\dot{\theta} = \frac{v}{r}.$$

As a result, the problem reduces to one unknown and the OCP for lateral flight is given by

$$J^* = \min_{v(t), t_d} \int_{t_c}^{t_d} (S_{FC}D + CI) dt$$

s.t.

$$\dot{\theta} = \frac{v}{r} \quad (3.35)$$

$$\dot{W} = -S_{FC}D$$

$$\theta(0) = \theta_0, \theta(t_f) = \theta_f$$

$$W(0) = W_0.$$

The following result states the solution of this OCP.

Theorem 3.3.2. *The optimal solution to the OCP stated in (3.35) is*

$$v = \sqrt{\frac{C_I + \sqrt{C_I^2 + 12(1 - J_W^*)^2 S_{FC}^2 C_{D,0} C_{D,2} W^2}}{(1 - J_W^*) S_{FC} C_{D,0} \rho S}} \quad (3.36)$$

Proof. The Hamiltonian is given by

$$H = S_{FC}D + C_I + J_\theta^* \frac{v}{r} - J_W^* S_{FC}D. \quad (3.37)$$

The necessary condition for optimality is

$$\frac{\partial H}{\partial v} = (1 - J_W^*)S_{FC}D_v + \frac{J_\theta^*}{r} = 0, \quad (3.38)$$

which allows solving for J_θ^*/r as follows:

$$\frac{J_\theta^*}{r} = -(1 - J_W^*)S_{FC}D_v \quad (3.39)$$

Similar to the longitudinal case, the sufficient condition for a minimum results in

$$\frac{\partial^2 H}{\partial v^2} = (1 - J_W^*)S_{FC}D_{vv} > 0,$$

from which we obtain

$$J_W^* < 1 \quad (3.40)$$

Noting that H is not a function of time and t_d is unspecified, the HJB equation reduces to $\inf_v H = 0$. By substituting (3.39) into (3.37) evaluated at the optimal speed, and making the expression equal to zero, we get

$$(1 - J_W^*)S_{FC}D - (1 - J_W^*)S_{FC}vD_v + C_I = 0. \quad (3.41)$$

This expression is identical to (3.27). The speed that satisfies this equation is

$$v^2 = \frac{C_I + \sqrt{C_I^2 + 12(1 - J_W^*)^2 S_{FC}^2 C_{D,0} C_{D,2} W^2}}{(1 - J_W^*)S_{FC}C_{D,0}\rho S},$$

which is the same as (3.21). □

The optimal μ is solved as a function of v using (3.34). As a result, we can conclude that, for a small μ , the speed that minimizes operating costs during cruise does not change, and the same results that were shown in section 3.3.1 apply to the lateral case as well. The

remainder of the chapter will present the shooting algorithm used for validation purposes and the simulation results.

3.4 Validation Results

3.4.1 Aircraft Model Used for the Simulations

The aircraft model used for all simulations in this work was borrowed from [46], and is based on the Gulfstream-IV (G-IV) business jet by Gulfstream Aerospace equipped with two Rolls-Royce Tay 611-8 turbofan engines. The drag coefficients, wing planform area, SFC and thrust characteristics are

$$C_{D,0} = 0.015$$

$$C_{D,2} = 0.08$$

$$S = 950 \text{ ft}^2$$

$$S_{FC} = 0.69 \text{ 1/h}$$

$$T_s = 27700 \text{ lbf}$$

$$T_i = 200 \text{ lbf}$$

$$m = 1.$$

The parameters T_s , T_i and m are not used for cruise, but are necessary for the modeling of maximum climb thrust and idle thrust in Chapter 4. The aircraft operating limits, taken

from [53], are given by

$$\begin{aligned} \text{Maximum Takeoff Weight} &= 74600 \quad \text{lbf} \\ \text{Maximum Zero-Fuel Weight} &= 49000 \quad \text{lbf} \\ \text{Service Ceiling}(h_{max}) &= 45000 \quad \text{ft} \\ M_{MO} &= 0.88. \end{aligned}$$

When choosing initial and final conditions for the simulations, it is important to ensure that the aforementioned limits are respected.

3.4.2 Shooting Method for Cruise

The general approach described in Section 2.2.4 will be adapted to solve (3.20) numerically. From the cruise dynamics (3.1) and (3.22), the augmented system is formed by

$$\begin{aligned} \dot{x} &= v \\ \dot{W} &= -S_{FC}D \\ \dot{J}_W^* &= (J_W^* - 1) \frac{4S_{FC}C_{D,2}W}{\rho S v^2} \\ x(t_c) &= x_c, x(t_d) = x_d \\ W(t_c) &= W_c, W(t_d) \quad \text{unspecified} \\ J_W^*(t_c) & \quad \text{unspecified}, J_W^*(t_d) = 0, \end{aligned} \tag{3.42}$$

where v is computed at every time-step using (3.21) (recall that J_x^* has been solved as a function of the other variables in (3.25), therefore its dynamics do not have to be included in the augmented system). The goal of the shooting method is to simulate (3.42) for different $J_W^*(t_c)$ until one is found for which $J_W^*(t_d) = 0$. Following the same notation as in Section 2.2.4, the following pseudo-code states the shooting algorithm for this particular OCP:

1. Choose $J_W^{*(0)}(t_c)$:

- (a) Estimate an initial value for the speed $v(t_c)$ from practical experience.
- (b) Solve for J_W^* from (3.27) and evaluate at $t = t_c$, yielding the following estimate:

$$J_W^{*(0)}(t_c) = 1 + \left(\frac{C_I}{S_{FC}(D - vD_v)} \right) \Big|_{t_c} \quad (3.43)$$

2. Let $k = 0$

3. Do:

- (a) Simulate (3.42) until $x(t) = x_d$, then $t_d = t$
- (b) Compute $\epsilon = J_W^{*(k)}(t_d) - J_W^*(t_d)$
- (c) Compute the next seed $J_W^{*(k+1)}(t_c)$ using the update law

$$J_W^{*(k+1)}(t_c) = J_W^{*(k)}(t_c) - \beta\epsilon \quad (3.44)$$

(d) $k = k + 1$

4. Until $|\epsilon| < \text{tolerance}$ OR $k \geq \text{Max. Iterations}$

Instead of proposing $J_W^{*(0)}(t_c)$ which is difficult to correlate with the physical variables of the problem, it is more convenient to estimate an initial cruise speed $v(t_c)$ from practical experience and then solve for $J_W^{*(0)}(t_c)$ using (3.43). β is a tuning parameter and was chosen to be equal to one for this problem. The algorithm presented in this subsection, as well as another algorithm that applies the sub-optimal feedback law (3.30), have been implemented in Matlab and Simulink. The implementation code and block diagrams can be found in Appendix A.

A simulation will now be carried out for the purpose of comparing the exact optimal trajectory found using the shooting method with the one using the sub-optimal feedback law.

3.4.3 Comparison between the optimal and sub-optimal trajectories

For this example the following initial and final conditions are used:

$$\begin{aligned}
 t_c &= 0 \quad \text{s} \\
 h_c &= 25000 \quad \text{ft} \\
 x_c &= 0 \quad \text{mi} \\
 x_d &= 2000 \quad \text{mi} \\
 W_c &= 70000 \quad \text{lb}
 \end{aligned}$$

Fig. 3.3 compares the sub-optimal true airspeeds with the optimal ones obtained using the shooting method for different CIs as a function of the aircraft range (time was not used for the horizontal axis as it changes significantly depending on CI, whereas the range is the same for all cases). The solid lines represent the optimal solution whereas the dashed lines represent the sub-optimal one. For a CI of zero both lines are identical. This is an expected result because the approximation that $J_W^* \approx 0$ becomes irrelevant when CI vanishes, as shown in Section 3.3. In fact, the obtained speed profile corresponds to the maximum range speed.

The optimal and sub-optimal references start to change when CI is different than zero. This is due to the approximation $J_W^* \approx 0$ being less precise at the start of the simulation, leading to a more pronounced difference between the optimal and sub-optimal speed. However, as the final time is reached, this assumption becomes more valid until $t = t_d$, where expressions (3.21) and (3.30) become identical. This is verified in Fig. 3.4 where J_W^* is plotted as a function of the range. As a result, it can be said that the sub-optimal control law is a good approximation for short range flights, and becomes less precise for longer distances.

For this example, it is possible to quantify how sub-optimal the analytical solution is by computing the total cost. Noting that $S_{FC}D = -\dot{W}$ in (3.19), the total cruise cost in units

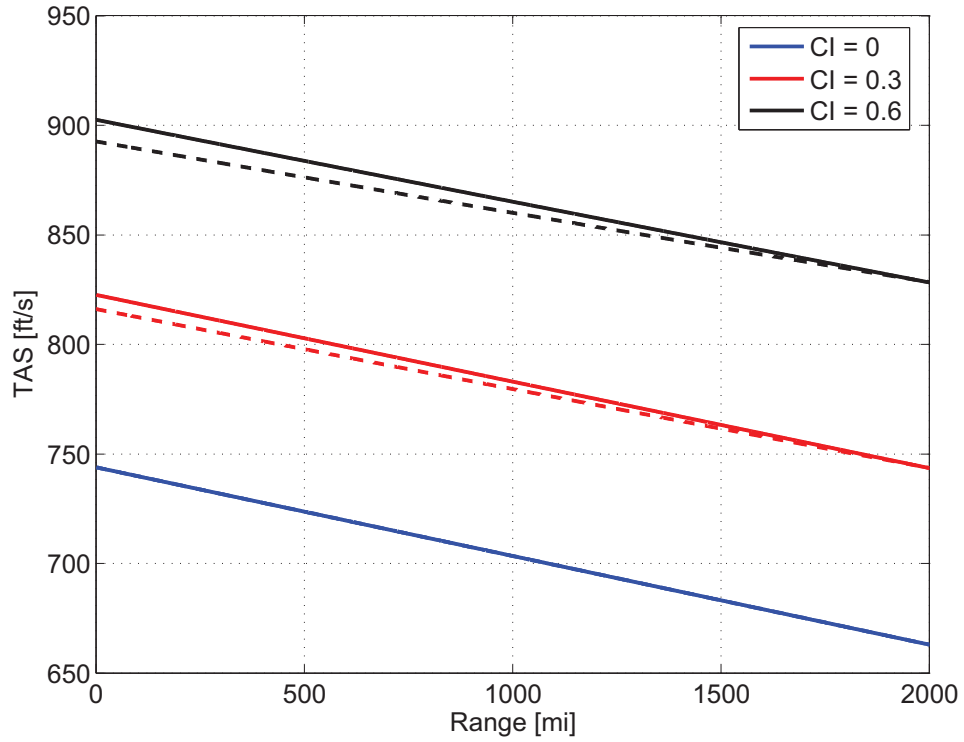


Figure 3.3: Comparison between the optimal and sub-optimal cruise speeds for different cost indexes. The solid line represents the optimal solution, while the dashed line is the sub-optimal one.

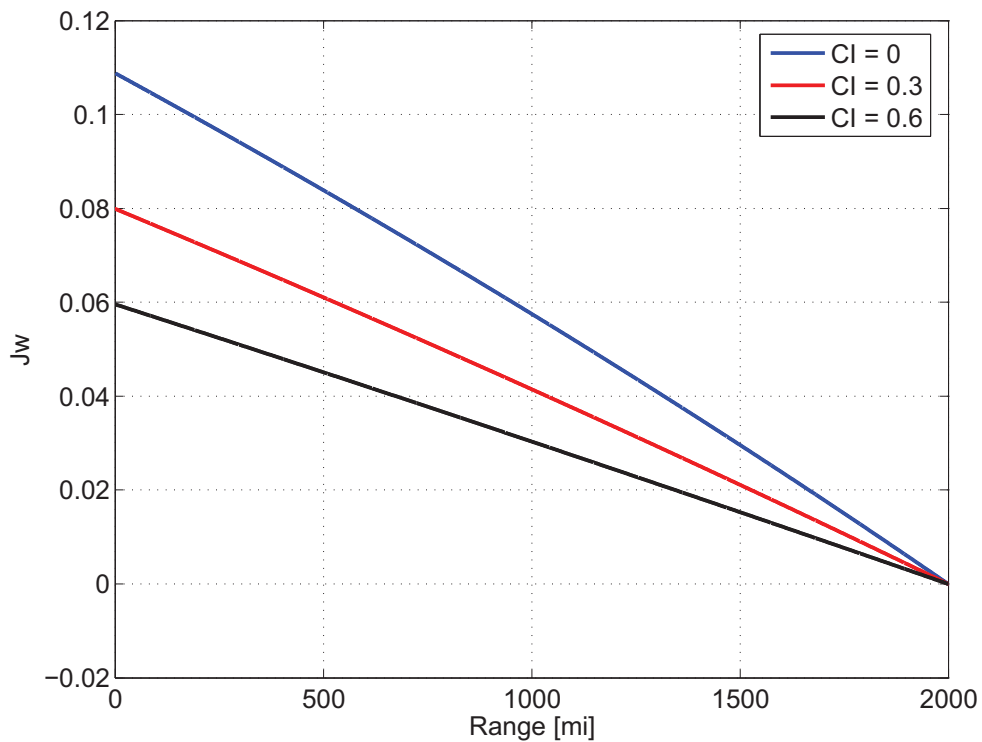


Figure 3.4: Costate J_W^* in cruise as a function of the range for different cost indexes.

of weight can be obtained as:

$$J = W(t_c) - W(t_d) + C_I(t_d - t_c)$$

Table 3.1 provides a comparison between the optimal and sub-optimal laws of the fuel consumed, time elapsed and cost computed using the above formula, for the same values of C_I used for the plots. The error column shows the percent relative error of the sub-optimal cost with respect to the optimal one, as specified by the formula:

$$\text{Error (\%)} = \left| \frac{\text{Sub-optimal cost} - \text{Optimal cost}}{\text{Optimal cost}} \right| \cdot 100 \quad (3.45)$$

It can be concluded that the discrepancy between these two laws does not introduce significant changes in the optimal cost, therefore the sub-optimal analytical solution is, in this example, close enough to the optimal one for practical purposes.

Table 3.1: Cruise fuel, time and cost comparison for different values of C_I .

		Fuel (lb)	Duration (min)	Cost (lb)	Error (%)
$C_I = 0$	Optimal	14407.0	250.5	14407.0	0
	Sub-optimal	14407.0	250.5	14407.0	
$C_I = 0.3$	Optimal	14630.0	225.0	18679.2	$2.4 \cdot 10^{-3}$
	Sub-optimal	14613.7	225.9	18679.6	
$C_I = 0.6$	Optimal	15202.6	203.5	22529.9	$3.8 \cdot 10^{-3}$
	Sub-optimal	15161.9	204.7	22530.8	

Chapter 4

Optimal Solutions for Climb and Descent

4.1 Assumptions

Similar to the approach taken in Chapter 3, this section presents the assumptions made to simplify the aircraft dynamics (2.6) during the climb and descent phases of the flight. The purpose of simplifying these equations is to allow solving the OCPs in this chapter analytically, which would be too difficult to do if the expressions involved are not tractable enough. Most of the assumptions made in this section are very similar to the ones made in the cruise phase. They will be repeated here for the sake of clarity.

The assumptions made for the climb and descent segments of the flight are the following:

- The altitude and speed values lie in the interior of the flight envelope given by the constraints (2.11). As a result, we do not need to enforce them in the mathematical formulation of the OCP.
- During climb, the thrust is constrained to be equal to a given, known value $T_c(h)$ known as the *maximum climb thrust*. Similarly, during the descent, the thrust is equal to a known value T_i known as the *idle thrust*.

- The angle of attack α and the flight path angle γ are small, allowing to write $\cos \alpha \approx 1$ and $\sin \alpha \approx \alpha$, and similarly for γ . This assumption is standard practice in performance analysis for commercial aircraft.
- The component of the thrust perpendicular to the velocity vector, $T\alpha$, is much smaller than L and W . The thrust force is usually around one order of magnitude smaller than the weight, therefore multiplying it by a small angle will effectively make it negligible.
- Climb and descent occur under steady flight conditions and as a result we will assume that \dot{v} and $\dot{\gamma}$ are zero. As explained in Section 1.2, the FMS supplies optimal references that are then followed by the autopilot using the aircraft's flight controls. Therefore, we can take v and γ as control signals, leaving their dynamics to the autopilot.

Taking these assumptions into consideration, we obtain the simplified aircraft model for quasi-steady climb and descent in the longitudinal plane

$$\begin{aligned} \dot{x} &= v \\ \dot{h} &= v\gamma \\ \dot{W} &= -S_{FC}T \end{aligned} \tag{4.1}$$

$$L = W \tag{4.2}$$

$$T = D + W\gamma, \tag{4.3}$$

Since $L = W$ from (4.2), equations (3.5), (3.6) and (3.7) are valid to compute the drag during the climb and descent. The last relation to consider is the constraint on the thrust:

$$T = \begin{cases} T_c(h) & : \gamma > 0 \quad (\text{during climb}) \\ T_i & : \gamma < 0 \quad (\text{during descent}) \end{cases}, \tag{4.4}$$

which will be applied in conjunction with (4.3) depending on the flight phase. T_i is considered constant and known for a particular aircraft, whereas $T_c(h)$ will follow the relation proposed in [46, 48] for turbojet and turbofan engines:

$$T_c(h) = T_s \left[\frac{\rho(h)}{\rho_s} \right]^m \quad (4.5)$$

In the above expression, T_s stands for the sea-level maximum climb thrust rating. T_s and m are given for a particular aircraft, and ρ obeys the ISA equations (2.1c) and (2.2b).

4.2 Maximum Rate of Climb and Minimum Rate of Descent OCPs

4.2.1 Maximum Rate of Climb

The OCP for maximum rate of climb can be stated as follows: It is desired to climb from a given initial altitude h_0 where the FMS is engaged to the desired cruise altitude h_c in minimum time. The point x_c at which h_c is reached is unspecified and constitutes the TOC, and $\gamma > 0$. As in (4.4), the thrust must be equal to T_c and γ is subject to the constraint (4.3). From there, we can solve for γ yielding:

$$\gamma = \frac{T_c - D}{W} \quad (4.6)$$

This leaves v as the single control input. In mathematical form the OCP is given by:

$$\begin{aligned}
J^* &= \min_{v, t_c} \int_0^{t_c} dt \\
\text{s.t.} \\
\dot{x} &= v \\
\dot{h} &= v\gamma \\
\dot{W} &= -S_{FC}T_c(h) \\
x(0) &= x_0 \\
h(0) &= h_0, \quad h(t_c) = h_c \\
W(0) &= W_0 \\
\gamma &= \frac{T_c - D}{W} > 0
\end{aligned} \tag{4.7}$$

The solution of this OCP is stated in the following theorem.

Theorem 4.2.1. *The optimal solution for the maximum ROC problem (4.7) is given by*

$$v = \sqrt{\frac{T_c + \sqrt{T_c^2 + 12C_{D,0}C_{D,2}W^2}}{3C_{D,0}\rho S}}. \tag{4.8}$$

Proof. The Hamiltonian

$$H = 1 + J_x^*v + J_h^*v\gamma - J_W^*S_{FC}T_c \tag{4.9}$$

must be minimized with respect to v . The necessary condition for optimality yields

$$\begin{aligned}
\frac{\partial H}{\partial v} &= 0 \\
&\equiv J_x^* + J_h^*(\gamma + v\gamma_v) = 0,
\end{aligned}$$

where γ_v is the partial derivative of γ with respect to v . The expression (4.6) can be differ-

entiated with respect to v to get

$$\gamma_v = \frac{\partial \gamma}{\partial v} = -\frac{D_v}{W}, \quad (4.10)$$

which is substituted into the necessary condition to get

$$J_x^* + J_h^* \left(\gamma - \frac{vD_v}{W} \right) = 0. \quad (4.11)$$

Note, however, that the following information can be obtained using the costate equations:

$$j_x^* = -\frac{\partial H}{\partial x} = 0, \quad (4.12)$$

and

$$\begin{aligned} j_h^* &= -\frac{\partial H}{\partial h} \\ &= J_W^* (S_{FC_h} T_c + S_{FC} T_{c_h}) - J_h^* v \gamma_h. \end{aligned} \quad (4.13)$$

Moreover, since the terminal cost is $\phi = 0$ and the terminal constraint function is $\psi = h - h_c$, we get:

$$J_x^*(t_c) = (\phi_x + \nu \psi_x)|_{t_c} = 0 \quad (4.14)$$

As a result, J_x^* is zero for all t and is eliminated from (4.11) yielding:

$$J_h^* \left(\gamma - \frac{vD_v}{W} \right) = 0$$

Since J_h^* has nonzero dynamics as in (4.13), it cannot be zero for all t , therefore

$$\gamma - \frac{vD_v}{W} = 0,$$

which, after substituting γ from (4.6) and the drag from (3.6), yields

$$\begin{aligned} T_c - D - vD_v &= 0 \\ \equiv 3d_0v^4 - T_cv^2 - d_1 &= 0. \end{aligned}$$

This equation is solved for the optimal speed obtaining

$$v^2 = \frac{T_c \pm \sqrt{T_c^2 + 12d_0d_1}}{6d_0},$$

or, after replacing d_0 and d_1 from (3.7) and taking the positive sign:

$$v^2 = \frac{T_c + \sqrt{T_c^2 + 12C_{D,0}C_{D,2}W^2}}{3C_{D,0}\rho S}$$

This equation yields the optimal speed that maximizes the ROC of the aircraft. It coincides with (2.19) with $T = T_c$, which is the expression commonly found in literature. Obtaining expressions for J_h^* , J_W^* and J^* is not relevant to this discussion, but they could be obtained by formulating and solving the rest of the equations.

It remains to verify the sufficient condition to minimize H , which is found by taking the partial derivative of (4.11) with respect to v (keeping in mind that J_x^* is zero) and substituting (4.10), yielding

$$\begin{aligned} \frac{\partial^2 H}{\partial v^2} &= J_h^* \left[\gamma_v - \frac{1}{W} \frac{\partial}{\partial v} (vD_v) \right] \\ &= \frac{J_h^*}{W} [-D_v - (D_v + vD_{vv})] \\ &= -\frac{J_h^*}{W} \left(6d_0v + \frac{2d_1}{v^3} \right) \end{aligned}$$

This partial derivative must be greater than zero. It follows that either

$$J_h^* < 0 \quad \text{and} \quad \left(6d_0v + \frac{2d_1}{v^3} \right) > 0,$$

or

$$J_h^* > 0 \quad \text{and} \quad \left(6d_0v + \frac{2d_1}{v^3}\right) < 0,$$

but, since $(6d_0v + 2d_1/v^3)$ is always positive as it involves only positive terms, the sufficient condition reduces to

$$J_h^* < 0. \tag{4.15}$$

Since H does not depend explicitly on time and t_c is unspecified, the HJB equation reduces to $\inf_v H = 0$. It follows from (4.9) evaluated at the optimal speed that

$$1 + J_x^*v + J_h^*v\gamma - J_W^*S_{FC}T_c = 0,$$

from which we solve for J_h^* to obtain

$$J_h^* = \frac{-1 + J_W^*S_{FC}T_c}{v\gamma}. \tag{4.16}$$

To satisfy (4.15), (4.16) must be less than zero. Since $\gamma > 0$ from (4.7) and v must be positive, we get

$$-1 + J_W^*S_{FC}T_c < 0,$$

from which a constraint on J_W^* is obtained as

$$J_W^* < \frac{1}{S_{FC}T_c} \tag{4.17}$$

Equation (4.17) implies that J_W^* is positive and smaller than a very small value, since $S_{FC}T_c$ is a generally a large quantity. \square

To close this section, we verify that the maximum ROC speed also coincides with the solution for minimum fuel consumption. Consider the OCP (4.7), but with the minimum

fuel cost functional:

$$J^* = \min_{v, t_c} \int_0^{t_c} S_{FC} T_c dt \quad (4.18)$$

The Hamiltonian changes to

$$H = (1 - J_W^*) S_{FC} T_c + J_x^* v + J_h^* v \gamma.$$

However, since the term $(1 - J_W^*) S_{FC} T_c$ does not depend on v , the necessary condition remains the same as (4.11). Furthermore, the same reasoning as the ROC problem can be followed: J_x^* satisfies (4.12) and (4.14) vanishing from the necessary condition, and yielding (4.8) for the optimal speed. The only equation that changes is \dot{J}_h^* and the constraint on J_W^* arising from the sufficient condition of optimality.

4.2.2 Minimum Rate of Descent

The minimum rate of descent problem is a very similar problem to the one discussed for climb. This time, the starting point x_d is unspecified, and the aircraft must descend from cruise altitude to a final value where the performance module of the FMS is disengaged and the approach phase begins. This takes place at a given final range x_f . Define the distance traveled as

$$\tilde{x} = x - x_d,$$

resulting in the dynamics and initial and final conditions

$$\dot{\tilde{x}} = v \cos(\gamma)$$

$$\tilde{x}(t_d) = 0$$

$$\tilde{x}(t_f) = x_f - x_d.$$

This change of variables allows formulating the OCP in standard form, given by

$$\begin{aligned}
J^* &= \max_{v, t_f} \int_{t_d}^{t_f} dt \\
\text{s.t.} \\
\dot{\tilde{x}} &= v \cos(\gamma) \\
\dot{h} &= v \sin(\gamma) \\
\dot{W} &= -S_{FC} T_i \\
\tilde{x}(t_d) &= 0 \\
h(t_d) &= h_c, \quad h(t_f) = h_f \\
W(t_d) &= W_d,
\end{aligned} \tag{4.19}$$

where $T = T_i$ and

$$\gamma = \frac{T_i - D}{W}. \tag{4.20}$$

The solution of OCP (4.19) is stated in the following theorem.

Theorem 4.2.2. *The optimal solution to OCP (4.19) is given by*

$$v = \sqrt{\frac{T_i + \sqrt{T_i^2 + 12C_{D,0}C_{D,2}W^2}}{3C_{D,0}\rho S}}. \tag{4.21}$$

Proof. Define the Hamiltonian

$$H = 1 + J_{\tilde{x}}^* v + J_h^* v \gamma - J_W^* S_{FC} T_i \tag{4.22}$$

from which the necessary condition of optimality can be obtained as follows:

$$\frac{\partial H}{\partial v} = J_{\tilde{x}}^* + J_h^* (\gamma + v \gamma_v)$$

Using the same approach as in the maximum ROC case, it can be shown that

$$\gamma_v = -\frac{D_v}{W}, \quad (4.23)$$

which is substituted into the necessary condition yielding

$$J_{\tilde{x}}^* + J_h^* \left(\gamma - \frac{vD_v}{W} \right) = 0. \quad (4.24)$$

Analogous to the climb problem, the costate equations yield

$$J_{\tilde{x}}^* = -\frac{\partial H}{\partial \tilde{x}} = 0 \quad (4.25)$$

$$J_{\tilde{x}}^*(t_f) = 0, \quad (4.26)$$

and

$$\begin{aligned} J_h^* &= -\frac{\partial H}{\partial h} \\ &= J_W^* S_{FC_h} T_i - J_h^* v \gamma_h \end{aligned} \quad (4.27)$$

It follows from (4.25) and (4.26) that $J_{\tilde{x}}^*$ is zero for all t , and (4.24) reduces to

$$J_h^* \left(\gamma - \frac{vD_v}{W} \right) = 0.$$

Given that J_h^* has the dynamics specified in (4.27), it cannot be zero for all t and the resulting equation can be solved for the minimum rate of descent speed in the same manner as in the climb:

$$\gamma - \frac{vD_v}{W} = 0$$

Substitute (4.20) to get

$$\begin{aligned} T_i - D - vD_v &= 0 \\ \equiv 3d_0v^4 - T_iv^2 - d_1 &= 0, \end{aligned}$$

which is solved for v yielding

$$\begin{aligned} v^2 &= \frac{T_i \pm \sqrt{T_i^2 + 12d_0d_1}}{6d_0} \\ &= \frac{T_i + \sqrt{T_i^2 + 12C_{D,0}C_{D,2}W^2}}{3C_{D,0}\rho S} \end{aligned}$$

The second partial derivative of H with respect to v is given by

$$\begin{aligned} \frac{\partial^2 H}{\partial v^2} &= J_h^* \left[\gamma_v - \frac{1}{W} \frac{\partial}{\partial v} (vD_v) \right] \\ &= -\frac{J_h^*}{W} \left(6d_0v + \frac{2d_1}{v^3} \right), \end{aligned}$$

which must be less than zero according to the sufficient condition of optimality. Since $(6d_0v + 2d_1/v^3)$ contains only positive terms, it follows that

$$J_h^* > 0. \tag{4.28}$$

In the same fashion as in the climb, the HJB equation reduces to $\inf_v H = 0$ which allows solving for J_h^* using (4.22) evaluated at the optimal v and equated to zero yielding

$$J_h^* = \frac{-1 + J_W^* S_{FC} T_i}{v\gamma}$$

The above expression must be greater than zero to satisfy (4.28). Since γ is negative dur-

ing the descent and v is positive, the numerator must be negative resulting in the constraint

$$J_W^* < \frac{1}{S_{FC}T_i}. \quad (4.29)$$

□

Equation (4.21) yields the minimum ROD speed and is very similar to (4.8), with the difference that T_c is changed to T_i . It also coincides with (2.19) with $T = T_i$. Moreover, just like in the climb phase, it can be shown that (4.21) is equivalent to the minimum fuel descent speed. The procedure to prove this statement is identical to the one followed in the previous subsection, and will not be repeated here.

4.3 Economy Mode OCP for Climb

The ECON mode for climb will now be derived and solved as an OCP. While it might seem tempting to formulate such problem by modifying the ROC minimum fuel cost functional (4.18) by adding C_I to the running cost, the truth is that doing this *will not* change the original problem. The Hamiltonian (4.9) would only be changed by the addition of C_I , which would disappear when the partial derivative w.r.t. v is taken for the necessary condition. As a result, the same procedure developed in Section 4.2.1 would hold and the speed target would remain unchanged.

The reason why this happens is because if the climb phase is considered alone without regard to the rest of the flight, reaching cruise altitude in minimum time is already equivalent to minimizing the fuel consumed during that phase, therefore using CI to quantify a tradeoff between these two criteria becomes meaningless. To obtain a relevant formulation, the impact of the climb phase on the rest of the flight must be considered, i.e. we will study the effect of choosing a given climb speed and flight path angle on the *overall* operating cost of the flight.

To take the rest of the phases into account, the *cost-to-go* from the TOC until the end of the flight must be added to the climb cost functional using the principle of optimality

as discussed in Section 2.2.5. However, doing so would require computing the optimal cost-to-go function of the cruise OCP (3.20), which involves finding analytic expressions for the costates J_x^* and J_W^* by solving the ODE (3.22) and the HJB equation subject to its boundary condition. Then, we would have to add the cost-to-go of the descent. This is obviously a very difficult proposition. Nevertheless, the objective of the next subsection is to develop a formulation that takes the cost-to-go into account an approximate manner, resulting in a meaningful OCP that can be approached analytically to obtain the cost-optimal speed.

Problem Formulation Using the Principle of Optimality

Suppose that it is desired for the aircraft to climb from a given initial point (x_0, h_0) to a prescribed cruise altitude h_c . The TOC, x_c , and the final time t_c are unspecified and must be determined such that the operating costs are minimized. The initial climb weight W_0 is known. From Section 1.3, we know that the total operating cost of the flight can be expressed in terms of the fuel flow rate f_f as

$$J = \int_0^{t_f} (f_f + C_I) dt, \quad (4.30)$$

which is split into the three phases of flight:

$$J = \int_0^{t_c} (f_{f_{cl}} + C_I) dt + \int_{t_c}^{t_d} (f_{f_{cr}} + C_I) dt + \int_{t_d}^{t_f} (f_{f_d} + C_I) dt \quad (4.31)$$

The terms $f_{f_{cl}}$, $f_{f_{cr}}$ and f_{f_d} denote the fuel flow rate during climb, cruise and descent respectively. Then, according to the principle of optimality defined in (2.36), we get

$$J^* = \inf_{v, t_c, 0 \leq t \leq t_c} \left\{ \int_0^{t_c} (f_{f_{cl}} + C_I) dt + J_{cr,d}^*(t_c, \zeta(t_c)) \right\}, \quad (4.32)$$

where

$$J_{cr,d}^* = \inf_{v, t_c \leq t \leq t_f} \left\{ \int_{t_c}^{t_d} (f_{f_{cr}} + C_I) dt + \int_{t_d}^{t_f} (f_{f_d} + C_I) dt \right\}.$$

The functional $J_{cr,d}^*$ computes the optimal cost-to-go from t_c until the end of the flight, and comprises both the cruise and the descent costs. To simplify the problem, we will assume that the descent cost is negligible when compared to the cruise cost. This is a reasonable assumption when considering that most commercial flights spend most of the time cruising, in addition to the thrust being small during the descent. As a result, the impact of the cruise on the overall flight time and fuel consumption is more significant than the descent. Furthermore, we know from Section 3.3 that the cruise cost is given by

$$J_{cr}(t_c) = \int_{t_c}^{t_d} (S_{FCD} + C_I) dt = \int_{t_c}^{t_d} (f_{f_{cr}} + C_I) dt.$$

Generally speaking, for a fixed cruise altitude, $f_{f_{cr}}$ changes slowly as the weight decreases due to fuel burnt and the speed is modified accordingly obeying (3.21). If $f_{f_{cr}}$ is computed for $W = W_0$, the total cruise cost-to-go can be estimated as follows:

$$J_{cr}^*(t_c) = \inf_{v_{cr}} \left\{ \int_{t_c}^{t_d} (S_{FCD} + C_I) dt \right\} \approx (f_{f_{cr}}|_{W_0} + C_I)(t_d - t_c).$$

Let us approximate $(t_d - t_c)$ by the expression

$$(t_d - t_c) \approx \frac{x_d - x_c}{v_{cr}},$$

where v_{cr} stands for the cruise speed and can be estimated by evaluating (3.30) at W_0 . Putting everything together, we will approximate $J_{cr,d}^* \approx J_{cr}^*$, and from (4.32) the following cost functional is obtained for the climb phase

$$J^*(0) \approx \inf_{v,t_c} \left\{ \int_0^{t_c} (f_{f_{cl}} + C_I) dt + (f_{f_{cr}} + C_I) \frac{x_d - x_c}{v_{cr}} \right\}, \quad (4.33)$$

where $f_{f_{cr}} = S_{FC}T_c$, and $f_{f_{cr}}, v_{cr}$ are assumed to be evaluated at W_0 . Then, the ECON

Climb OCP can be stated mathematically as follows:

$$\begin{aligned}
J^*(0) &= \min_{v, t_c} \left\{ \int_0^{t_c} (S_{FC}T_c + C_I) dt + (f_{fcr} + C_I) \frac{x_d - x_c}{v_{cr}} \right\} \\
\text{s.t.} \\
\dot{x} &= v \\
\dot{h} &= v\gamma \\
\dot{W} &= -S_{FC}T_c \\
x(0) &= x_0 \\
h(0) &= h_0, \quad h(t_c) = h_c \\
W(0) &= W_0,
\end{aligned} \tag{4.34}$$

where γ satisfies (4.6) and T_c is given by (4.5).

Optimal solution

The following result gives the solution to OCP (4.34).

Theorem 4.3.1. *The optimal solution to the ECON mode OCP for climb stated in (4.34) is given by the solution v of the equation*

$$[(1 - J_W^*)S_{FC}T_c + C_I](T_c - D - vD_v) - J_x^*v^2D_v = 0, \tag{4.35}$$

where γ is obtained from (4.6), J_x^* is given by

$$J_x^* = -\frac{f_{fcr} + C_I}{v_{cr}}, \tag{4.36}$$

and the time derivative of J_W^* equals

$$j_W^* = -\left(\frac{J_x^*v}{W}\right) \left(\frac{d_0v^4 - T_cv^2 - d_1}{3d_0v^4 - T_cv^2 - d_1}\right), \tag{4.37}$$

with final condition

$$J_W^*(t_c) = 0. \quad (4.38)$$

Proof. Define the Hamiltonian as

$$H = (1 - J_W^*)S_{FC}T_c + J_x^*v + J_h^*v\gamma + C_I. \quad (4.39)$$

To minimize (4.39) with respect to v , the necessary condition for optimality must be satisfied:

$$\frac{\partial H}{\partial v} = J_x^* + J_h^*(\gamma + v\gamma_v) = 0$$

Substitute γ_v from (4.10) to get

$$J_x^* + J_h^*\left(\gamma - \frac{vD_v}{W}\right) = 0 \quad (4.40)$$

Up to this point, the minimum-cost problem seems identical to the maximum ROC one from Section (4.2.1). In fact, (4.40) and (4.11) are the same. However, the problem changes drastically once the costate J_x^* is taken into account. We get:

$$j_x^* = -\frac{\partial H}{\partial x} = 0 \quad (4.41)$$

Moreover, since there is a terminal cost

$$\phi(x) = (f_{f_{cr}} + C_I)\frac{x_d - x}{v_{cr}}, \quad (4.42)$$

and

$$\psi(h) = h - h_c, \quad (4.43)$$

then the following value for J_x^* is obtained:

$$J_x^*(t_c) = J_x^* = (\phi_x + \nu\psi_x)|_{t_c} = -\frac{f_{f_{cr}} + C_I}{v_{cr}}$$

The main difference between this OCP and the maximum ROC is that J_x^* does not vanish, but has a constant, known value given by the above equation. The costate J_W^* can be solved directly as a function of the rest of the variables from (4.40) yielding

$$J_h^* = -\left(\frac{J_x^*}{\gamma - \frac{vD_v}{W}}\right), \quad (4.44)$$

therefore we do not have to compute its time derivative or final value. For J_W^* , the costate equation gives

$$\dot{J}_W^* = -\frac{\partial H}{\partial W} = -J_h^* v \gamma_W \quad (4.45)$$

Differentiating (4.6) with respect to W yields

$$\gamma_W = \frac{1}{W^2} (-D_W W - T_c + D).$$

From (3.5)

$$D_W = \frac{4C_{D,2}W}{\rho S v^2},$$

which is substituted into γ_W along with (3.6) and (3.7) to get

$$\begin{aligned} \gamma_W &= \frac{1}{W^2} \left(-\frac{4C_{D,2}W^2}{\rho S v^2} - T_c + d_0 v^2 + \frac{d_1}{v^2} \right) \\ &= \frac{1}{W^2} \left(-\frac{2d_1}{v^2} - T_c + d_0 v^2 + \frac{d_1}{v^2} \right) \\ &= -\frac{1}{W^2} \left(T_c - d_0 v^2 + \frac{d_1}{v^2} \right) \end{aligned} \quad (4.46)$$

Substituting (4.46) into (4.45) results in

$$\dot{J}_W^* = \left(\frac{J_h^* v}{W^2} \right) \left(T_c - d_0 v^2 + \frac{d_1}{v^2} \right).$$

If J_h^* is replaced by (4.44) one obtains the expression

$$\dot{J}_W^* = - \left(\frac{J_x^* v}{W^2} \right) \left(\frac{T_c - d_0 v^2 + \frac{d_1}{v^2}}{\gamma - \frac{v D_v}{W}} \right)$$

in which γ is substituted using (4.6) and D by (3.6) yielding

$$\begin{aligned} \dot{J}_W^* &= - \left(\frac{J_x^* v}{W} \right) \left(\frac{T_c - d_0 v^2 + \frac{d_1}{v^2}}{T_c - D - v D_v} \right) \\ &= - \left(\frac{J_x^* v}{W} \right) \left(\frac{T_c - d_0 v^2 + \frac{d_1}{v^2}}{T_c - 3d_0 v^2 + \frac{d_1}{v^2}} \right) \\ &= - \left(\frac{J_x^* v}{W} \right) \left(\frac{d_0 v^4 - T_c v^2 - d_1}{3d_0 v^4 - T_c v^2 - d_1} \right) \end{aligned}$$

Its final value is given by

$$J_W^*(t_c) = (\phi_W + \nu \psi_W)|_{t_c} = 0.$$

We will now apply the same result from optimal control theory that we used in the cruise problem to simplify the HJB equation. Since H and ϕ are not explicit functions of t and t_c is unspecified, the HJB equation

$$0 = J_t^* + \min_v H,$$

reduces to

$$\min_v H = 0.$$

Replacing the Hamiltonian (4.39) into the HJB equation yields

$$\min_v \{(1 - J_W^*)S_{FC}T_c + J_x^*v + J_h^*v\gamma + C_I\} = 0,$$

or, at the optimal speed

$$(1 - J_W^*)S_{FC}T_c + J_x^*v + J_h^*v\gamma + C_I = 0. \quad (4.47)$$

Substitute (4.44) into (4.47) to yield

$$(1 - J_W^*)S_{FC}T_c + J_x^*v + C_I - \frac{J_x^*v\gamma}{\left(\gamma - \frac{vD_v}{W}\right)} = 0.$$

The above expression can be further manipulated to obtain an equation in terms of v , J_W^* and γ as follows:

$$\begin{aligned} & [(1 - J_W^*)S_{FC}T_c + C_I + J_x^*v] \left(\gamma - \frac{vD_v}{W} \right) - J_x^*v\gamma = 0 \\ \equiv & [(1 - J_W^*)S_{FC}T_c + C_I] \left(\gamma - \frac{vD_v}{W} \right) - \frac{J_x^*v^2D_v}{W} = 0 \end{aligned}$$

Using (4.6) yields

$$[(1 - J_W^*)S_{FC}T_c + C_I] (T_c - D - vD_v) - J_x^*v^2D_v = 0.$$

□

Remark: As opposed to the cruise phase, if C_I vanishes in (4.35) then the Maximum ROC solution presented in Section 4.2.1 is not attained, which was shown to be equivalent to the minimum fuel case for a standalone climb. This happens as a result of the interaction between climb and cruise phases. The only way for both speeds to coincide is to ignore the cruise cost-to-go, which would make J_x^* vanish in (4.40) thus recovering the Maximum ROC solution, regardless of the value of C_I .

Deriving a sub-optimal control law

Equation (4.35) gives the exact solution to the speed that minimizes operating costs, but requires deriving an expression J_W^* . We would like to obtain a simplified, sub-optimal expression that does not depend on J_W^* and that can be solved either analytically or by the means of a fast-converging numerical method for implementation in a FMS.

Note that the right bracket term in (4.37) involves a quotient of two expressions that are in a similar order of magnitude. The term v^4 is usually large, as well as $T_c v^2$ (and d_1 since it involves a term in W^2 , see (3.7)). On the other hand, the left bracket from (4.37) results in a very small quantity, since $W \gg v$. Note that the constant J_x^* is also small as $v_c \gg f_{f_{cr}} + C_I$. We will therefore assume that the left bracket term in (4.37) is much smaller than the right one, therefore $W \gg v J_x^*$ and $\dot{J}_W^* \approx 0$.

To validate these assumptions with an example, we will use the G-IV model presented in section 3.4.1. Suppose that the aircraft is at 5000 ft, where $\rho = 2 \times 10^{-3}$ slug/ft³ as computed using (2.1c) and $T_c = 24867$ lbf calculated from (4.5). The aircraft gross weight is $W = 70000$ lbf and the desired cruise altitude is $h_c = 25000$ ft. For $C_I = 0$, the cruise fuel flow rate is $f_{f_{cr}} = 1.07$ lbf/s and the optimal speed is $v_{cr} = 536.48$ ft/s. These values were obtained using the CruiseOptimalSPeedAndFuelFlow.m function from Appendix A. Then from (4.36) we get $J_x^* = -0.002$ and, referring to (4.37), the following values of the left bracket term, right bracket term and \dot{J}_W^* are obtained for different climb speeds

$$\begin{aligned}
 v = 750 \text{ ft/s} : & \quad \text{Left bracket} = -2.15 \times 10^{-5}, \quad \text{Right bracket} = -393.15, \quad \dot{J}_W^* = -8.40 \times 10^{-3} \\
 v = 800 \text{ ft/s} : & \quad \text{Left bracket} = -2.29 \times 10^{-5}, \quad \text{Right bracket} = -4.31, \quad \dot{J}_W^* = -9.86 \times 10^{-5} \\
 v = 850 \text{ ft/s} : & \quad \text{Left bracket} = -2.43 \times 10^{-5}, \quad \text{Right bracket} = -1.93, \quad \dot{J}_W^* = -4.69 \times 10^{-5}.
 \end{aligned}$$

The considerations written above make sense from a physical point of view. As a result, we will make the assumption that \dot{J}_W^* is negligible and J_W^* is approximately zero for all t as

in (4.38). This assumption allows simplifying (4.35) to

$$(S_{FC}T_c + C_I)(T_c - D - vD_v) - J_x^*v^2D_v = 0,$$

which yields a 5th degree polynomial in terms of v

$$\begin{aligned} & (S_{FC}T_c + C_I) \left(T_c - d_0v^2 - \frac{d_1}{v^2} - 2d_0v^2 + 2\frac{d_1}{v^2} \right) - J_x^*v^2 \left(2d_0v - 2\frac{d_1}{v^3} \right) = 0 \\ \equiv & (S_{FC}T_c + C_I) (T_cv^2 - 3d_0v^4 + d_1) - 2J_x^*(d_0v^5 - d_1v) = 0 \\ \equiv & 2J_x^*d_0v^5 + 3(S_{FC}T_c + C_I)d_0v^4 - (S_{FC}T_c + C_I)T_cv^2 - 2J_x^*d_1v - (S_{FC}T_c + C_I)d_1 = 0 \end{aligned} \tag{4.48}$$

Equation (4.48) constitutes a sub-optimal feedback law for the optimal speed v . When compared to (4.35), it has the advantage that it does not require prior knowledge of J_W^* . An expression for v cannot be found analytically, but computing a positive real root of a polynomial such as (4.48) that lies within the flight envelope of the aircraft can be achieved numerically in a few iterations using an algorithm such as Newton's method. The exact methodology used for on-board implementation is not discussed in this thesis. Instead, to evaluate the accuracy of the sub-optimal policy, Matlab is used to compute the required root of (4.48), and the resulting trajectory is compared to the numerical solution found via the shooting method as described in the next section.

4.4 Validation of Climb Results

All simulations conducted in this section use the aircraft model presented in Section 3.4.1.

4.4.1 Shooting Method for Climb

Following the procedure of Section 3.4.2, we form the augmented system with the specified initial and final conditions from (4.1) and (4.37) as follows:

$$\begin{aligned}
 \dot{x} &= v \\
 \dot{h} &= v\gamma \\
 \dot{W} &= -S_{FC}T_c \\
 j_W^* &= -\left(\frac{J_x^*v}{W}\right)\left(\frac{d_0v^4 - T_cv^2 - d_1}{3d_0v^4 - T_cv^2 - d_1}\right) \\
 x(0) &= x_0, x(t_c) \quad \text{unspecified} \\
 h(0) &= h_0, h(t_c) = h_c \\
 W(0) &= W_0, W(t_c) \quad \text{unspecified} \\
 J_W^*(0) &\text{ unspecified, } J_W^*(t_c) = 0
 \end{aligned} \tag{4.49}$$

As explained previously, J_x^* is constant and given by (4.36) and J_h^* has been solved in terms of the other variables in (4.44). At each time-step, the control inputs v and γ are obtained by solving (4.6) and (4.35) simultaneously. The following pseudo-code discusses the algorithm of the climb shooting method:

1. Compute J_x^* from (4.36), with $f_{f_{cr}}$ and v_{cr} evaluated at h_c, W_0 .
2. Choose $J_W^{*(0)}(0)$:
 - (a) Estimate an initial value for the speed $v(0)$ based on experience
 - (b) Compute $\gamma(0)$ from (4.6)
 - (c) Solve for J_W^* from (4.35) and evaluate at $t = 0$, yielding the following estimate:

$$J_W^{*(0)}(0) = \left[1 + \frac{C_I}{S_{FC}T_c} - \frac{J_x^*v^2D_v}{S_{FC}T_c(T_c - D - vD_v)} \right] \Big|_{t=0} \tag{4.50}$$

3. Let $k = 0$

4. Do:

(a) Simulate (4.49) until $h(t) = h_c$, then $t_c = t$

(b) Compute $\epsilon = J_W^{*(k)}(t_c) - J_W^*(t_c)$

(c) Compute next seed $J_W^{*(k+1)}(0)$ using the update law:

$$J_W^{*(k+1)}(0) = J_W^{*(k)}(0) - \beta\epsilon \quad (4.51)$$

(d) $k = k + 1$

5. Until $|\epsilon| < \text{tolerance}$ OR $k \geq \text{Max. Iterations}$

Estimating $v(0)$ then solving for $J_W^{*(0)}(0)$ is easier than proposing a value for $J_W^{*(0)}(0)$ directly, as the former has a direct physical meaning and can be guessed from experience. β is a tuning parameter and equals one for this problem. Appendix B contains the code developed in Matlab to implement this method, as well as the sub-optimal law from (4.48). In what follows, both approaches will be compared in simulations.

4.4.2 Comparison between the optimal and sub-optimal trajectories

For this demonstration we use the following initial and final conditions, where x_d is relevant only to compute the cost:

$$x_0 = 0 \quad \text{mi}$$

$$x_d = 1000 \quad \text{mi}$$

$$h_0 = 2000 \quad \text{ft}$$

$$h_c = 25000 \quad \text{ft}$$

$$W_0 = 73000 \quad \text{lb}$$

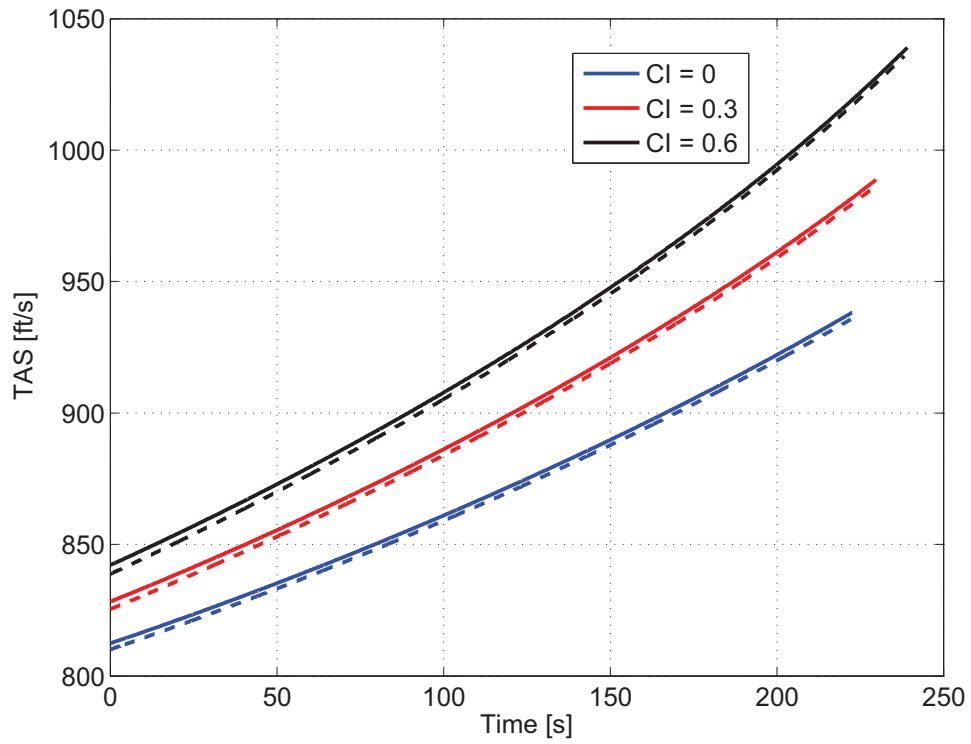


Figure 4.1: Comparison between the optimal and sub-optimal climb speeds for different cost indexes. The solid line represents the optimal solution, while the dashed line is the sub-optimal one.

The result of the simulation is displayed in Fig. 4.1, where the optimal speed profiles are compared for different values of CI. The solid line represents the shooting method solution and the dashed line represents the sub-optimal one. It can be determined by inspection that the distance between each pair of curves is not significant. Moreover, Fig. 4.2 shows a plot of J_W^* as a function of time for each of the examples, where we can verify that its value stays below 8×10^{-3} throughout the simulation, making it very close to zero. As a result, the assumptions made in section 4.3 that lead to (4.48) are valid.

To quantify the impact of the small discrepancies between the optimal and sub-optimal speeds as well as the value of J_W^* , Table 4.1 compares the fuel consumed, time elapsed, range and cost incurred during the phase for each example. The cost was computed by manipulating (4.33) to obtain

$$J = W(0) - W(t_c) + C_I t_c + \left(\frac{f_{fcr} + C_I}{v_{cr}} \right) (x_d - x_c).$$

Table 4.1: Climb fuel, time, range and cost comparison for different values of CI.

		Fuel (lb)	Duration (min)	Range (mi)	Cost (lb)	Error (%)
$C_I = 0$	Optimal	748.19	3.71	36.38	8244.63	$1.21 \cdot 10^{-4}$
	Sub-optimal	746.96	3.70	36.22	8244.64	
$C_I = 0.3$	Optimal	769.17	3.83	38.90	10232.23	$4.89 \cdot 10^{-4}$
	Sub-optimal	767.30	3.82	38.68	10232.28	
$C_I = 0.6$	Optimal	795.99	3.99	41.80	12056.17	$6.64 \cdot 10^{-4}$
	Sub-optimal	792.97	3.97	41.48	12056.25	

Note that, as CI increases, the time spent in the climb phase is larger. While this might seem incorrect at first, it is important to remember that spending more time in the climb results in less time spent during the cruise, which reduces the overall flight time. This interaction between climb and cruise is measured in the cost. Secondly, a climb time of approximately 3.8 might seem unreasonable. However, as explained in [46], the G-IV airplane used in this simulation is a very high performance business jet with an unusually high thrust-to-weight ratio, making it capable of reaching the desired height in the specified time. Moreover, in real flights aircraft must go through standard departure procedures and

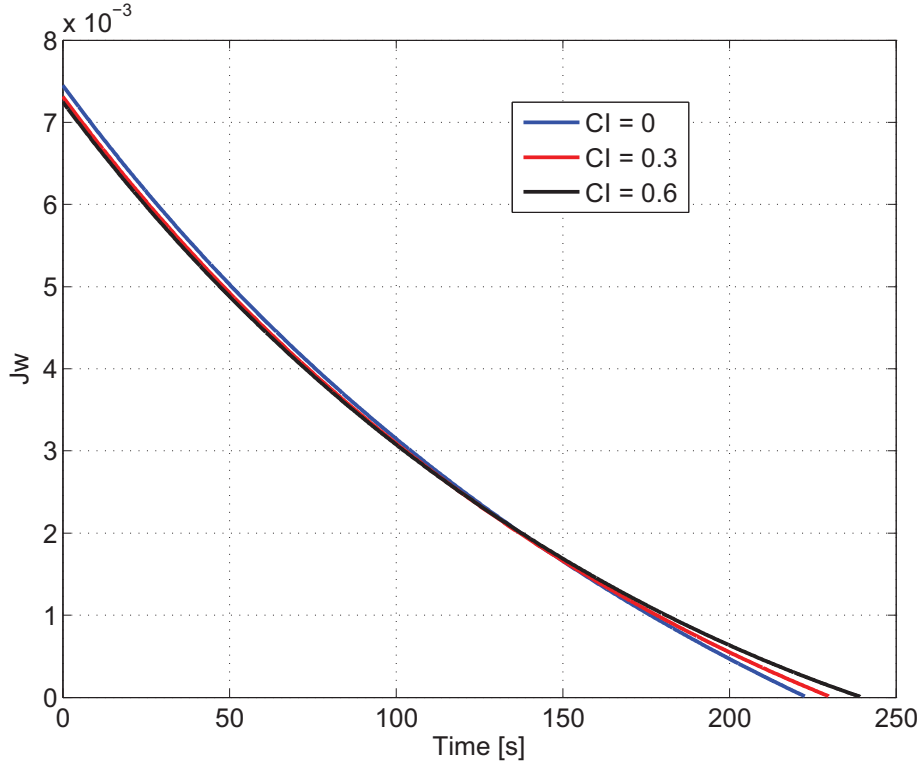


Figure 4.2: Costate J_W^* in climb as a function of time for different cost indexes.

a series of speed and altitude constraints after takeoff that add to the overall duration of the takeoff and climb phases [21]. The problem formulation in this thesis neglects these constraints allowing the aircraft to climb in an unconstrained manner, and as a result it reaches the desired cruise altitude in a short amount of time.

Overall, it can be seen in Table 4.1 that the relative error resulting from the cost difference between both control laws, computed as in (3.45), can be considered negligible for practical purposes. Moreover, increasing CI results in a longer range, pushing the TOC farther, which is the expected behavior as shown in Fig. 1.2 of section 1.3. This is also attested in Fig. 4.3 which shows the vertical profile of the aircraft as an range-altitude plot, generated using the sub-optimal solution, for the different values of CI. Finally, a noticeable change in the flight path angle during the phase can be appreciated from the graph.

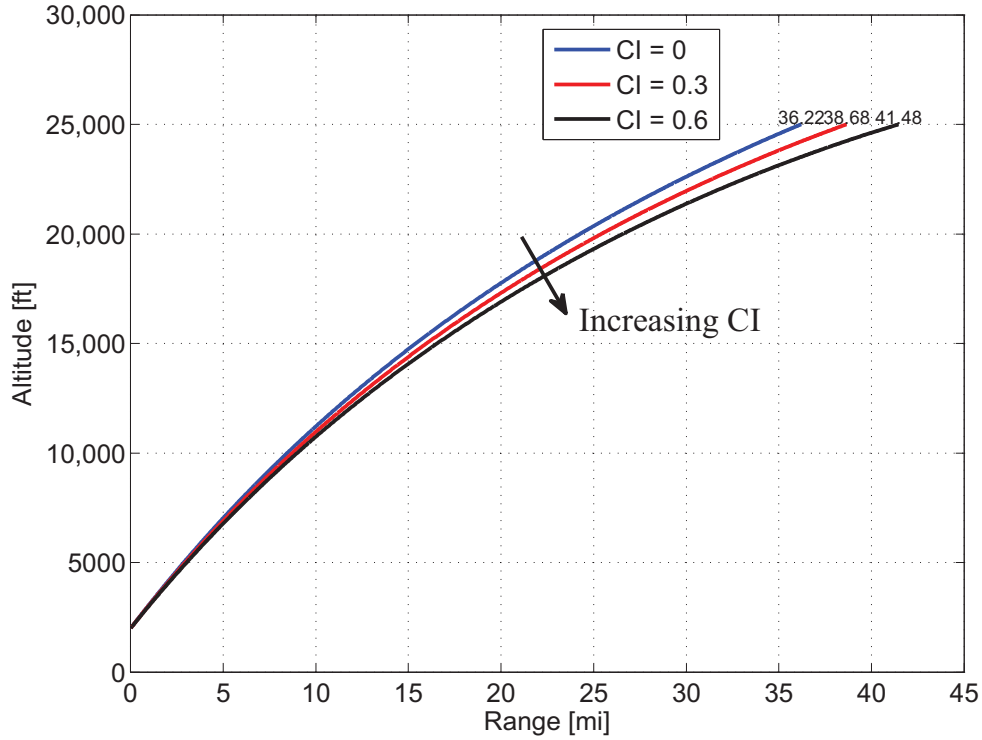


Figure 4.3: Climb vertical profile for different values of CI.

4.5 Economy Mode OCP for Descent

Formulating a descent OCP presents the same challenge as the climb, in the sense that the interaction between the descent and the other flight phases must be taken into account in order to achieve a meaningful result. However, if the descent is observed as a climb phase carried out backwards in time, it is possible to apply a similar approach to the one used in section 4.3, as explained below.

Problem Formulation Using the Principle of Optimality

During the descent, it is desired to go from an initial cruise altitude h_c to a specified final point (x_f, h_f) where the FMS is disengaged and the approach phase begins. The TOD, x_d , and the final time t_f are unknown and must be determined such that the operating costs are minimized. The initial descent weight W_d is considered given (the aircraft cruises before

descending, therefore when x_d is known W_d will be automatically determined). We go back to (4.32) which expresses the overall trip cost in integral form. Instead, this work proposes applying the same approach as the climb by solving the descent backwards in time, with the cruise cost-to-go added as a terminal cost function. Define

$$\tau(t) = t_f - t, \quad (4.52)$$

which implies

$$\frac{d\tau}{dt} = -1$$

$$\tau(0) = t_f \equiv \tau_f \quad (4.53)$$

$$\tau(t_c) = t_f - t_c \equiv \tau_c \quad (4.54)$$

$$\tau(t_d) = t_f - t_d \equiv \tau_d \quad (4.55)$$

$$\tau(t_f) = 0. \quad (4.56)$$

As a result, we can rewrite (4.32) in terms of τ yielding

$$J^* = \inf_{v, \tau_d, 0 \leq \tau \leq \tau_d} \left\{ \int_0^{\tau_d} (f_{f_{cl}} + C_I) d\tau + J_{cr,cl}^*(\tau_d, \zeta(\tau_d)) \right\}, \quad (4.57)$$

where

$$J_{cr,cl}^* = \inf_{v, \tau_d \leq \tau \leq \tau_f} \left\{ \int_{\tau_d}^{\tau_c} (f_{f_{cr}} + C_I) d\tau + \int_{\tau_c}^{\tau_f} (f_{f_{cl}} + C_I) d\tau \right\}.$$

In a similar manner as in section 4.3, we will assume that the climb cost is negligible when compared to the cruise, allowing to express $J_{cr,cl}^*$ as the cruise cost only. This is a stronger assumption than neglecting the descent with respect to the cruise, which becomes specially inaccurate in short flights. Longer flights, however, spend most of the time in the cruising segment, with the other two phases making a very small portion of the overall trip. As a result, the developments presented in this section can be considered valid for longer,

transcontinental flights.

As a result of the new time variable in (4.52), system dynamics (4.1) change to

$$\begin{aligned}\frac{dx}{d\tau} &= -v \\ \frac{dh}{d\tau} &= -v\gamma \\ \frac{dW}{d\tau} &= S_{FC}T_i.\end{aligned}\tag{4.58}$$

The initial and final conditions, specified in the initial paragraph of this subsection, must also change to match τ :

t	τ
$x(t_d) = x_d$	$x(\tau_d) = x_d$ unspecified
$x(t_f) = x_f$	$x(0) = x_f$
$h(t_d) = h_c$	$h(\tau_d) = h_c$
$h(t_f) = h_f$	$h(0) = h_f$
$W(t_d) = W_d$	$W(\tau_d) = W_d$
$W(t_f) = W_f$	$W(0) = W_f$ unspecified

Following the same procedure as in the climb, the optimal cruise cost is approximated by

$$J_{cr}^*(\tau_d) = \inf_{v, \tau_d \leq \tau \leq \tau_c} \left\{ \int_{\tau_d}^{\tau_c} (f_{f_{cr}} + C_I) d\tau \right\} \approx (f_{f_{cr}} + C_I) \frac{x_d - x_c}{v_{cr}},$$

which allows substituting $J_{cr,cl}^* \approx J_{cr}^*$ into (4.57) to obtain the descent cost functional

$$J^*(0) \approx \inf_{v, \tau_d} \left\{ \int_0^{\tau_d} (S_{FC}T_i + C_I) d\tau + (f_{f_{cr}} + C_I) \frac{x_d - x_c}{v_{cr}} \right\}.\tag{4.59}$$

In (4.59), f_{fcr} and v_{cr} are computed at a given initial descent weight W_d and

$$f_{fd} = S_{FC}T_i.$$

Before stating the OCP formally, an additional change of variables has to be made to account for the fact that $W(\tau)$ is known at the final time τ_d , but not at $\tau = 0$. Define the *fuel consumed* as

$$\widetilde{W}(\tau) = W(\tau) - W_f, \quad (4.60)$$

such that its dynamics are the same as $W(\tau)$ and its initial and final conditions become

$$\begin{aligned} W(0) = W_f \quad \text{unspecified} &\equiv & \widetilde{W}(0) = 0 \quad \text{given} \\ W(\tau_d) = W_d \quad \text{given} &\equiv & \widetilde{W}(\tau_d) = W_d - W_f \quad \text{unspecified} \end{aligned}$$

The ECON Descent OCP can then be stated mathematically in terms of the new variables τ and \widetilde{W} as follows:

$$J^*(0) = \min_{v, \tau_d} \left\{ \int_0^{\tau_d} (S_{FC}T_i + C_I) d\tau + (f_{fcr} + C_I) \frac{x_d - x_c}{v_{cr}} \right\}$$

s.t.

$$\dot{x} = -v$$

$$\dot{h} = -v\gamma$$

$$\dot{\widetilde{W}} = S_{FC}T_i$$

$$x(0) = x_f$$

$$h(0) = h_f, \quad h(\tau_d) = h_c$$

$$\widetilde{W}(0) = 0,$$

(4.61)

In (4.61), γ satisfies (4.20) and T_i is constant. Note the slight abuse of notation, where

\dot{x} denotes the derivative of x with respect to τ , and the same applies to the rest of the state variables.

Optimal solution

The following theorem states the solution to OCP (4.61).

Theorem 4.5.1. *The optimal solution to the ECON mode OCP for descent stated in (4.61) is given by the solution v of the equation*

$$[(1 + J_{\widetilde{W}}^*)S_{FC}T_i + C_I] (T_i - D - vD_v) + J_x^*v^2D_v = 0, \quad (4.62)$$

where γ is obtained from (4.20), J_x^* is given by

$$J_x^* = \frac{f_{cr} + C_I}{v_{cr}}, \quad (4.63)$$

and the time derivative of $J_{\widetilde{W}}^*$ equals

$$\dot{J}_{\widetilde{W}}^* = \left(\frac{J_x^*v}{\widetilde{W}} \right) \left(\frac{d_0v^4 - T_iv^2 - d_1}{3d_0v^4 - T_iv^2 - d_1} \right), \quad (4.64)$$

with final condition

$$J_{\widetilde{W}}^*(\tau_d) = 0. \quad (4.65)$$

Proof. The procedure presented in this section mirrors the one shown in the climb ECON problem. The Hamiltonian is defined as

$$H = (1 + J_{\widetilde{W}}^*)S_{FC}T_i - J_x^*v - J_h^*v\gamma + C_I, \quad (4.66)$$

which is minimized with respect to v by satisfying the necessary condition

$$\frac{\partial H}{\partial v} = -J_x^* - J_h^* (\gamma + v\gamma_v) = 0.$$

Substitute γ_v using (4.23) to obtain

$$J_x^* + J_h^* \left(\gamma - \frac{vD_v}{W} \right) = 0. \quad (4.67)$$

Equation (4.67) is identical to (4.40), the necessary condition for the climb. The costate J_x^* is constant since

$$\dot{J}_x^* = -\frac{\partial H}{\partial x} = 0. \quad (4.68)$$

In this OCP, the terminal cost is

$$\phi(x) = (f_{fcr} + C_I) \frac{x - x_c}{v_{cr}}, \quad (4.69)$$

and

$$\psi(h) = h - h_c. \quad (4.70)$$

As a result of J_x^* being constant, its value is given by its boundary condition, which yields

$$J_x^*(\tau_d) = J_x^* = (\phi_x + \nu\psi_x)|_{\tau_d} = \frac{f_{fcr} + C_I}{v_{cr}}.$$

When compared to (4.36), the above equation differs only in the positive sign. Solving for J_h^* in (4.67) gives

$$J_h^* = - \left(\frac{J_x^*}{\gamma - \frac{vD_v}{W}} \right), \quad (4.71)$$

therefore we do not need to study its time derivative and final value. For $J_{\widetilde{W}}^*$, we get

$$\dot{J}_{\widetilde{W}}^* = -\frac{\partial H}{\partial \widetilde{W}} = J_h^* v \gamma_{\widetilde{W}} \quad (4.72)$$

Differentiating (4.20) with respect to \widetilde{W} yields

$$\gamma_{\widetilde{W}} = \gamma_W = \frac{1}{W^2} (-D_W W - T_i + D).$$

Using the same procedure as the climb phase, (3.5) is differentiated with respect to W and substituted into $\gamma_{\widetilde{W}}$ along with (3.6) and (3.7) to get

$$\gamma_{\widetilde{W}} = -\frac{1}{W^2} \left(T_i - d_0 v^2 + \frac{d_1}{v^2} \right). \quad (4.73)$$

Substitute (4.73) into (4.72) to obtain

$$\dot{j}_{\widetilde{W}}^* = - \left(\frac{J_h^* v}{W^2} \right) \left(T_i - d_0 v^2 + \frac{d_1}{v^2} \right),$$

which results in the following equation after accounting for (4.20) and (4.71)

$$j_{\widetilde{W}}^* = \left(\frac{J_x^* v}{W} \right) \left(\frac{d_0 v^4 - T_i v^2 - d_1}{3d_0 v^4 - T_i v^2 - d_1} \right).$$

Again, it is important to remember that in this OCP the time derivatives are with respect to τ . The final value of this costate is given by

$$J_{\widetilde{W}}^*(\tau_d) = (\phi_{\widetilde{W}} + \nu \psi_{\widetilde{W}})|_{\tau_d} = 0.$$

We have that (4.66) and (4.69) do not depend explicitly on τ and τ_d is unspecified, therefore the HJB equation

$$0 = J_{\tau}^* + \min_v H,$$

reduces to

$$\min_v H = 0.$$

Replacing the Hamiltonian (4.66) into the HJB equation yields

$$\min_v \left\{ (1 + J_{\widetilde{W}}^*) S_{FC} T_i - J_x^* v - J_h^* v \gamma + C_I \right\} = 0,$$

or, at the optimal speed

$$(1 + J_{\widetilde{W}}^*) S_{FC} T_i - J_x^* v - J_h^* v \gamma + C_I = 0. \quad (4.74)$$

Substitute (4.71) into (4.74) to get

$$\begin{aligned} & (1 + J_{\widetilde{W}}^*) S_{FC} T_i - J_x^* v + C_I + \frac{J_x^* v \gamma}{\left(\gamma - \frac{v D_v}{W}\right)} = 0 \\ \equiv & \left[(1 + J_{\widetilde{W}}^*) S_{FC} T_i + C_I \right] \left(\gamma - \frac{v D_v}{W} \right) + \frac{J_x^* v^2 D_v}{W} = 0, \end{aligned}$$

or, after using (4.20)

$$\left[(1 + J_{\widetilde{W}}^*) S_{FC} T_i + C_I \right] (T_i - D - v D_v) + J_x^* v^2 D_v = 0.$$

□

Remark: The same situation happens in descent as in the climb regarding the minimum fuel solution. If C_I is zero in (4.62), the minimum ROD speed shown in Section 4.2.2 is not obtained. The only way for both solutions to coincide is to eliminate the terminal cost in the OCP, making J_x^* vanish in (4.67).

Deriving a sub-optimal control law

Equation (4.62) yields the exact solution to the optimal true airspeed v , provided that $J_{\widetilde{W}}^*$ is known a-priori. Following the same procedure as the climb, assumptions will be made to derive a simplified polynomial that can be solved for a sub-optimal control input in state feedback form.

It will be assumed that the left bracket term in (4.64) is much smaller than the rightmost one, implying that $W \gg J_x^*v$, then $\dot{J}_{\widetilde{W}}^* \approx 0$. Using the G-IV model presented in 3.4.1, an example will be shown to validate this assumption. Suppose $h = 5000$ ft, corresponding to a density of $\rho = 2 \times 10^{-3}$ slug/ft³, the desired cruise altitude is $h_c = 25000$ ft and the aircraft gross weight is $W = 70000$ lbf. For $C_I = 0$, the cruise fuel flow rate is $f_{f_{cr}} = 1.07$ lbf/s and the optimal speed is $v_{cr} = 536.48$ ft/s, as computed using the CruiseOptimalSPeedAndFuelFlow.m function from Appendix A. Recall from the aircraft model that $T_i = 200$ lbf. Then from (4.63) we get $J_x^* = 0.002$ and, referring to (4.64), the following values of the left bracket term, right bracket term and $\dot{J}_{\widetilde{W}}^*$ are obtained for different descent speeds

$$\begin{aligned}
v = 350 \text{ ft/s} : \quad & \text{Left bracket} = 1.00 \times 10^{-5}, \quad \text{Right bracket} = -0.91, \quad \dot{J}_{\widetilde{W}}^* = -9.10 \times 10^{-6} \\
v = 400 \text{ ft/s} : \quad & \text{Left bracket} = 1.15 \times 10^{-5}, \quad \text{Right bracket} = -0.09, \quad \dot{J}_{\widetilde{W}}^* = -1.02 \times 10^{-6} \\
v = 450 \text{ ft/s} : \quad & \text{Left bracket} = 1.29 \times 10^{-5}, \quad \text{Right bracket} = 0.12, \quad \dot{J}_{\widetilde{W}}^* = 1.48 \times 10^{-6}.
\end{aligned}$$

We can conclude from this example that the above considerations appear reasonable from a physical point of view. As a result, we assume that $\dot{J}_{\widetilde{W}}^*$ is negligible and that $J_{\widetilde{W}}^* \approx 0$, which is its final value according to (4.65). In light of this assumption, (4.62) is simplified to

$$(S_{FC}T_i + C_I)(T_i - D - vD_v) + J_x^*v^2D_v = 0,$$

which yields a 5th degree polynomial in v given by

$$-2J_x^*d_0v^5 + 3(S_{FC}T_i + C_I)d_0v^4 - (S_{FC}T_i + C_I)T_iv^2 + 2J_x^*d_1v - (S_{FC}T_i + C_I)d_1 = 0. \quad (4.75)$$

The sub-optimal equation (4.75) differs with respect to the climb solution (4.48) because T_c was replaced by T_i and the signs of the terms involving J_x^* are symmetric. Nevertheless, J_x^* itself is negative during climb and positive during descent, so when replaced in the respective equations the opposite signs cancel resulting in the same expression for both phases, with

$T = T_c$ for climb and $T = T_i$ for descent. Equation (4.75) involves only the speed, J_x^* and the state variables, therefore it can be thought of as a state-feedback law. To obtain the optimal v , a numerical method has to be implemented for finding the roots of a polynomial.

The validation scheme designed to demonstrate the accuracy of the result and of the assumption $J_W^* \approx 0$ will be presented in the next section.

4.6 Validation of Descent Results

All simulations conducted in this section use the aircraft model presented in Section 3.4.1.

4.6.1 Shooting Method for Descent

To form the augmented system, the dynamics in terms of τ are taken from (4.58), that is, with $W(\tau)$ instead of $\widetilde{W}(\tau)$. The latter was used to correctly formulate the OCP in a standard form as in (2.24), where all initial conditions are specified. However, a value for the weight W is required for the aerodynamic calculations. In the simulations we will assign a value to $W(0) = W_f$. In a practical setting the final aircraft weight W_f cannot be known in advance, but this modification of the problem does not invalidate the results since the measurements that assess the optimality of the solution are the amount of fuel consumed during the phase and the phase duration. Moreover, $J_W^* = J_{\widetilde{W}}^*$, therefore the conclusions drawn for the former also apply to the latter.

The augmented system is formed from (4.58) and (4.64), resulting in

$$\begin{aligned}
\dot{x} &= -v \\
\dot{h} &= -v\gamma \\
\dot{W} &= S_{FC}T_i \\
j_W^* &= \left(\frac{J_x^* v}{W} \right) \left(\frac{d_0 v^4 - T_i v^2 - d_1}{3d_0 v^4 - T_i v^2 - d_1} \right) \\
x(0) &= x_f, x(\tau_d) \quad \text{unspecified} \\
h(0) &= h_f, h(\tau_d) = h_c \\
W(0) &= W_f, W(\tau_d) \quad \text{unspecified} \\
J_W^*(0) &\text{ unspecified, } J_W^*(\tau_d) = 0,
\end{aligned} \tag{4.76}$$

where the control inputs are obtained at each time-step by solving (4.20) and (4.62) simultaneously, with $J_W^* = J_W^*$. The system (4.76) is given in terms of τ , but the results can be recovered forward in time by mirroring the plots with respect to the time axis. The algorithm implements the following pseudo-code:

1. Compute J_x^* from (4.63), evaluating $f_{f_{cr}}$ and v_{cr} at h_c and W_f .
2. Choose $J_W^{*(0)}(0)$:
 - (a) Estimate an initial value for the speed $v(0)$ from practical experience
 - (b) Compute $\gamma(0)$ from (4.20)
 - (c) Solve for J_W^* from (4.62) and evaluate at $\tau = 0$, yielding the following estimate:

$$J_W^{*(0)}(0) = - \left[1 + \frac{C_I}{S_{FC}T_i} + \frac{J_x^* v^2 D_v}{S_{FC}T_i (T_i - D - v D_v)} \right] \Big|_{\tau=0} \tag{4.77}$$

3. Let $k = 0$

4. Do:

- (a) Simulate (4.76) until $h(\tau) = h_c$, then $\tau_d = \tau$
- (b) Compute $\epsilon = J_W^{*(k)}(\tau_d) - J_W^*(\tau_d)$
- (c) Compute next seed $J_W^{*(k+1)}(0)$ using the update law:

$$J_W^{*(k+1)}(0) = J_W^{*(k)}(0) - \beta\epsilon \quad (4.78)$$

- (d) $k = k + 1$

5. Until $|\epsilon| < \text{tolerance}$ OR $k \geq \text{Max. Iterations}$

The tuning parameter β equals one for this problem. An example will now be shown that compares the numerical solution with the sub-optimal one resulting from (4.75). The Matlab code that implements the algorithms is presented in Appendix C.

4.6.2 Comparison between the optimal and sub-optimal trajectories

The initial and final conditions for this exercise are

$$x_c = 0 \quad \text{mi}$$

$$x_f = 1000 \quad \text{mi}$$

$$h_c = 25000 \quad \text{ft}$$

$$h_f = 2000 \quad \text{ft}$$

$$W_f = 55000 \quad \text{lb},$$

where x_c is only relevant to compute the cost. As explained previously, the simulation is carried out backwards in time, but the plots presented in this section have been corrected to show the results forward in time. Fig. 4.4 compares the optimal speed profile as a function of time for different values of CI, with the solid line representing the shooting-method and the

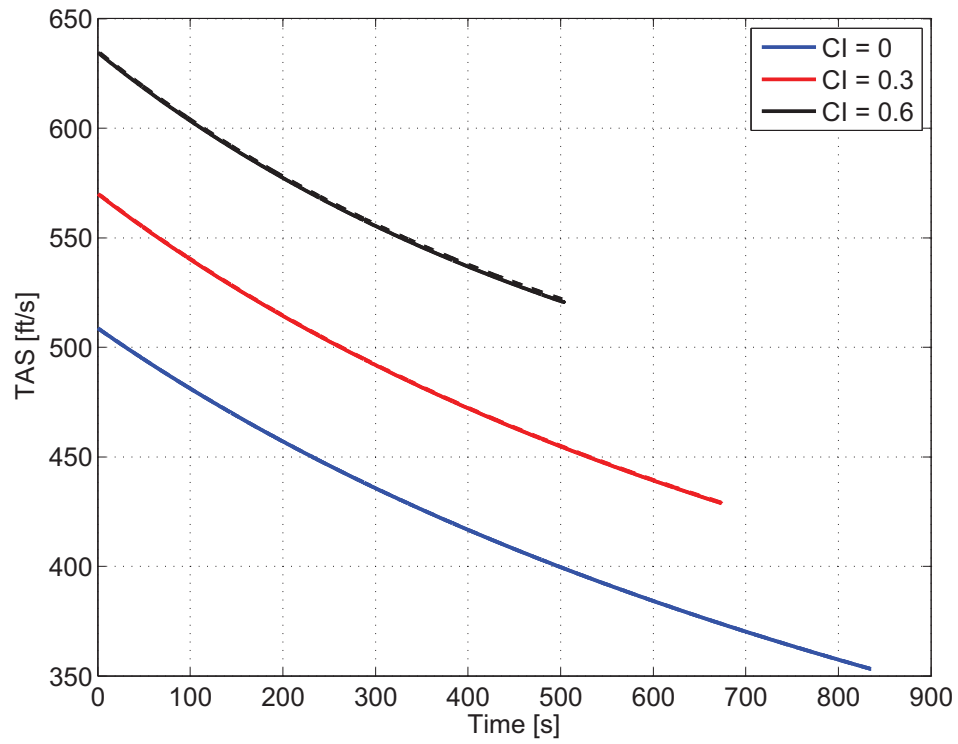


Figure 4.4: Comparison between the optimal and sub-optimal descent speeds for different cost indexes. The solid line represents the optimal solution, while the dashed line is the sub-optimal one.

dashed line representing the sub-optimal law. There is no discernible difference between each pair of curves: they look identical to the naked eye. In addition, a plot of J_W^* as a function of time for each CI is shown in Fig. 4.5 (recall that the plots are being shown forward in time, therefore J_W^* starts at zero, which is its “final value” when the problem is solved backwards in time). We have that $|J_W^*| < 3 \times 10^{-3}$, which validates the assumption that $J_W^* \approx 0$. It can be shown that the sign changes in \dot{J}_W^* occur in the right bracket term of (4.64), which does not happen in the climb because T_c is much larger than T_i .

In Table 4.2 the fuel consumed, time elapsed, range and cost incurred are compared for each example. Just like in the climb section, the cost was computed from (4.59), manipulated as follows:

$$J = W(\tau_d) - W(0) + C_I \tau_d + \left(\frac{f_{fcr} + C_I}{v_{cr}} \right) (x_c - x_d)$$

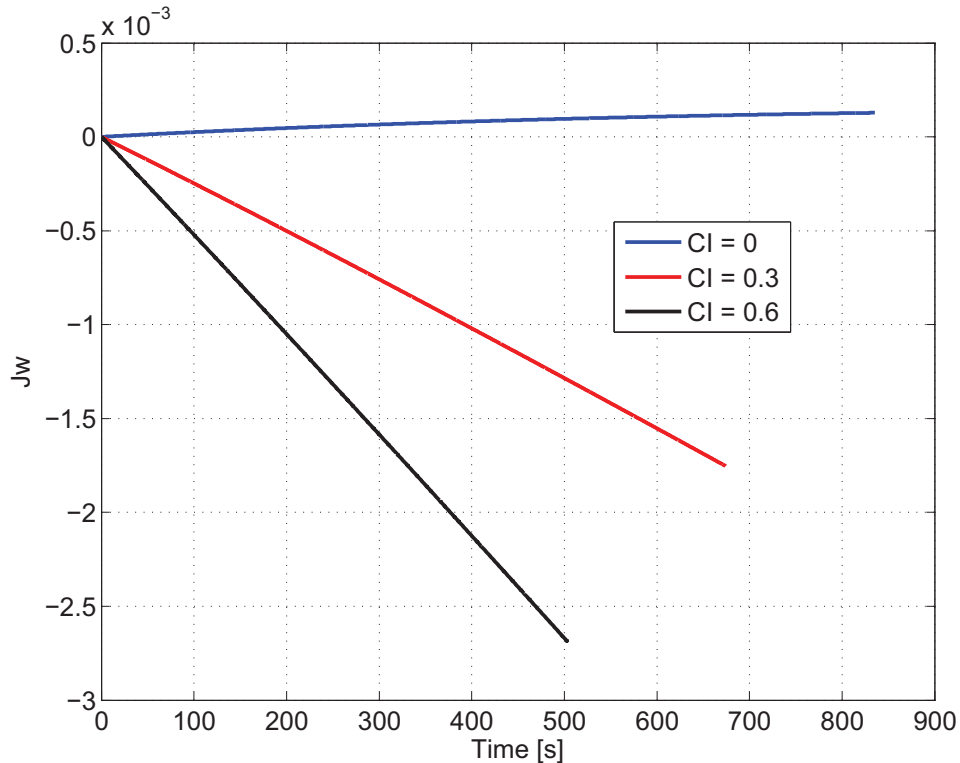


Figure 4.5: Costate J_W^* in descent as a function of time for different cost indexes.

Note that, as CI increases, the fuel consumed during the descent decreases, which might appear as incorrect. However, spending less time in the descent (which translates into less

Table 4.2: Descent fuel, time, range and cost comparison for different values of CI.

		Fuel (lb)	Duration (min)	Range (mi)	Cost (lb)	Error (%)
$C_I = 0$	Optimal	32.02	13.92	66.18	6337.76	0
	Sub-optimal	32.02	13.92	66.18	6337.76	
$C_I = 0.3$	Optimal	25.85	11.24	62.33	8684.42	$1.15 \cdot 10^{-4}$
	Sub-optimal	25.83	11.23	62.31	8684.43	
$C_I = 0.6$	Optimal	19.31	8.39	54.14	10761.87	$1.86 \cdot 10^{-4}$
	Sub-optimal	19.24	8.36	54.03	10761.89	

fuel consumed the descent) implies that more time is spent cruising, thereby increasing the overall trip fuel consumption in favor of a shorter flight time. Secondly, the descent phase takes much longer than the climb, which lasted about 3.8 minutes in the example of section 4.4.2. This is a direct result of the idle thrust being much smaller than the maximum climb thrust because, as shown in (2.18), the rate of descent depends on the difference between the thrust and the drag. For a small $T = T_i$, this difference is not as significant as the case $T = T_c$ and therefore the resulting vertical speed is smaller.

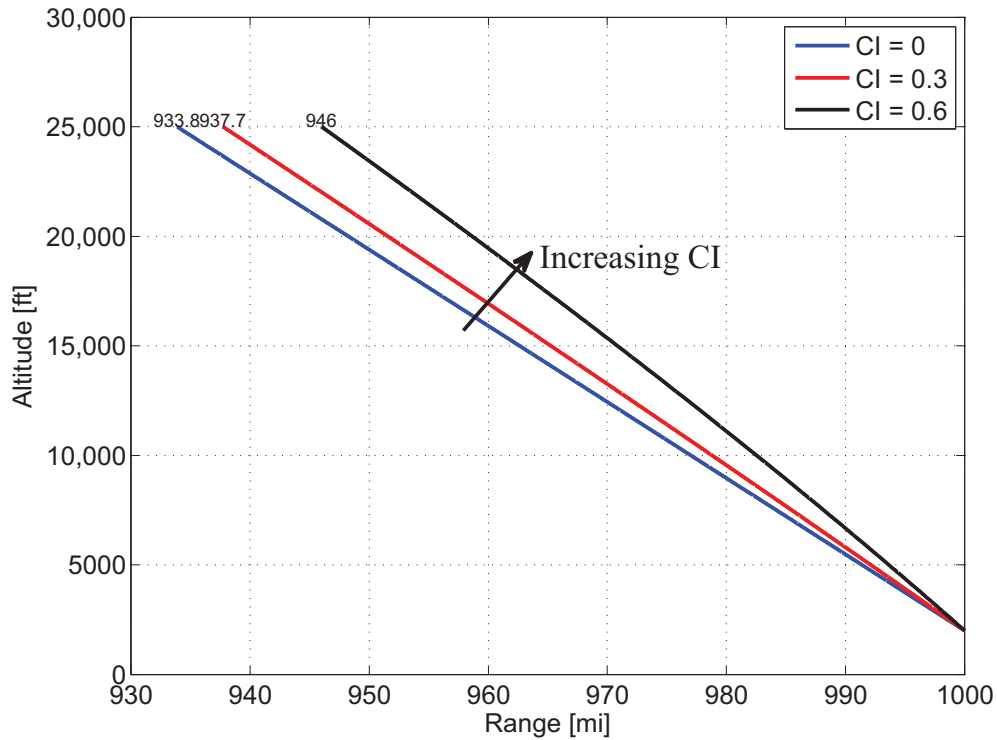


Figure 4.6: Descent vertical profile for different values of CI.

Overall, Table 4.6 shows that the relative error, computed as in (3.45), can be considered negligible for practical purposes. Moreover, the expected behavior for the TOD, depicted in Fig. 1.2 of section 1.3, is recovered: increasing CI results in a shorter range pushing this waypoint farther and making the cruise phase longer. This is also attested in Fig. 4.6 which shows the descent profile as a range-altitude plot, generated using the sub-optimal solution for each value of CI. An important difference between the climb and descent is that there is no noticeable change in the flight path angle in the latter. In fact, the TOD and the final waypoint seem to be connected by a straight line. This finding is considered in the next section, where a scheme is proposed to estimate the TOD waypoint during the cruise segment of the flight.

4.7 Practical consideration: Estimation of the Top-of-Descent

The descent solution proposed in this work has been attained by proposing an OCP that is solved backwards in time. This approach has allowed to obtain sub-optimal expressions for the speed and flight path angle that minimize operating costs. However, real aircraft do not fly backwards in time, thus the TOD waypoint must be estimated a-priori during the cruise segment. This waypoint can be estimated following the approach presented in this section.

Looking at the simulation results, it can be concluded that the descent flight path angle does not change significantly during the phase. Suppose that we can approximate γ by a constant value. Then we have the situation depicted in Fig. 4.7. For a constant γ , the following relation is satisfied

$$\tan(\gamma) = -\frac{h_c - h_f}{x_f - x_d},$$

where the negative sign results from the descent angle being negative. Then, we can solve

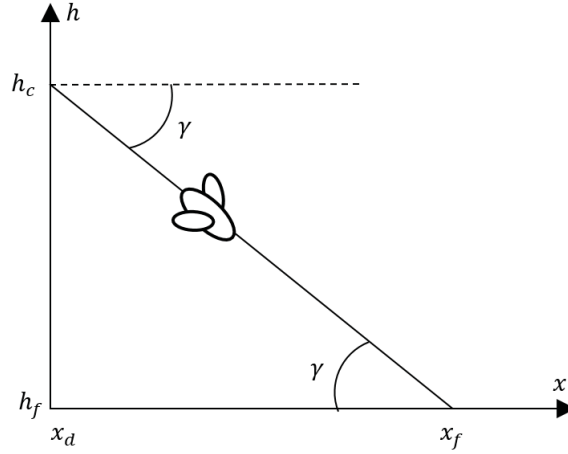


Figure 4.7: Estimating the top-of-descent.

for the descent range yielding

$$(x_f - x_d) = -\frac{h_c - h_f}{\tan(\gamma)} \quad (4.79)$$

Provided that γ is nonzero (which is the case in the descent phase), then (4.79) allows computing the TOD which equals x_d , because x_f is known. During cruise, estimations of the optimal descent v and γ can be made using (4.75) and (4.20) evaluated at the current aircraft gross weight. Then, using those estimates, (4.79) gives an approximate TOD. As the aircraft approaches the real x_d , its gross weight converges to the real weight at the start of the descent phase, W_d . As a result the estimate of the TOD will converge to the real TOD. The only assumption made here is that γ can be approximated by its value at the start of the descent but, as shown in the simulations, this is a perfectly reasonable assumption.

Chapter 5

Conclusions and Future Work

5.1 Conclusions

This thesis has presented a novel approach for solving the Economy Mode problem in FMS. Using techniques from optimal control theory and algebraic manipulations, an analytic sub-optimal solution has been found for the true airspeed that minimizes operating costs for the cruise phase of the flight. For climb and descent, finding a root of the resulting polynomial that lies in the flight envelope of the aircraft is proposed for on-board implementation using an iterative approach, such as Newton's method. In all the examples shown, the relative error between the optimal and the sub-optimal costs is less than $1 \cdot 10^{-2}\%$, which is small enough to be considered negligible in practical scenarios.

The merits of the contributions of this thesis are:

- The airspeed target is in a state-feedback form, thereby avoiding time dependencies that require offline computations which are common in the open literature and in some implementations. Moreover, a state-feedback law is more robust in the sense that will correct small deviations from the optimal trajectory due to possible disturbances. From a control systems point of view, the FMS under this scheme works as an outer feedback loop, while the inner loop consists of the autopilot.

- Solving for the speed directly eliminates the need of having a performance database storing the optimal speed schedules in the system. Thus, errors due to interpolation between points are avoided and the implementation becomes faster. If a performance database is needed, a look-up table can be created as a function of CI and the state variables using the proposed sub-optimal equations.
- The climb and descent solutions are not analytic, but the roots of the polynomial involved can be found using very simple numerical methods, such as Newton's method. To ensure a fast convergence, the speed computed at the previous time-step can be used. This is an effective solution because, as shown in the simulations, the optimal speed does not change much over small periods of time. In fact, the FMS does *not* have to obtain new targets at a very high frequency. The flight management computer would have plenty of time to compute the next set-point numerically between time-steps.
- From a theoretical standpoint, this formulation provides a significant contribution as it falls in line with the well-known performance theory present in most books today. Using this methodology, the maximum-range solution has been recovered when CI vanishes during cruise, and (3.30) extends the theory naturally and elegantly to a more general case where CI is not zero. In addition, it unifies all the well-known performance results, such as maximum endurance and rate of climb, under a single approach.

From this work we can conclude that:

- Practically relevant problems such as the FMS Economy Mode can be formulated as optimal control problems that can be treated analytically, provided that the correct assumptions and simplifications are made. While the cruise formulation was simple enough to perform algebraic manipulations, the climb and descent problems required that the terminal cost (which is the optimal cost-to-go of the cruise phase) be approximated by a simpler expression involving the cruise fuel flow evaluated at the initial aircraft weight. This allowed approaching the problem analytically, something that

would have been otherwise impossible. As a result, making the right assumptions is an important step in profiting from the optimal control techniques described in this work.

- The behavior of the TOC and TOD, stated but not derived formally in publications such as [10, 11], can be verified and explained using Bellman’s principle of optimality, which models the correlation between the time spent climbing/descending and the time spent cruising. In addition, because each phase utilizes different thrust settings, their impact on the overall fuel consumption and flight time is different. As a result the placement of these two waypoints becomes an important factor in the optimization. Considering the climb and descent as isolated phases would not have yielded the same results: in fact, as shown in Chapter 4, the inclusion of the cost index into the problem does not make sense until the influence of the cruise phase is taken into account.

5.2 Extensions

Several extensions to this work can be proposed for future research, namely:

- Account for wind speeds during the flight. In reality, the existence of wind is one of the most important factors in a commercial flight, thus the assumption that the wind speed is zero is the strongest one in this work. Suppose that v_w denotes the speed of the headwind (pointing in the direction of $-\hat{x}_h$, which is part of the horizon axes system as defined in section 2.1.3), then the \dot{x} equation from the aircraft model in (2.6) would change to [47]

$$\dot{x} = v \cos(\gamma) - v_w,$$

with \dot{h} and the dynamic equations being unchanged. The aerodynamic forces and specific fuel consumption would remain as functions of the true airspeed. Therefore the assumptions and OCPs in this thesis would have to account for this modified state-space model. Even for this simple modification, it will not be possible to obtain a polynomial in the cruise phase that is solvable analytically because cross terms that multiply v and

v_w appear in the HJB equation. A similar problem would be present in the climb and descent phases. The equations of motion for more complex wind scenarios are discussed in [47].

- Study the impact of the flight length on the validity of the assumptions made to obtain the sub-optimal solutions. For each flight phase, the costate J_W^* (or $J_{\bar{W}}^*$ for the descent) was approximated by zero, which is its final value. This assumption is less valid for longer flights. On the other hand, when using the principle of optimality, the assumption that the optimal cost-to-go for the rest of the flight can be approximated by the cruise cost holds only for long flights, where the cruise phase dominates. As a result, an interesting extension would involve finding the best compromise between the flight length and the error due to these assumptions between the sub-optimal trajectory and the optimal one.
- Find better approximations for J_W^* . Note that making $J_W^* \approx 0$ is a zero-order Taylor series expansion in the backward time variable τ , around $\tau = 0$, which is the final condition. However, if its time derivative \dot{J}_W^* could be estimated at the final time, then a first-order Taylor series expansion could be made about that point yielding a better estimate for this costate. A potential drawback of this approach is that the resulting expression would depend on time. As a result, when substituting J_W^* on the optimal solutions, a time-dependent state-feedback law would be obtained.
- Consider transition periods between phases. Note that the optimal speed for the climb found using (4.35) does not coincide with the cruise optimal solution (3.21) when $h = h_c$, and similarly between cruise and descent. Therefore, a period has to exist between these phases where the aircraft transitions from one speed target to the other. Initially, this period could be handled by the autopilot. However, it would be an interesting extension to find the optimal way to change phases, based on the theory of optimal control.
- Extend the formulation to support step climbs during cruise. The main idea is to allow

the aircraft to change between ATC-allowed flight levels during cruise to account for changes in its optimum altitude. Current FMS already support step-climb, but they must be initiated manually by the pilot. An interesting optimal control formulation would be finding the “best” point to change altitude while cruising.

- Explicitly account for state and input constraints in the mathematical formulation, given by the flight envelope of the aircraft. While the current assumption that all points lie inside the flight envelope is valid for most practical scenarios, it is important to guarantee that the aircraft does not exceed its structural limits specially when flying at a high CI value. Using the current formulation, either one can compute CI to ensure the constraints are verified (see remark 2 in section 3.3) or, otherwise, these constraints must be enforced *after* the optimal set-points are found. To obtain an optimal trajectory when close to the boundaries of the flight envelope, the constraints must be explicitly incorporated in the optimal control problem.
- Compute the optimum altitude, defined as the height where operating costs are minimal. Current FMS compute this value.
- Formulate and solve a Required Time of Arrival (RTA) problem. This mode was mentioned in Section (1.2), and its purpose is to ensure that a particular waypoint is reached within a prescribed time window. It would also allow accounting for strict time of arrival constraints at the destination airport. From an optimal control point of view, these situations would imply that the final times in the OCPs are now prescribed. Accounting for these modifications is out of the scope of this thesis, and a preliminary approach could be to change CI such that the given time constraint is satisfied.

Bibliography

- [1] P. N. E. A. Agency, “Trends in global co2 emissions report,” 2014. Accessed January 2015.
- [2] U. E. I. A. (EIA), “U.s. energy-related carbon dioxide emissions in 2013,” 2014. Accessed January 2015.
- [3] T. Guardian, “Air traffic growth rates will outpace emissions reductions, research shows,” 2014. Accessed January 2015.
- [4] N. Rivers, “Are low oil prices good for the environment?,” December 2014. From the Ottawa Citizen. Accessed January 2015.
- [5] F. A. Administration, *Instrument Flying Handbook*. U.S. Department of Transportation, 2007.
- [6] S. Liden, “The evolution of flight management systems,” in *13th AIAA/IEEE Digital Avionics Systems Conference*, pp. 157–169, October 1994.
- [7] R. Walter, *The Avionics Handbook, Chapter 15: Flight Management Systems*. CRC Press, 2001.
- [8] Z. Sibin, L. Guixian, and H. Junwei, “Research and modelling on performance database of flight management systems,” in *2nd International Asia Conference on Informatics in Control Automation and Robotics (CAR)*, pp. 295–298, March 2010.

- [9] A. Industries, “Getting to grips with the cost index.” Flight Operations Support and Line Assistance, 1998.
- [10] Boeing, “Jet transport performance methods (d6-1420),” 2009.
- [11] B. Roberson, “Fuel conservation strategies: Cost index explained.” Boeing AERO Magazine QTR_02, 2007.
- [12] W. Roberson, “Fuel conservation strategies: Cruise flight.” Boeing AERO Magazine QTR_04, 2007.
- [13] A. Industries, “Getting to grips with aircraft performance.” Flight Operations Support and Line Assistance, 2002.
- [14] D. E. Kirk, *Optimal Control Theory: An Introduction*. Prentice-Hall, 1970.
- [15] M. Athans and P. L. Falb, *Optimal Control: An Introduction to the Theory and its Applications*. Dover Publications, 2006.
- [16] D. Liberzon, *Switching in Systems and Control*. Boston, USA: Birkhuser, 2003.
- [17] A. E. Bryson and Y. Ho, *Applied Optimal Control: Optimization, Estimation and Control*. Taylor and Francis Group, 1975.
- [18] L. S. Pontryagin, V. Boltyanskii, R. V. Gamkrelidze, and E. F. Mischenko, *The Mathematical Theory of Optimal Processes*. Interscience Publishers, Inc., 1962.
- [19] R. E. Bellman, *Dynamic Programming*. Princeton University Press, 1957.
- [20] P. L. et M. G. Grandall, “Viscosity solutions of hamilton-jacobi equations,” *Trans. Amer. Math. Soc.* 277, pp. 1–42, 1983.
- [21] W. Roberson, “Fuel conservation strategies: Takeoff and climb.” Boeing AERO Magazine QTR_04, 2008.

- [22] W. Roberson and J. A. Johns, “Fuel conservation strategies: Descent and approach.” Boeing AERO Magazine QTR.02, 2010.
- [23] S. Liden, “Optimum 4d guidance for long flights,” in *Digital Avionics Systems Conference*, pp. 262–267, October 1992.
- [24] S. Liden, “Flight management system providing minimum total cost,” 1988. US Patent 4,760,530.
- [25] S. Liden, “Apparatus and method for computing wind-sensitive optimum altitude steps in a flight management system,” 1996. US Patent 5,574,647.
- [26] N. Chui, “The development of a dynamic test bed for flight management systems,” 2002. M. A. Sc. thesis, Concordia University.
- [27] A. Tewari, *Advanced Control of Aircraft, Spacecraft and Rockets*. John Wiley and Sons, 2011.
- [28] H. Erzberger, “Optimum climb and descent trajectories for airline missions,” in *AGARD Theory and Applications of Optimal Control in Aerospace Systems*, July 1981.
- [29] J. Sorensen, S. A. Morello, and H. Erzberger, “Applications of trajectory optimization principles to minimize aircraft operating costs,” in *18th IEEE Conference on Decision and Control including the Symposium on Adaptive Processes*, pp. 415–421, December 1979.
- [30] S. Wu and Y. Shen, “Studies on the flight performance optimization of commercial aircrafts,” in *IEEE Region 10 Conference on Computer, Communication, Control and Power Engineering*, vol. 4, pp. 139–145, October 1993.
- [31] S. Wu and S. Guo, “Optimum flight trajectory guidance based on total energy control of aircraft,” *Journal of Guidance, Control, And Dynamics*, vol. 17, March 1994.

- [32] J. Burrows, “Fuel-optimal aircraft trajectories with fixed arrival times,” *Journal of Guidance, Control and Dynamics*, vol. 6, pp. 14–19, January 1983.
- [33] P. Hagelauer and F. Mora-Camino, “Evaluation of practical solutions for onboard aircraft four-dimensional guidance,” *Journal of Guidance, Control and Dynamics*, vol. 20, no. 5, pp. 1052–1054, 1997.
- [34] Y. Diaz-Mercado, S. Lee, M. Egerstedt, and S.-Y. Young, “Optimal trajectory generation for next generation flight management systems,” in *IEEE/AIAA 32nd Digital Avionics Systems Conference*, pp. 3C5–1–3C5–10, October 2013.
- [35] M. C. Waller, “Considerations in the application of dynamic programming to optimal aircraft trajectory generation,” in *Proceedings of the IEEE Aerospace and Electronics Conference*, vol. 2, pp. 574–579, May 1990.
- [36] P. Hagelauer and F. Mora-Camino, “A soft dynamic programming approach for on-line aircraft 4d-trajectory optimization,” *European Journal of Operational Research* 107, pp. 87–95, 1998.
- [37] H. Wu, N. Cho, H. Bouadi, L. Zhong, and F. Mora-Camino, “Dynamic programming for trajectory optimization of engine-out transportation aircraft,” in *24th IEEE Chinese Control and Decision Conference*, pp. 98–103, 2012.
- [38] N. K. Wickramasinghe, A. Harada, H. Totoki, T. Miyamoto, and Y. Miyazawa, “Flight trajectory optimization for modern jet passenger aircraft with dynamic programming,” in *Lecture Notes in Electrical Engineering: Air Traffic Management and Systems*, pp. 87–104, Springer, 2014.
- [39] R. Almgren and A. Tourin, “Optimal soaring via hamilton-jacobi-bellman equations.” Social Science Research Network (SSRN), February 2014.

- [40] S. Khardi, “Applied methods validating aircraft flight path optimization. theoretical and experimental considerations,” in *HIKARI Ltd. Applied Mathematical Sciences*, vol. 7, pp. 2209–2228, 2013.
- [41] B. Tian and Q. Zong, “3dof ascent phase trajectory optimization for aircraft based on adaptive gauss pseudospectral method,” in *IEEE Third International Conference on Intelligent Control and Information Processing*, pp. 431–435, July 2012.
- [42] P. Bonami, A. Olivares, M. Soler, and E. Staffetti, “Multiphase mixed-integer control approach to aircraft trajectory optimization,” *Journal of Guidance, Control and Dynamics*, vol. 36, pp. 1267–1277, September 2013.
- [43] S. G. Park and J. Clarke, “Fixed rta fuel optimal profile descent based on analysis of trajectory performance bound,” in *IEEE/AIAA 31st Digital Avionics Systems Conference*, pp. 3D3-1 – 3D3-13, October 2012.
- [44] R. Drury, A. Tsourdos, and A. Cooke, “Real-time trajectory generation: Improving the optimality and speed of an inverse dynamics method,” in *IEEE Aerospace Conference*, pp. 1–12, March 2010.
- [45] R. S. Shevell, *Fundamentals of Flight*. Prentice Hall, 2 ed., 1988.
- [46] J. D. Anderson, *Aircraft Performance and Design*. WCB/McGraw-Hill, 1999.
- [47] D. G. Hull, *Fundamentals of Airplane Flight Mechanics*. Springer, 2007.
- [48] M. Saarlal, *Aircraft Performance*. John Wiley and Sons Inc., 2007.
- [49] S. Boyd, *Convex Optimization*. Cambridge University Press, 2004.
- [50] D. Liberzon, *Calculus of Variations and Optimal Control Theory: A Concise Introduction*. Princeton University Press, 2012.
- [51] R. Horn and C. Johnson, *Matrix Analysis*. Cambridge University Press, 1990.

- [52] R. E. Bellman and S. E. Dreyfus, *Applied Dynamic Programming*. Princeton University Press, 1962.
- [53] G. Aerospace, “Gulfstream g450 technical specifications.” <http://www.gulfstream.com/aircraft/gulfstream-g450>. Accessed 12-2014.

Appendix A

Validation Code for the Cruise Phase

The code developed for validation purposes is composed of the following Matlab and Simulink files:

atmosphere_standard.m

This function returns the International Standard Atmosphere (ISA) temperature, pressure and density at a given altitude h . It follows the model in Section 2.1.1. The code is shown below.

```
1 %%%%%%%%%%%%%%%%%%%%%%%%%%%%%%%%%%%%%%%%%%%%%%%%%%%%%%%%%%%%%%%%%%%%%%%%%%
2 %
3 % Filename: atmosphere_standard.m
4 %
5 % Purpose: Returns the International Standard Atmosphere characteristics at
6 %           the given
7 %           density altitude , in imperial units .
8 %%%%%%%%%%%%%%%%%%%%%%%%%%%%%%%%%%%%%%%%%%%%%%%%%%%%%%%%%%%%%%%%%%%%%%%%%%
9
10 function [temperature , pressure , density]=atmosphere_standard(h)
11
12 % Obtain atmosphere parameters at a given altitude for standard sea level
```

```

13 % conditions:
14 % Ts=518.69 R
15 % ps=2116.2 lb/ft^2
16 % rho_s=2.3769e-3 slugs/ft^3
17
18 if ((h>=0) && (h<=36150)) % Troposphere
19     temperature = 518.69 - 3.5662e-3*h;
20     pressure     = 1.1376e-11*temperature^5.256;
21     density      = 6.6277e-15*temperature^4.2560;
22 elseif ((h>36150) && (h<=82300)) % Stratosphere I
23     temperature = 389.99;
24     pressure     = 2678.4*exp(-4.8063e-5*h);
25     density      = 1.4939e-6*pressure;
26 elseif (h>82300) % Stratosphere II
27     temperature = 389.99+5.4864e-4*(h-65617);
28     pressure     = 3.7930e90*temperature^-34.164;
29     density      = 2.2099e87*temperature^-35.164;
30 end
31
32 end

```

aircraft_data.m

This script contains the drag coefficients, specific fuel consumption and thrust data of the aircraft model used for the simulations, specified in Section 3.4.1. The source code is displayed below.

```

1 %%%%%%%%%%%%%%%%%%%%%%%%%%%%%%%%%%%%%%%%%%%%%%%%%%%%%%%%%%%%%%%%%%%%%%%%%%
2 %
3 % Filename: aircraft_data.m
4 %
5 % Purpose: Contains the drag coefficients , specific fuel consumption and
           thrust characteristics of an aircraft modeled after the Gulfstream

```

```

    Aerospace's G-IV jet.
6 %
7 % Model source: J. D. Anderson. Aircraft Performance and Design. Chapter 5,
    Airplane Performance: Steady Flight. Pages 199-232.
8 %
9 % Source for operating limits: http://www.gulfstream.com/aircraft/gulfstream-
    g450
10 %%%%%%%%%%%%%%%%%%%%%%%%%%%%%%%%%%%%%%%%%%%%%%%%%%%%%%%%%%%%%%%%%%%%%%%%%%
11
12 % Some definitions:
13 M.HOUR.TO.SEG    = 3600;
14
15 % Gulfstream Aerospace's G-IV data:
16 SFC              = 0.69/M.HOUR.TO.SEG; % (1/s). At 30000 ft.
17 Cd0              = 0.015;
18 Cd2              = 0.08;
19 S                = 950;                % (ft^2).
20 T0               = 2 * 13850; % Each Rolls-Royce Tay 611-8 engine is rated at
    13850 (lbf) at sea level.
21 Ti               = 200.0;            % (lbf).
22 m                = 1;
23 Mmo              = 0.88;            % Maximum operating Mach.
24
25 % Make sure that the initial conditions do not exceed these limits:
26 % Maximum usable fuel weight = 29500 lb.
27 % Maximum take-off weight    = 74600 lb.
28 % Maximum zero fuel weight   = 49000 lb.
29 % Service ceiling            = 45000 ft.

```

shooting_method_cruise.m

This script loads the model from aircraft_data.m, sets the shooting method and simulation parameters, and implements the pseudo-code shown in Section 3.4.2. The desired initial,

final conditions, CI and initial speed estimate must be specified in this file as well. The sub-optimal trajectory given by (3.30) is obtained as well. To perform all these functions, the script makes use of Simulink models `sim_2pbvp_cruise.mdl` and `sim_analytic_cruise.mdl`. The code is shown below. It is important to note that the costate J_W^* is named `lambda2` in the implementation.

```

1 %%%%%%%%%%%%%%%%%%%%%%%%%%%%%%%%%%%%%%%%%%%%%%%%%%%%%%%%%%%%%%%%%%%%%%%%%%
2 %
3 % Filename: shooting_method_cruise.m
4 %
5 % Purpose: Implements the shooting method for the cruise phase. Also simulates
6 %           the system sim_analytic_cruise.mdl which implements the sub-optimal
7 %           analytic solution.
8 %
9 %%%%%%%%%%%%%%%%%%%%%%%%%%%%%%%%%%%%%%%%%%%%%%%%%%%%%%%%%%%%%%%%%%%%%%%%%%
10 % Run the script for the aircraft model:
11 aircraft_data;
12 % Some definitions:
13 Ts          = 0.1; % Simulation sampling time.
14 CI          = 0.0;
15 M_MILE_TO_FT = 5280; % Conversion from miles to feet.
16 rhosea     = 0.002377; % (slug/ft^2) sea level density.
17
18 % Shooting method parameters:
19 tolerance   = 1e-5; % Tolerance on the final condition of lambda2.
20 error       = 1e3; % Difference between final lambda2 and
21               lambda2f.
22 iter        = 1; % Iteration count.
23 maxiter     = 30; % Maximum number of iterations.
24 beta        = 1; % Used in the update law of lambda2.
25 lambdas20(1:maxiter) = 0.0; % Store initial values of lambda2 here.

```

```

25
26 % Initial and final conditions:
27 hc          = 25000;                % (ft).
28 x0          = 0.0;                % (ft).
29 xf          = 1000*M_MILE_TO_FT;   % (ft).
30 W0          = 70000;                % (lbf).
31 lambda2f    = 0;                    % % Known boundary
      condition of lambda2.
32
33 % Estimate an initial value for the speed:
34 V0          = 900;
35
36 % ISA and drag computations:
37 [~,~,rho,] = atmosphere_standard(hc);
38 d0          = 0.5*Cd0*rho*S;
39 d1          = 2*Cd2*W0*W0/(rho*S);
40 D          = d0*V0^2 + d1/V0^2;
41
42 % Compute initial value of lambda2 from V0:
43 if (CI ~ = 0)
44     lambda20 = 1 + CI/(SFC*(D - 2*d0*V0^2 + 2*d1/V0^2));
45 else
46     % lambda2 cannot be equal to 1. When CI is zero, it is best to
      estimate a small value for lambda20.
47     lambda20 = 1e-3;
48 end
49 lambdas20(iter) = lambda20;
50
51 % Begin loop:
52 while (error > tolerance) && (iter <= maxiter)
53     sim('sim_2pbvp_cruise');
54     iter = iter + 1

```

```

55
56     % Next seed for lambda20:
57     error          = abs(lambda2(end)-lambda2f);
58     lambda20       = lambda20 - beta*(lambda2(end)-lambda2f);
59     lambdas20(iter) = lambda20;
60 end
61
62 % Display a warning if the maximum number of iterations was reached:
63 if (iter >= maxiter)
64     disp('Maximum number of iterations reached. Check value of error');
65 end
66
67 % Simulate the analytic sub-optimal solution:
68 sim('sim_analytic_cruise');
69
70 % End of script.

```

sim_2pbvp_cruise.mdl

This Simulink model, shown in Fig. A.1, implements the 2PBVP given by (3.42), where v at each time-step is computed using (3.21). The blocks x , W , λ_2 , V and t store those variables in the Matlab workspace for further analysis. The block `aircraft2pbvp` is a Matlab Level-2 S-Function that specifies the dynamics of the system to Simulink. This function must comply with a specific template¹, and its implementation does not provide additional information regarding the developments of this thesis. As a result, source code for the S-functions will not be provided.

¹For more information regarding Matlab Level-2 S-Functions, consult the following website: <http://www.mathworks.com/help/simulink/sfg/writing-level-2-matlab-s-functions.html>

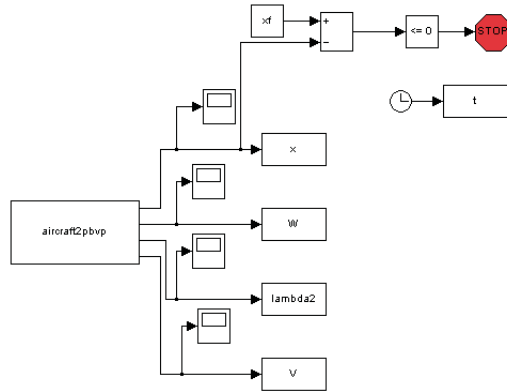


Figure A.1: Simulink block diagram of the cruise 2PBVP.

sim_analytic_cruise.mdl

This system, depicted in Fig. A.2, is used to obtain the sub-optimal trajectories resulting from applying the feedback law (3.30). The blocks `aircraft_cruise` and `optimal_controller` are Level-2 S-Functions, the latter making use of the script `CruiseOptimalSpeedAndFuelFlow.m`, shown below.

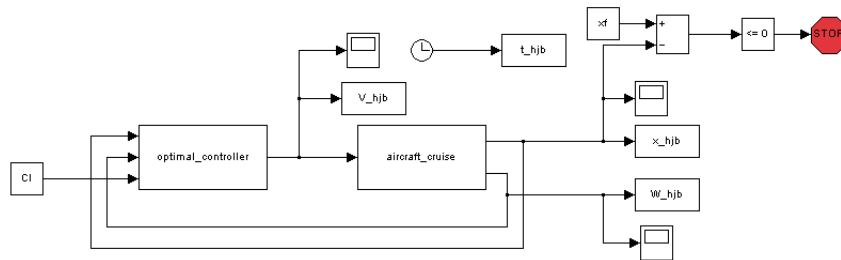


Figure A.2: Simulink block diagram of the sub-optimal cruise validation system.

CruiseOptimalSpeedAndFuelFlow.m

This function is a direct implementation of (3.30). For a given cruise altitude h , W , and CI , the function returns the sub-optimal cruise speed and the cruise fuel flow, which is equal to $f_f = S_{FC}D$. This information will be used during climb and descent to compute the constant value of J_x^* . The code is presented below.

1 %%

```

2 %
3 % Filename: CruiseOptimalSpeedAndFuelFlow.m
4 %
5 % Purpose: Computes the sub-optimal cruise speed for minimum operating costs,
      as well as the cruise fuel flow at the given weight.
6 %
7 %%%%%%%%%%%%%%%%%%%%%%%%%%%%%%%%%%%%%%%%%%%%%%%%%%%%%%%%%%%%%%%%%%%%%%%%%%
8
9 function [vTAS,ffc]=CruiseOptimalSpeedAndFuelFlow(h,W,CI,Cd0,Cd2,SFC,S)
10
11 % ISA computation:
12 [~,~,density] = atmosphere_standard(h);
13
14 vTAS    = sqrt((CI+sqrt(CI*CI + 12*SFC*SFC*Cd0*Cd2.*W.*W))./(SFC*Cd0*S*density
      )));
15
16 % Compute cruise fuel flow:
17 d0      = 0.5*Cd0*density*S;
18 d1      = 2*Cd2*W*W/(density*S);
19 ffc     = SFC*(d0*vTAS*vTAS + d1/(vTAS*vTAS));
20
21 end

```

Appendix B

Validation Code for the Climb Phase

The climb implementation makes use of `atmosphere_standard.m`, `aircraft_data.m` and `CruiseOptimalSpeedAndFuelFlow.m` from Appendix A. The following scripts and systems are exclusive to the climb phase:

`shooting_method_climb.m`

This script is analogous to `shooting_method_cruise.m`, and its code can be found below. As its name implies, it implements the shooting method provided in Section 4.4.1, and then computes the sub-optimal trajectory resulting from the application of the control law (4.48). Desired initial and final conditions must be specified inside this script. For the simulations, it runs systems `sim_2pbvp_climb.mdl` and `sim_analytic_climb.mdl`. Note that J_x^* is referred to as `lambda1` and J_W^* is called `lambda3` in the code.

```
1 %%%%%%%%%%%%%%%%%%%%%%%%%%%%%%%%%%%%%%%%%%%%%%%%%%%%%%%%%%%%%%%%%%%%%%%%%%
2 %
3 % Filename: shooting_method_climb.m
4 %
5 % Purpose: Implements the shooting method for the climb phase. Also simulates
   the system sim_analytic_descent.mdl which implements the sub-optimal
   solution.
6 %
```

```

7  %%%%%%%%%%%%%%%%%%%%%%%%%%%%%%%%%%%%%%%%%%%%%%%%%%%%%%%%%%%%%%%%%%%%%%%%%%
8
9  % Run the script for the aircraft model:
10 aircraft_data;
11
12 % Some definitions:
13 Ts          = 0.2;           % Simulation sampling time.
14 CI          = 0.0;
15 MDEG_TO_RAD = pi/180;       % Conversion from degrees to radians.
16 M_MILE_TO_FT = 5280;       % Conversion from miles to feet.
17 rhosea      = 0.002377;    % (slug/ft^2) sea level density.
18
19 % Shooting method parameters:
20 tolerance   = 1e-4;        % Tolerance on the final condition of lambda3.
21 error       = 1e3;         % Difference between final lambda3 and
    lambda3f.
22 iter        = 1;           % Iteration count.
23 maxiter     = 30;          % Maximum number of iterations.
24 beta        = 1;           % Used in the update law of lambda3.
25 lambdas30(1:maxiter) = 0.0; % Store initial values of lambda3 here.
26
27 % Initial and final conditions:
28 h0          = 2000;         % (ft).
29 hc          = 25000;        % (ft).
30 x0          = 0*M_MILE_TO_FT; % (ft).
31 W0          = 70000;        % (lbf).
32 lambda3f    = 0.0;         % Known boundary condition of
    lambda3.
33
34 % Estimate an initial value for the speed:
35 V0          = 780.0;       % (ft/s).
36
37 % ISA, thrust and drag computations:

```

```

38  [~,~,rho] = atmosphere_standard(h0);
39  d0 = 0.5*Cd0*rho*S;
40  d1 = 2*Cd2*W0*W0/(rho*S);
41  D = d0*V0^2 + d1/V0^2;
42  Dv = 2*d0*V0 - 2*d1/V0^3; % Derivative of D with respect to V.
43  Tclimb = T0*(rho/rhosea)^m;
44
45  % Initial gamma corresponding to V0:
46  gamma0 = asin( (Tclimb - D)/W0 );
47
48  % Compute lambda1 and initial lambda3:
49  [M,vTAS,vKTAS,vKEAS,vKCAS,ffc] = CruiseOptimalSpeedAndFuelFlow(hc,W0,CI,Cd0,
    Cd2,SFC,S); % Estimated cruise TAS and fuel flow.
50  lambda1 = - (ffc + CI)/vTAS;
51  lambda30 = 1 + CI/(SFC*Tclimb) - lambda1*V0*V0*Dv/(SFC*Tclimb*(W0*
    gamma0 - V0*Dv));
52  lambdas30(iter) = lambda30;
53
54  % Run the iterative process:
55  while (abs(error) > tolerance) && (iter <= maxiter)
56      sim('sim_2pbvp_climb'); % Run the system.
57      iter = iter + 1
58
59      % Next seed for lambda30:
60      error = lambda3(end)-lambda3f;
61      lambda30 = lambda30 - beta*error;
62      lambdas30(iter) = lambda30;
63  end
64
65  ROCfpm = ROC.*60; % Change ROC to feet per minute.
66
67  % Display a warning if the maximum number of iterations was reached:
68  if (iter >= maxiter)

```

```

69     disp('Maximum number of iterations reached, possibly without a solution');
70 end
71
72 % Simulate the sub-optimal solution:
73 sim('sim_analytic_climb');
74
75 ROC_hjbfpm = ROC_hjb.*60; % Change ROC to feet per minute.
76
77 % End of script.

```

sim_2pbvp_climb.mdl

This model implements the 2PBVP (4.49). To compute v and γ at each time-step, (4.6) and (4.35) must be solved simultaneously. This task is carried out using `GetControlsClimb.m`, provided in the next subsection, in conjunction with Matlab function `fsolve.m`¹, which solves systems of nonlinear equations of the form $F(u) = 0$. The block `aircraft2pbvp` is a Level-2 S-Function implementing the dynamics of the system. See Fig. B.1.

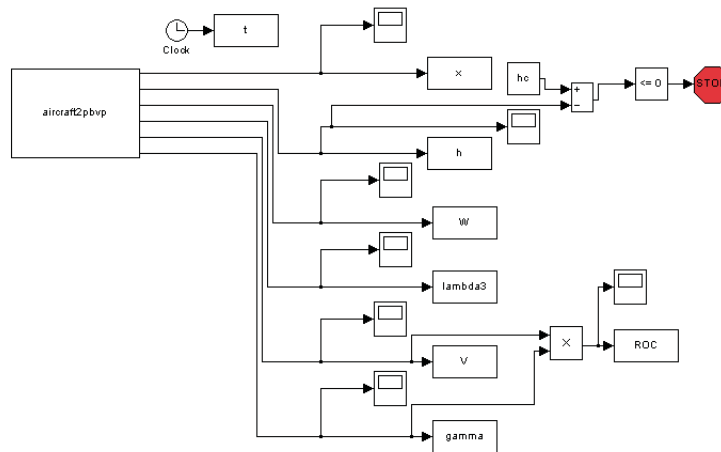


Figure B.1: Simulink block diagram of the climb 2PBVP.

¹For more information on `fsolve.m`, visit: <http://www.mathworks.com/help/optim/ug/fsolve.html>

GetControlsClimb.m

This function is meant to be used in conjunction with Matlab's function `fsolve.m`. The code evaluates (4.6) and (4.35) at a given $u = [v \ \gamma]^T$. Using `fsolve.m`, these two expressions are continuously evaluated until both equal zero, in which case the optimal point is found.

```
1 %%%%%%%%%%%%%%%%%%%%%%%%%%%%%%%%%%%%%%%%%%%%%%%%%%%%%%%%%%%%%%%%%%%%%%%%%%
2 %
3 % Filename: GetControlsClimb.m
4 %
5 % Purpose: Returns the value of the system of nonlinear equations that must be
6 %           solved to get the optimal controls (V,gamma), at u. For use with fsolve.
7 %%%%%%%%%%%%%%%%%%%%%%%%%%%%%%%%%%%%%%%%%%%%%%%%%%%%%%%%%%%%%%%%%%%%%%%%%%
8
9 function output = GetControlsClimb(rho,W,lambda1,lambda3,SFC,Cd0,Cd2,S,Tclimb,
10    u,CI)
11 % u contains V and gamma:
12 V           = u(1);
13 gamma      = u(2);
14
15 % Drag components:
16 d0          = 0.5*Cd0*rho*S;
17 d1          = 2*Cd2*W*W/(rho*S);
18
19 % Return the system of nonlinear equations evaluated at u:
20 output      = zeros(2,1);
21
22 Dv          = 2*d0*V - 2*d1/(V^3); % Derivative of the drag.
23 output(1)   = ((1-lambda3)*SFC*Tclimb + CI)*(sin(gamma) - V*Dv/W) -
24             lambda1*V*V*Dv/(W*cos(gamma));
25 output(2)   = Tclimb - (d0*V*V + d1/V/V) - W*sin(gamma);
```

sim_analytic_climb.mdl

This system, shown in Fig. B.2, is used to generate the sub-optimal climb trajectories resulting from applying the feedback law (4.48). To obtain the roots of the 5th degree polynomial, Matlab function `roots.m` is used², and an iterative loop is carried out to find the solution that lies within the operating limits of the aircraft. The blocks `aircraft_climb` and `optimal_controller` are Level-2 S-Functions implementing climb dynamics and the sub-optimal controller, respectively.

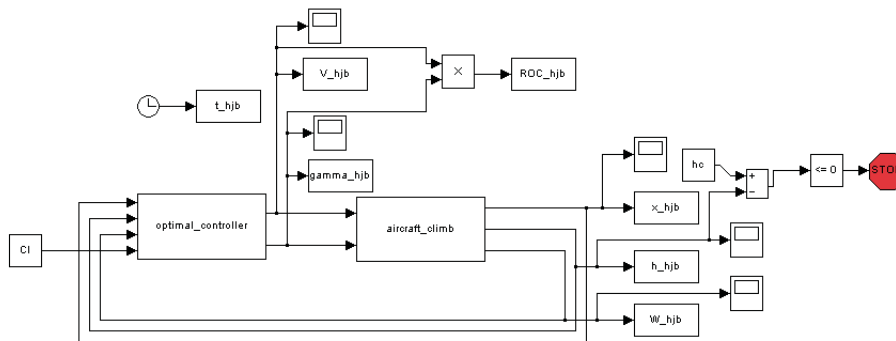


Figure B.2: Simulink block diagram of the sub-optimal climb validation system.

²More information regarding `roots.m` can be found at the website: <http://www.mathworks.com/help/matlab/ref/roots.html>

Appendix C

Validation Code for the Descent Phase

The descent implementation makes use of `atmosphere_standard.m`, `aircraft_data.m` and `CruiseOptimalSpeedAndFuelFlow.m` from Appendix A, as well as the following scripts and systems:

`shooting_method_descent.m`

Just like in the previous appendices, this script implements the shooting method provided in Section 4.6.1, and then computes the sub-optimal trajectory resulting from the application of the control law (4.75). Desired initial and final conditions must be specified inside this script. For the simulations, it runs systems `sim_2pbvp_descent.mdl` and `sim_analytic_descent.mdl`. Note that J_x^* is referred to as `lambda1` and J_W^* is called `lambda3` in the code.

```
1 %%%%%%%%%%%%%%%%%%%%%%%%%%%%%%%%%%%%%%%%%%%%%%%%%%%%%%%%%%%%%%%%%%%%%%%%%%
2 %
3 % Filename: shooting_method_descent.m
4 %
5 % Purpose: Implements the shooting method for the descent phase. Also
           simulates the system sim_analytic_descent.mdl which implements the sub-
           optimal solution.
6 %
7 %%%%%%%%%%%%%%%%%%%%%%%%%%%%%%%%%%%%%%%%%%%%%%%%%%%%%%%%%%%%%%%%%%%%%%%%%%
8
```

```

9 % Run the script for the aircraft model:
10 aircraft_data;
11
12 % Some definitions:
13 Ts          = 0.2;           % Simulation sampling time.
14 CI          = 0.6;
15 MDEG_TO_RAD = pi/180;       % Conversion from degrees to radians.
16 M_MILE_TO_FT = 5280;       % Conversion from miles to feet.
17
18 % Shooting method parameters:
19 tolerance   = 1e-4;         % Tolerance on the final condition of lambda3.
20 error       = 1e3;          % Difference between final lambda3 and lambda3f.
21 iter        = 1;            % Iteration count.
22 maxiter     = 30;           % Maximum number of iterations.
23 beta        = 1;            % Used in the update law of lambda3.
24 lambdas30(1:maxiter) = 0.0; % Store initial values of lambda3 here.
25
26 % Initial and final conditions:
27 hc          = 25000;         % (ft).
28 hf          = 2000;          % (ft).
29 xf          = 0*M_MILE_TO_FT; % (ft).
30 Wf          = 70000;         % (lbf). "Given" final weight
    at end of flight , which becomes an initial condition.
31 lambda3f    = 0.0;           % Known boundary condition of lambda3.
32 % REMINDER: The descent is solved backwards in time!
33
34 % Estimate an initial value for the speed:
35 V0          = 520.0; % (ft/s).
36
37 % ISA and drag computations:
38 [~,~,rho]   = atmosphere_standard(hf);
39 d0          = 0.5*Cd0*rho*S;
40 d1          = 2*Cd2*Wf*Wf/(rho*S);

```

```

41 D = d0*V0^2 + d1/V0^2;
42 Dv = 2*d0*V0 - 2*d1/V0^3; % Derivative of D with respect to V.
43
44 % Initial gamma corresponding to V0:
45 gamma0 = asin( (Ti - D)/Wf );
46
47 % Compute lambda1 and initial lambda3:
48 [M,vTAS,vKTAS,vKEAS,vKCAS,ffc]=CruiseOptimalSpeedAndFuelFlow(hc,Wf,CI,Cd0,Cd2,
SFC,S); % Estimated cruise TAS and fuel flow.
49 lambda1 = (ffc + CI)/vTAS; % Positive for descent.
50 lambda30 = -1 - CI/(SFC*Ti) - lambda1*V0*V0*Dv/(SFC*Ti*(Wf*gamma0 - V0*
Dv));
51 lambdas30(iter) = lambda30;
52
53 % Run the iterative process:
54 while (abs(error) > tolerance) && (iter <= maxiter)
55     sim('sim_2pbvp_descent');
56     iter = iter + 1
57
58     % Next seed for lambda30:
59     error = lambda3(end)-lambda3f;
60     lambda30 = lambda30 - beta*error;
61     lambdas30(iter) = lambda30;
62
63 end
64
65 RODfpm = ROD.*60; % Change ROD to feet per minute.
66
67 % Display a warning if the maximum number of iterations was reached:
68 if (iter >= maxiter)
69     disp('Maximum number of iterations reached, possibly without a solution');
70 end
71

```

```

72 % Simulate the sub-optimal solution :
73 sim('sim_analytic_descent');
74
75 ROD_hjbfpm = ROD_hjb.*60; % Change ROD to feet per minute.
76
77 % End of script.

```

sim_2pbvp_descent.mdl

The model in Fig. C.1 implements the 2PBVP (4.6.1). Just like in the climb, v and γ are computed at each time-step by solving (4.20) and (4.62) simultaneously with the aid of using GetControlsDescent.m and fsolve.m. The block aircraft2pbvp is a Level-2 S-Function implementing the dynamics of the augmented system.

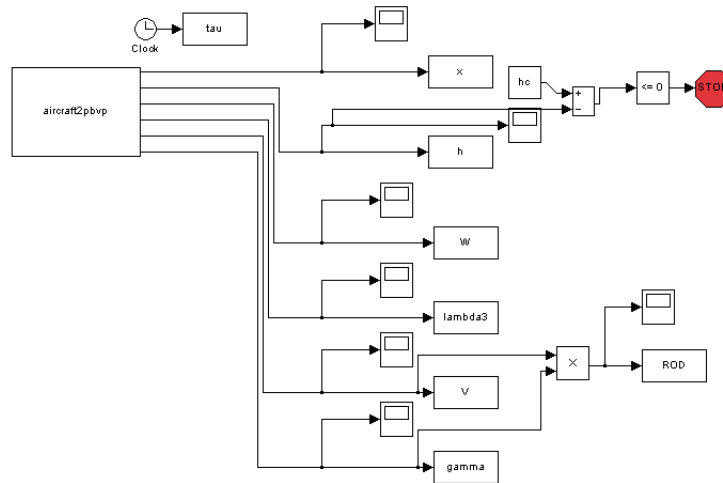


Figure C.1: Simulink block diagram of the descent 2PBVP.

GetControlsDescent.m

This function is meant to be used in conjunction with Matlab’s function fsolve.m. The code evaluates (4.20) and (4.62) at a given $u = [v \ \gamma]^T$. Using fsolve.m, these two expressions are continuously evaluated until both equal zero, in which case the optimal control is found.

1 %%

```

2 %
3 % Filename: GetControlsDescent.m
4 %
5 % Purpose: Returns the value of system of nonlinear equations that must be
        solved
6 % simultaneously in order to get the optimal controls (V,gamma). For use with
        fsolve.
7 %
8 %%%%%%%%%%%%%%%%%%%%%%%%%%%%%%%%%%%%%%%%%%%%%%%%%%%%%%%%%%%%%%%%%%%%%%%%%%
9
10 function output = GetControlsDescent(rho,W,lambda1,lambda3,SFC,Cd0,Cd2,S,Ti,u,
        CI)
11
12 % u contains V and gamma.
13 V          = u(1);
14 gamma     = u(2);
15
16 % Drag components:
17 d0          = 0.5*Cd0*rho*S;
18 d1          = 2*Cd2*W*W/(rho*S);
19
20 % Return the system of nonlinear equations evaluated at u:
21 output      = zeros(2,1);
22
23 Dv          = 2*d0*V - 2*d1/(V^3); % Derivative of the drag.
24 output(1)   = ((1+lambda3)*SFC*Ti + CI)*(sin(gamma) - V*Dv/W) + lambda1*V*V*Dv
        /(W*cos(gamma));
25 output(2)   = Ti - (d0*V*V + d1/V/V) - W*sin(gamma);
26
27 end

```

sim_analytic_descent.mdl

This system is used to generate the sub-optimal descent trajectories resulting from applying the feedback law (4.75). `roots.m` is used to get the roots of the 5th degree polynomial. The blocks `aircraft_descent` and `optimal_descent` are Level-2 S-Functions implementing descent dynamics and the sub-optimal controller, respectively. See Fig. C.2.

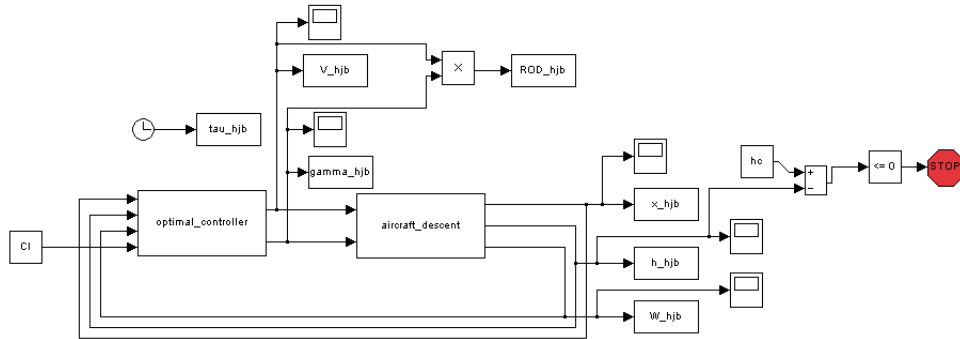


Figure C.2: Simulink block diagram of the sub-optimal descent validation system.